GRID
GLOBAL RESOURCE INFORMATION DATABASE

GRID
CASE STUDY SERIES
NO. 4

NAIROBI
JULY 1991

GLOBAL DIGITAL DATASETS FOR LAND DEGRADATION STUDIES: A GIS APPROACH

Uwe Deichmann
Lars Eklundh

GEMS
GLOBAL ENVIRONMENT MONITORING SYSTEM
UNITED NATIONS ENVIRONMENT PROGRAMME

Uwe Deichmann is a Consultant to UNEP from the Department of Geography, University of California, Santa Barbara, USA.

Lars Eklundh is a Systems Analyst at GRID-Nairobi on leave from the Remote Sensing and GIS Laboratory, Department of Physical Geography, University of Lund, Sweden.

The authors are indebted for their support and helpful comments to: Dr. Michael Norton-Griffiths, GEMS/UNITAR Africa Programme, who co-ordinated the project at GEMS, and to Dr. Harvey Croze, GRID-Co-ordinator and Dr. Michael Gwynne, GEMS Director.

The authors would also like to thank Dr. R. Oldeman, International Soil Reference and Information Centre, Wageningen, and Dr. M. Hulme, Climatic Research Unit, University of East Anglia, for their cooperation in integrating and producing the GLASOD and climate datasets.

GRID
GLOBAL RESOURCE INFORMATION DATABASE

GRID
CASE STUDY SERIES
NO. 4

NAIROBI
JULY 1991

GLOBAL DIGITAL DATASETS FOR LAND DEGRADATION STUDIES: A GIS APPROACH

Uwe Deichmann
Lars Eklundh

GEMS
GLOBAL ENVIRONMENT MONITORING SYSTEM
UNITED NATIONS ENVIRONMENT PROGRAMME

TABLE OF CONTENTS

Part 1

INTRODUCTION TO THE REPORT

The 1977 UNESCO/UNEP desertification map of the world and the 1984 FAO/UNEP map covering Africa are some of the first important attempts to characterize the spatial extent and distribution of desertification on a global and regional level. Based on the experiences of these efforts, the twelfth session of UNEP's governing council recommended in 1984 that the complexity of desertification phenomena required the characterization of the problem as a series of thematic maps. It was therefore decided to produce a World Atlas of Thematic Indicators of Desertification together with a global assessment of desertification in time for the United Nations Conference on Environment and Development in 1992.

The definition of desertification adopted by the Consultation Meeting on the Assessment of Global Desertification (Odingo, 1990) is:

Desertification/land degradation, in the context of assessment, is land degradation in arid, semiarid and dry subhumid areas resulting from adverse human impact.

The breadth of this definition requires a wide variety of variables to be included into the atlas such as soil degradation processes, climatic conditions, vegetation resources, as well as socioeconomic factors. The atlas will contain a global section, aimed at providing a better understanding of the global distribution of desertification and the factors underlying it, and a regional section highlighting desertification problems on the African continent. A third section presents case studies of desertification compiled by research institutions around the globe.

The global assessment as well as the thematic atlas are coordinated by UNEP's Desertification Control Programme Activity Centre (DC/PAC). The Global Resource Information Database (GRID) programme was involved to establish the database on which the project draws. More specifically, GRID's task was comprised of two parts:

(1) to provide numeric data (e.g. area statistics) on indicators of desertification and of the interactions of land degradation indicators with other variables. These data are used to accompany maps in the thematic atlas, and it will also aid the global assessment of desertification.

(2) to produce a series of maps of thematic indicators of desertification to be included in the global and regional sections of the atlas.

One of the drawbacks of the 1977 approach to desertification mapping was the fact that the outputs, e.g. the maps, were static products. The methodology chosen for the current project in contrast is based on the design of a dynamic database. This is achieved by storing and processing all data in a common reference system in a geographic information system (GIS). This means that as new and better information becomes available, the database can be continuously augmented, updated, modified and corrected. Furthermore, since the data is stored in a generic format, it can be made available to scientists and decision makers worldwide. Because there is no universally accepted approach to the analysis of desertification and land degradation, other analysts might want to look at the data from a different angle, for example, using alternative data sources in combination with the soil degradation data.

This report describes GRID's work in assembling the core data sets used in the production of the global and regional sections of the thematic atlas. Its aim is to serve as a source of background information rather than as a detailed analysis of the data generated. In the course of the project, new data sets as well as existing ones stored in the GRID archive have been utilized. All coverages have been prepared or generated by GRID analysts in close cooperation with internationally acknowledged experts in the relevant fields. The datasets are now part of the GRID archive and are distributed freely.

Part 2 of this report gives a technical background to the study. Concepts of geographic analysis are introduced, and methodologies for the production of numeric and cartographic output are presented.

The core data set of the project, the Global Assessment of Soil Degradation (GLASOD) is discussed in Part 3. Emphasized here are the modifications implemented by GRID to allow statistics to be derived, and to make the data compatible with the other coverages. Two versions of the GLASOD data set have been used in this study: a global one based on the 1:10 million scale wall chart, and a more detailed African data set for the regional section of the atlas based on a 1:6 million scale map.

Part 4 deals with the production of a coverage of climatic zones. Since desertification is defined as degradation of the land surface in arid, semi-arid and dry-subhumid zones, climatic boundaries to delineate those areas are needed. Acknowledging the fact that climate changes over time, it was decided to produce a new climatic coverage based on recent data rather than utilize an existing map.

The importance of vegetation cover in the land degradation context is undisputed. Global data sets on vegetation characteristics, however, are hardly available. A data set that can be obtained on a frequent basis is the Global Vegetation Index (GVI). Part 5 of this report presents the methodology chosen by GRID analysts to include these data in the global and regional desertification study.

Many desertification processes are human-induced, and thus socioeconomic factors play a large role in the degradation of land resources. Global or regional data on factors such as population pressure or population carrying capacity, which link human habitation to land use and land cover, are scarce. As an approximation it was decided to include a map of population densities for Africa into the regional section of the atlas. The construction of this dataset is discussed in Part 6 of this report.

The data sets collected and assembled in the course of this study offer many possibilities for analysis. The study of individual thematic indicators and combinations of factors provide numerous insights into the problem of desertification. Results from some analyses conducted at GRID are displayed in Part 7 of this report as a selection of cross-tabulations (area calculations) of the GLASOD datasets with other data layers. The information presented in Part 7 is by no means exhaustive. More information can be derived from the existing data sets, and including additional variables would open up even more possibilities.

Odinga, R.S., 1990: Desertification Revisited. Proceedings of an Ad-Hoc Consultative Meeting on the Assessment of Desertification. UNEP-DC/PAC, Nairobi, 15-17 February 1990.

Part 2

GEOGRAPHICAL ANALYSIS

TABLE OF CONTENTS

1. INTRODUCTION

All the land degradation information discussed in this report is stored in a digital database and forms part of the Global Resource Information Database (GRID). The major part of the data has been collected by international institutions and experts outside GRID, and then transferred to the database at GRID-Nairobi, UNEP, either in digital form, or as maps and tables for later conversion into digital format.

All data in the database are geographically referenced in the sense that each point in every data layer is related to a physical location on the earths surface. All data are therefore compatible with all the other data layers, and with all other data layers in the GEMS/GRID global environmental database.

Different information layers that are stored in a common reference system in the database can be combined or analyzed in the computer to cross check, validate or create new information layers from the input data. Data can be changed and updated as new information is obtained, and geographical modelling and surfacing can be performed. Storing geographical data digitally also makes the creation of various types of outputs possible, like tabular statistics, graphs and maps. All data can be distributed in digital form on various media, such as optical disks, magnetic tapes or floppy disks. This enables other researchers to use the data in the most suitable way, and to combine it with their own choice of data.

2. GEOGRAPHIC INFORMATION SYSTEMS - A TECHNICAL BACKGROUND

It is necessary to include a short discussion of GIS methods, in order to give a background to the analyses that have been performed and presented in other parts of this report. The field of GIS is very wide, and only the parts that have been applied in this project will be touched upon here. The interested reader is referred to a standard textbook like Burrough (1986).

The input of analog data, like a map, into a GIS can be done automatically through optical scanning, or manually by digitizing. The computerized data in the database are stored and analyzed in either raster or vector format. It is possible to change between these formats through conversion programs, thereby utilizing the advantages of both systems.

Raster or grid-cell format is the most convenient format for continuous variables, like precipitation or elevation. It is also used for satellite data. The data files consist of columns and rows, where each cell or pixel represents a particular area on the map. Each cell contains a number representing the value of the variable that is being mapped. The format allows operations such as mean value calculations or interpolations. Interpolation is the technique of transforming point data into a continuous surface by estimating the value of a variable for a particular location as a function of neighboring values. An example is the conversion of rainfall station data to a continuous rainfall surface. A classification can then transform the surface into discrete rainfall classes. Spatial filtering is a common way of smoothing or enhancing raster data. A filter consists of a window of a specified number of pixels that moves over the image, replacing the centre pixel with, for example, the mean or the mode value in the window.

Vector format stores geographic features as pairs or series of x and y co-ordinates. It is more efficient for storage than raster format, if the variability in the data is not very high. The format retains larger accuracy, but programming is complicated and not intuitive. The features of a vector coverage usually consist of either points, lines or polygons. A polygon denotes a series of connected lines forming a closed area, and is mostly used for categorical data such as soil units or land use classes.

In a vector GIS each feature, such as a polygon, has a series of attributes associated with it which are stored in a table. The attributes can denote, for example, the area of the polygon, the class value, the name, the colour it should have on the map, or any other connected information. This table is handled by a relational database management system which allows the user to perform statistical and logical operations on the attribute data.

Combining or overlaying vector GIS data is a process whereby the computer intersects the lines in two or more input data layers that are stored in the same spatial reference system. The result of such a process is a merged dataset which contains all features from the input datasets. Assuming that the input datasets are correctly referenced the output areas will be calculated with very high accuracy. The attribute information is also merged so that the resulting attribute table contains all the attributes from both input datasets. The principle of GIS overlay is shown in the example in Figure 1 where a climate dataset is overlayed with a dataset on erosion. The new attribute table, created by the overlay, can be used for performing a large range of geographical analyses, for example of the co-variation of the features from both input datasets.

3. DATA ANALYSIS

Many of the input data layers for the land degradation project were originally processed in raster, or grid-cell, format. This was the case with the climate, population and the NOAA NDVI satellite data. Typical raster operations were performed on the data, like point data interpolation, classification and filtering. Other data, such as the GLASOD datasets, were delivered in vector format. For the purpose of overlaying with the other datasets and for map production, all classified raster files were subsequently converted into vector format.

After the preprocessing stage and before any analyses were attempted, all land degradation information was thoroughly error checked by plotting the map data and through contextual cross checking. Outliers and logically "impossible" combinations were detected and corrected.

In the vectorized format the data could be transformed into various different map projections. The two projections used for this project were Mollweide and Van der Grinten. Mollweide is an equal-area projection which has been used for all area calculations, to insure correct area estimates. Van der Grinten is a projection well suited for global map drawing, since it fairly well retains both size, shape and distances. It exaggerates the size of the near-polar areas to a lesser extent than many other popular projections such as Mercator. Van der Grinten was thus used for all map plotting.

Most of the analysis of the land degradation data is based on the overlaying of maps as described in the example above. These combinations of data play a very important role in geographic analysis because they reveal information about relationships between different variables. Overlay of environmental data forms the basis for all the tables presented in this report.

The area calculations produced in the geographical information system were exported from the relational database system into a spread-sheet programme for percentage calculations, layout and production of graphs.

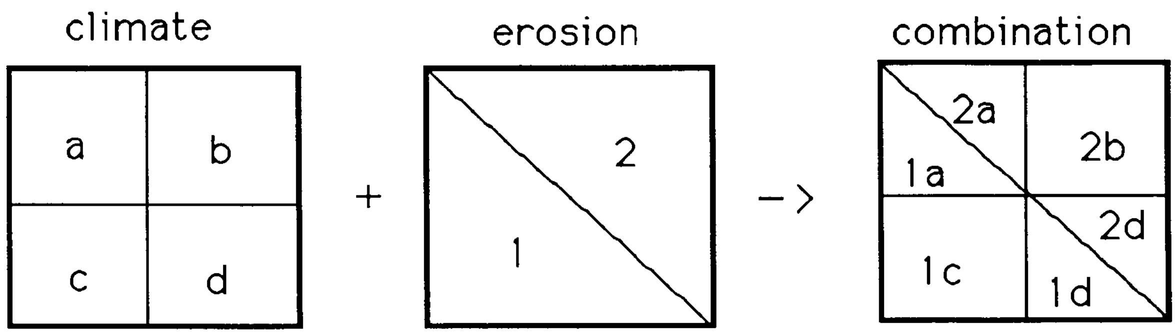

Attribute tables:

Climate	Erosion	Combination
a = arid b = semi-arid c = subhumid d = humid	1 = low 2 = high	1a = arid climate, low erosion 2a = arid climate, high erosion 1b = semi-arid climate, low erosion 2b = semi-arid climate, high erosion etc...

Figure 1: Example of overlay between a dataset on climate and a dataset on erosion degree.

4. PRODUCTION OF OUTPUT

Besides the statistical information obtained and printed from the attribute tables the digital information has also been presented in map form. Maps can be plotted on paper or as colour separations directly from the database, using graphics software. Plot files can also be converted to postscript format for direct typesetting. For the production of map output for the Thematic Atlas of Desertification the following production line will be used: (1) Processing of all raw data files at GRID-Nairobi. (2) Production of map plot files using UNIRAS and Arc/Info at GRID-Nairobi. (3) Plotting of the maps on a Calcomp high-resolution electrostatic plotter at GRID-Arendal. (4) Verification and final design of the plotted maps at GRID-Arendal and Nairobi. (5) Production of postscript format files at GRID-Arendal. (6) Transfer of the postscript files to the publisher for direct typesetting.

5. HARDWARE AND SOFTWARE USED

All analyses have been performed on an IBM PS2-80 under DOS and a DEC Microvax III under VMS. Some of the data processing was done on an IBM 9370 mainframe running under VM/IS. The raster analyses have been conducted using IDRISI (Eastman, 1990) and routines programmed in Turbo-C on the PS-2 and FORTRAN on the VAX. The vector analyses have been conducted in Arc/Info (ESRI 1988). Tables were processed in Lotus-123 and graphs produced with Harvard Graphics. Map outputs have been produced with the Arc/Info Arcplot module, and with UNIRAS (Uniras, 1988).

6. REFERENCES

Burrough, P.A., 1986, *Principles of Geographical Information Systems for Land Resources Assessment.* Monographs on Soil and Resources Survey, Gen. Ed. P.H.T. Beckett. Clarendon Press, Oxford.

Eastman, J.R., 1990, IDRISI A Grid-Based Geographic Analysis System. Clark University, Graduate School of Geography.

ESRI, 1988, Arc/Info, Users Guide. Environmental Systems Research Institute, Redlands, California.

UNIRAS, 1988, FGL/Graphics User Guide, Version 6. Uniras A/S Soborg, Denmark.

Part 3

THE GLOBAL ASSESSMENT OF SOIL DEGRADATION (GLASOD)

TABLE OF CONTENTS

1. INTRODUCTION

The Global Assessment of Human Induced Soil Degradation (GLASOD) is the core dataset for UNEP's desertification assessment and for the production of an atlas of thematic indicators of desertification. The GLASOD dataset was commissioned by the soil unit of UNEP's Terrestrial Ecosystems Branch (TEB/Soils) and assembled by the International Soil Reference and Information Centre (ISRIC) on the basis of questionnaires completed by soil experts all over the world. The dataset exists as a global wall chart produced by ISRIC and as a digital geographic database to be used in a geographic information system (GIS). The digital database was used in the desertification atlas project for the production of more detailed maps of individual variables, for the combination of GLASOD data with other datasets (climate, vegetation etc.), and for the calculation of area statistics.

The GLASOD data are stored in digital form in UNEP's Global Resource Information Database (GRID). Thus, the data can be made available to scientists and decision makers all over the world for query and analysis. The GLASOD dataset contains a wealth of information on soil degradation processes. Due to the scale of the analysis and the nature of the variables included, the database is highly complex. This explanatory note describes the conventions used in the analysis of the dataset. This documentation does not replace, however, the information already provided by ISRIC to accompany the global wallchart (Oldeman, 1991). Specific information about the compilation of the data, and about the variables that are relevant to soil degradation processes should be taken from there.

After modifications on the original GLASOD dataset from ISRIC, the database now contains a number of additional items necessary for area calculations and map production. At various stages during the project adjustments had to be made to the database.The expertise and judgement from ISRIC was sought before any modifications were done.

The following section of this report describes the preliminary steps that were necessary to prepare the GLASOD coverage for analysis. The global GLASOD coverage is discussed in section 3. Section 4 presents issues related to the more detailed GLASOD African dataset. A selection of area calculations derived from the GLASOD datasets has been included in part seven of this report.

2. PRELIMINARY WORK

The topological information of the GLASOD dataset was delivered to GRID as point and line data in a format that can be used by the Arc/Info GIS. The attribute information was included as a standard database file. ISRIC had digitized directly from the global wall chart which was registered in the Mercator projection. Similar to the wallchart the coverage was divided into three separate parts (files) which had to be joined to produce a continuous coverage.

In contrast to the global wall chart which has an origin at 150 degrees West, all maps prepared by GRID for the desertification atlas have a left edge corresponding to 180 degrees West and are centered over the Greenwich meridian. From the ISRIC coverage a rectangular part with a width of 30 degrees was therefore moved from the right (East) to the left (West) edge of the map. Up to this point, the coverage was still registered in digitizing units. The latitude/longitude coordinates of the control points provided by ISRIC, were projected into

Mercator coordinates. These were used in a linear transformation in Arc/Info, such that the whole coverage was registered in Mercator units. From this correctly registered map two coverages were derived for use in the project: in the equal area Mollweide projection, to be used in all area calculations, and in the Van der Grinten projection which was used for the production of cartographic output.

3. THE GLASOD DATABASE

ISRIC's concept of data collection has to be discussed briefly, in order to clarify the structure of the GLASOD database (see Oldeman 1991). For a given region (e.g. Eastern Africa), ISRIC asked experts to delineate a set of areas that could be considered homogeneous according to physical geographic criteria. These areas are called map units or polygons and represent the smallest spatial unit in the GLASOD database. For each map unit, the soil experts answered a questionnaire about soil degradation processes occuring *within* the unit. The most important of the variables are:

DEGREE: A measure of how strongly the soil is affected by degradation, estimated in relation to changes in agricultural suitability, to declined productivity and to biotic functions of the soil; Four levels of degree are distinguished: light, moderate, strong and extreme.

EXTENT: The percentage of the area of the map unit that is actually affected; five classes from infrequent to dominant are considered: 0-5%, 5-10%, 10-25%, 25-50% and 50-100%.

TYPE: Twelve individual types of soil degradation are recognized. These can be grouped into four major types: water and wind erosion, chemical and physical degradation. Furthermore three types of stable terrain and six types of unproductive wastelands are indicated.

CAUSE: The term human induced soil degradation refers to social processes leading to a diminishing agricultural potential of the land. The cause variable indicates the kind of human interference that has triggered the degradation process. The five major factors inducing soil degradation are: deforestation, overgrazing, agricultural activities, overexploitation of vegetative cover for domestic use, and (bio)-industrial activities.

RATE: The speed at which degradation occured in the recent past, medium or rapid. The rate variable is not clearly defined according to ISRIC and has therefore not been used in this study.

The GLASOD database contains information only about the degradation processes *within* a map unit. Two degradation processes can occur in each map unit of the global coverage. This could mean, for example, that one part of the map unit (e.g. 5-10%) is affected by water erosion, another (e.g. 10-25%) by wind erosion. Within the map unit, however, it is unknown exactly where the processes occur. One could argue that the data has thus been collected on the wrong spatial scale. On the other hand, many degradation processes might be scattered over the area of the map unit. A particular erosion process (e.g. gully erosion) might affect approximately 10% of the area but since it is dispersed over the whole terrain, it is impossible to display it as a coherent area.

The fact that more than one degradation process can be present in one map unit is crucial in understanding the structure of the GLASOD database since it complicates the processing of the data considerably, both for mapping and for deriving statistics. Many of the adjustments that were made for the analysis were required because of this feature. As an example, consider the problem of mapping where the spatial units are shaded according to the attributes stored with the polygon. Shading the entire polygon provokes the impression that the entire map unit is affected by degradation, even if the extent is only 0-5%. Furthermore, using two colors to shade a polygon, indicating that two different types are present, might indicate that both processes are equally important even if one clearly dominates the other.

In the global wallchart, ISRIC resolved the issue by including the full attribute information in each polygon as a map unit symbol. Still it is likely that the influence of the first visual impression of a map unit completely colored will exaggerate the magnitude of degradation. The inclusion of the attribute information was not possible in the Thematic Atlas of Desertification due to the limited size of the maps. The display of the maps therefore has to rely on a clear explanation of the cartographic conventions used.

It is necessary to use three different variables indicating the strength of a process in a given map unit, because of the problems outlined above. These are now discussed in turn.

1) Degree

Degree is provided by ISRIC in the original database and is divided into four classes: light, moderate, strong and extreme. An explanation of these classes is given in the ISRIC documentation. For area calculations, degree has to be used in combination with the Extent variable. For a given map unit, the actual area affected by degradation type 1 and degree 1 is calculated as the total area of the polygon times the midpoint of the percent range indicated by extent I divided by 100 (e.g. 0.025 for the 0-5% range). As an example, for a map unit of 1000 sqkm and an extent of 0-5%, only 25 sqkm are thus affected by degradation. For map units within which two types are causing soil degradation, the actual areas affected can be calculated separately and summed.

An additional problem in some map units occured when one type has an extent of 25-50%, and the other of 50-100%. Taking the midpoint of the ranges would result in a total affected area of more than 100% of the total map unit. In these cases, the percentages were reduced to sum to 100%.

A more complicated issue is encountered when statistics from overlays are compiled (e.g. GLASOD combined with a coverage of climate zones). Assume a climatic boundary between the arid and semi-arid zone cuts through a map unit splitting it in half. Assume further that 7.5% of the map unit is actually affected. It might now very well be that the degraded area is located within only one, e.g. the arid half. However, there is no way to know this. It was therefore assumed in all area calculations performed by GRID, that all degradation processes are distributed completely homogenously over the map unit. In our example, the degradation would therefore be equally distributed to each climate zone. Thus, 3.75% of the map unit area would be allocated to the total of degradation in the arid zone, and 3.75% to the semi-arid zone.

2) Severity of Soil Degradation (Status)

The severity variable relates degree and extent and was calculated for each degradation type separately. The table "Soil Degradation Severity Classes" in Figure 1 shows the conventions used. Note that the twenty classes that result as combinations of the four degree and five extent classes may be combined into four composite categories. These range from the combination of low degrees and extents in the upper left corner to high ones in the lower right corner. These four categories are called low, medium, high and very high. The four classes have been indicated as varying color intensities in the maps of types of degradation included in the atlas. A very high severity can therefore mean that either extreme degradation is occuring in only 10-25% of the map unit, or that moderate degradation affects 50-100% of the map unit. Examples from the global coverage of the severity of the four major types of soil degradation are shown in Figures 2-5.

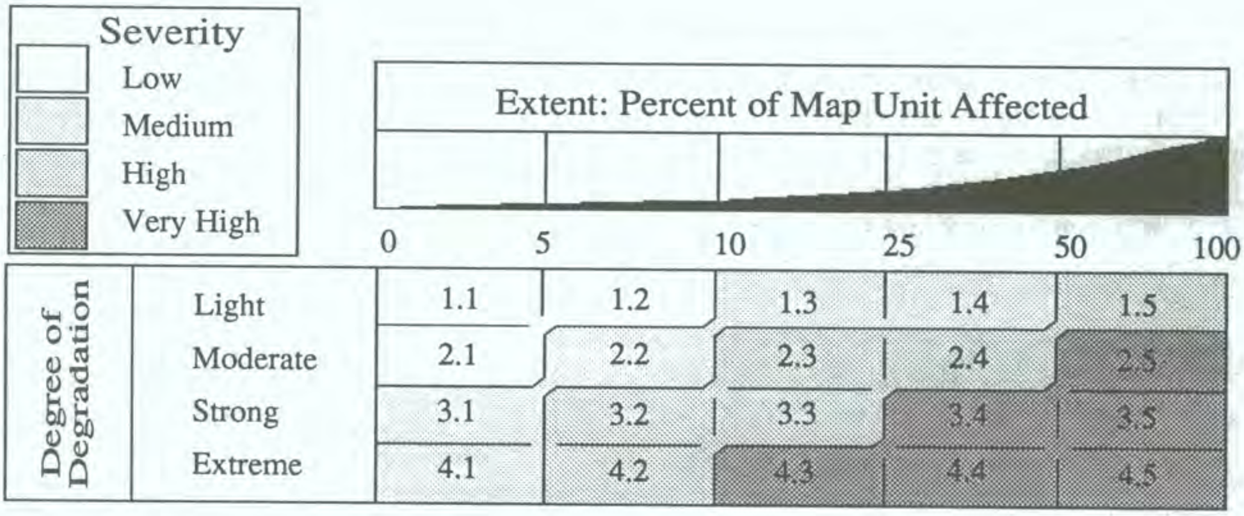

Figure 1: Soil degradation severity classes

3) Aggregate Severity

One of the tasks involved in the production of the desertification atlas was the design of a map showing the overall intensity of degradation processes on the globe. For each map unit one measure had to be defined that considers the degree and extent of *both* types of degradation that occur within the polygon. The aggregate severity variable was created to indicate this measure.

For map units within which only one type occurs, aggregate severity is identical to the severity of the individual type. For map units with two types, a look-up table set up by soil scientists from ISRIC was used to define the severity class. It contains some polygons where it was felt that the combined impact of two processes in a map unit were not adequately expressed by the individual severity for each type. In some cases, for example, the ISRIC experts upgraded severity to very high where both processes involved only have a high status.

In summary, like individual severity, aggregate severity indicates the strength at which degradation processes act within a map unit. In contrast to the severity of only one type of degradation (status), severity takes both types occuring within a map unit into consideration. It is thus an indicator of the overall importance of degradation. Figure 6 shows the overall soil degradation severity for the globe.

While a maximum of two types, degrees and extents of soil degradation are given in the GLASOD dataset, only one cause variable is included. Often however, a combined cause such as "ai" (agricultural and bio-industrial) is entered. The problem in calculating areas affected by various causes is that it is not directly clear which cause is associated with which type and extent. This information would be necessary as well for calculating totals of soil degradation causes (e.g. by region) as for calculating areas of for example cause by type or by degree of degradation.

Figure 2: Water erosion severity derived from the GLASOD dataset

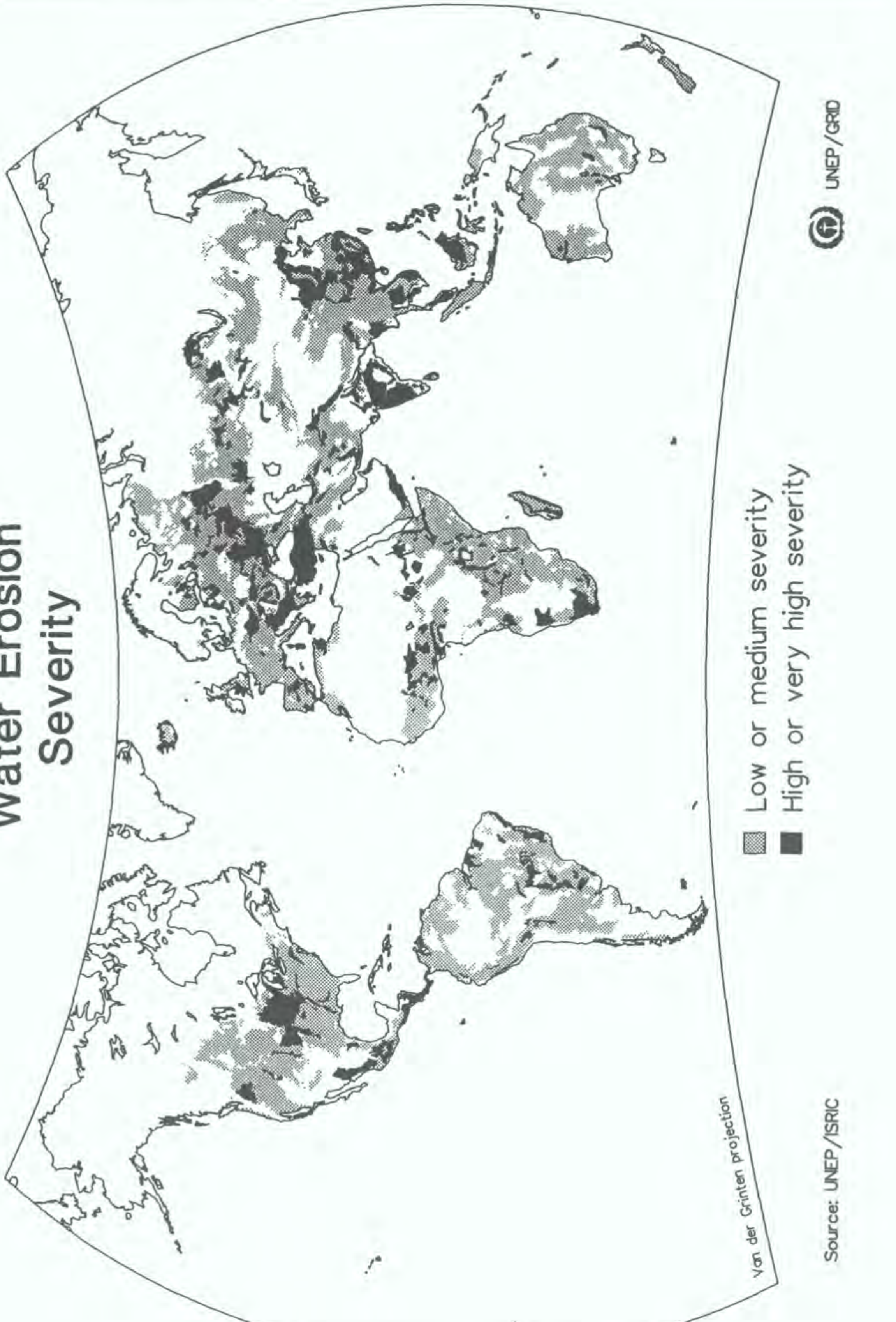

Figure 3: Wind erosion severity derived from the GLASOD dataset

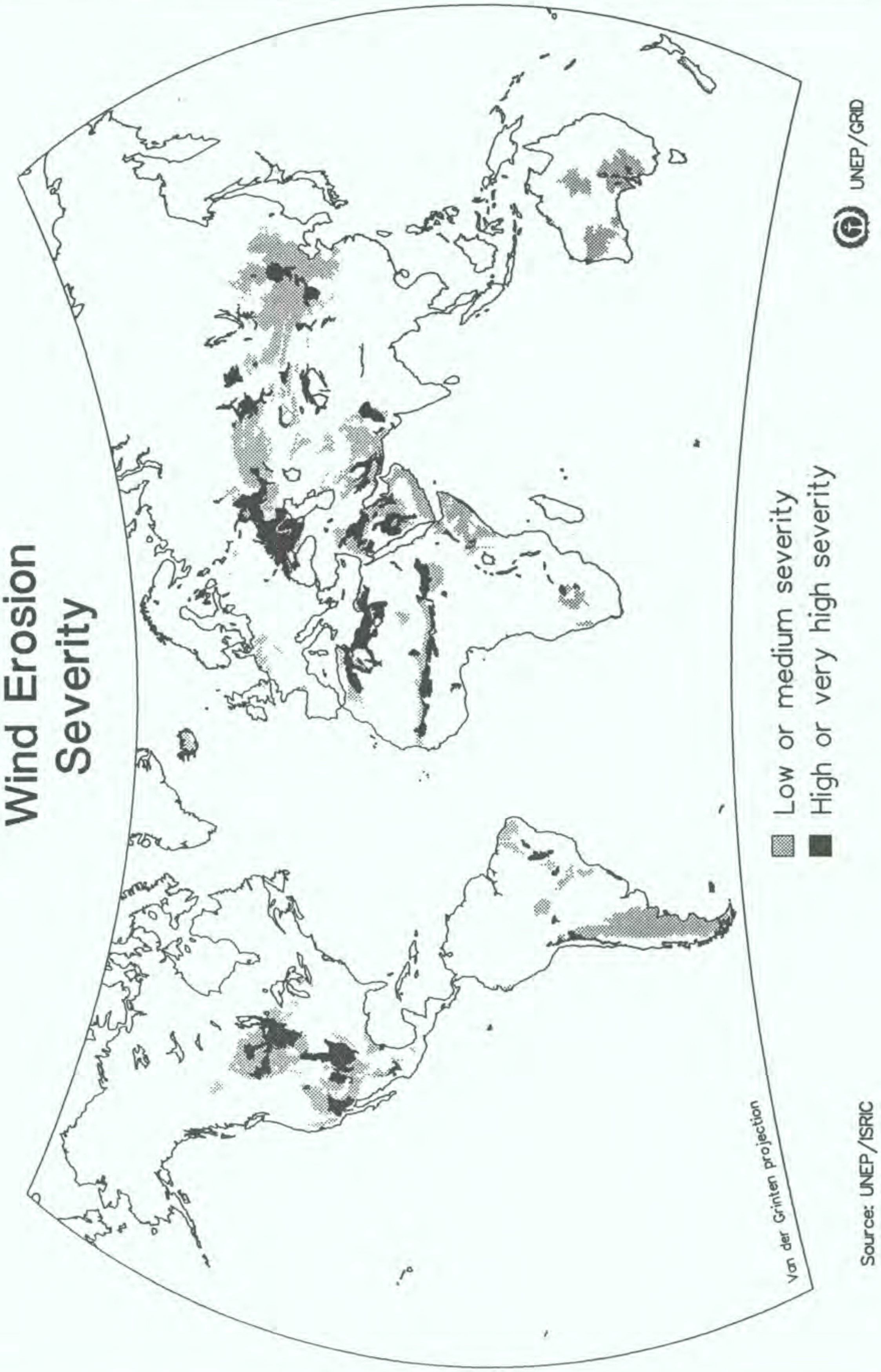

Figure 4: Chemical deterioration severity derived from the GLASOD dataset

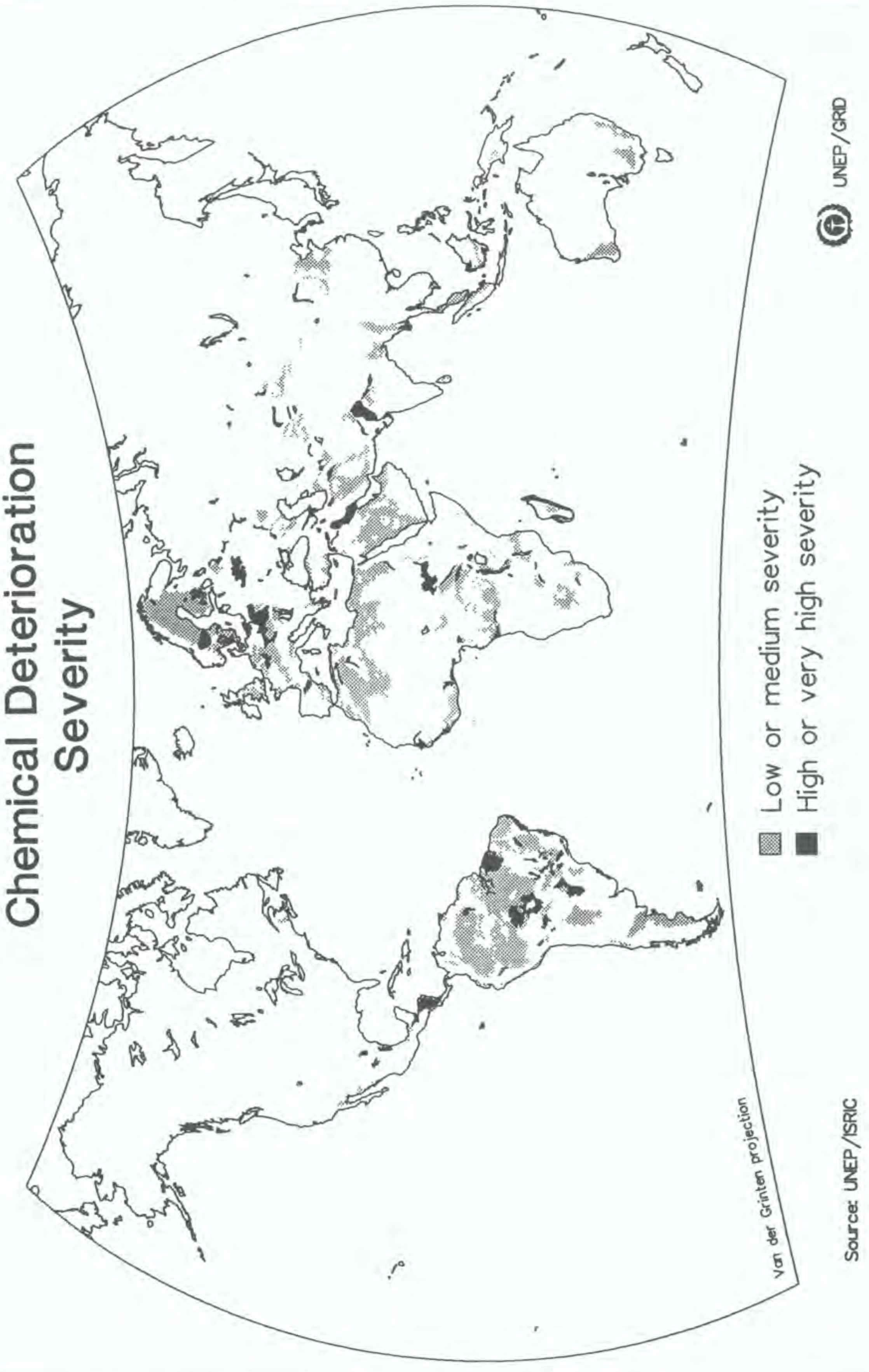

Figure 5: Physical deterioration severity derived from the GLASOD dataset

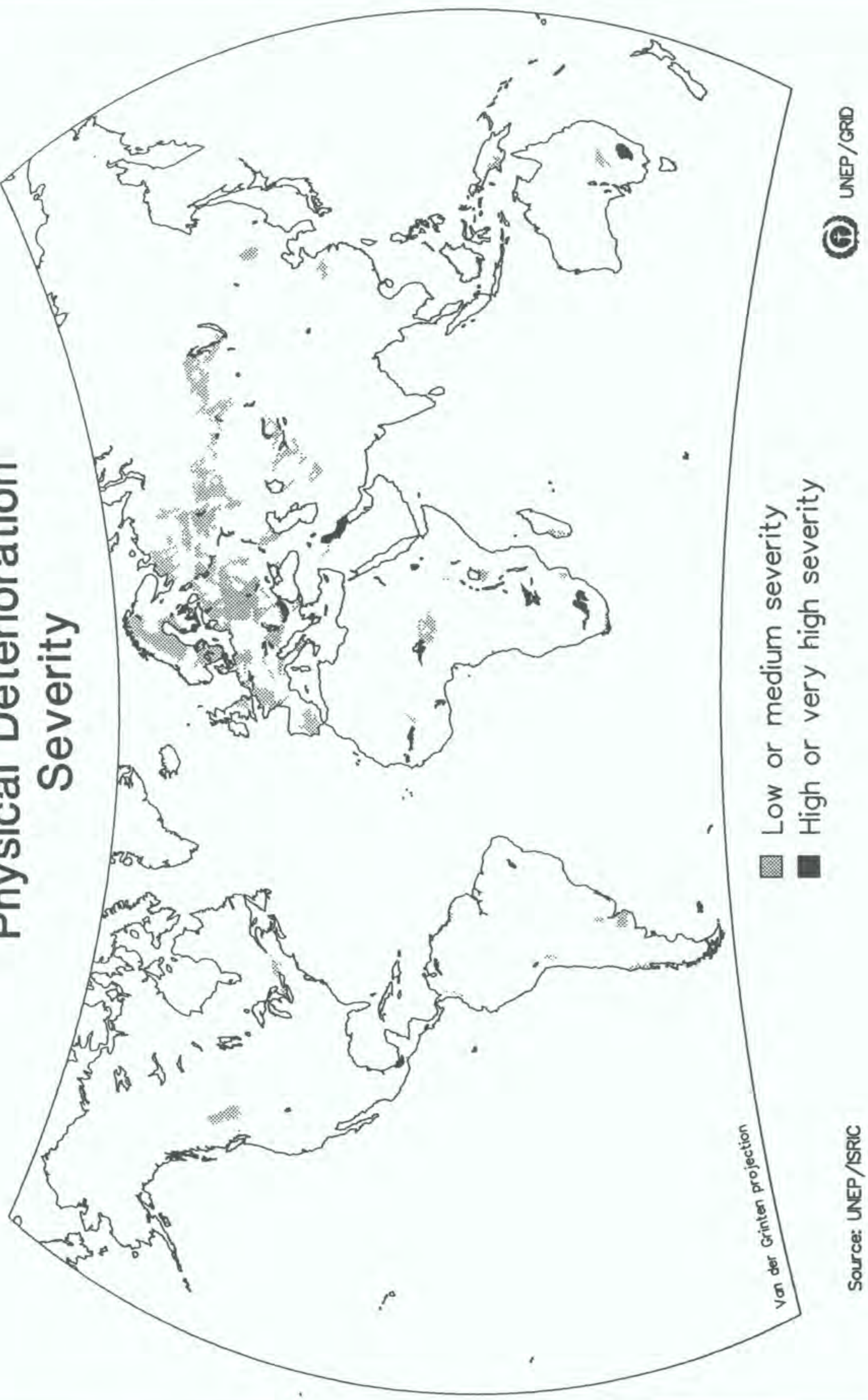

Figure 6: Aggregate soil erosion severity derived from the GLASOD dataset

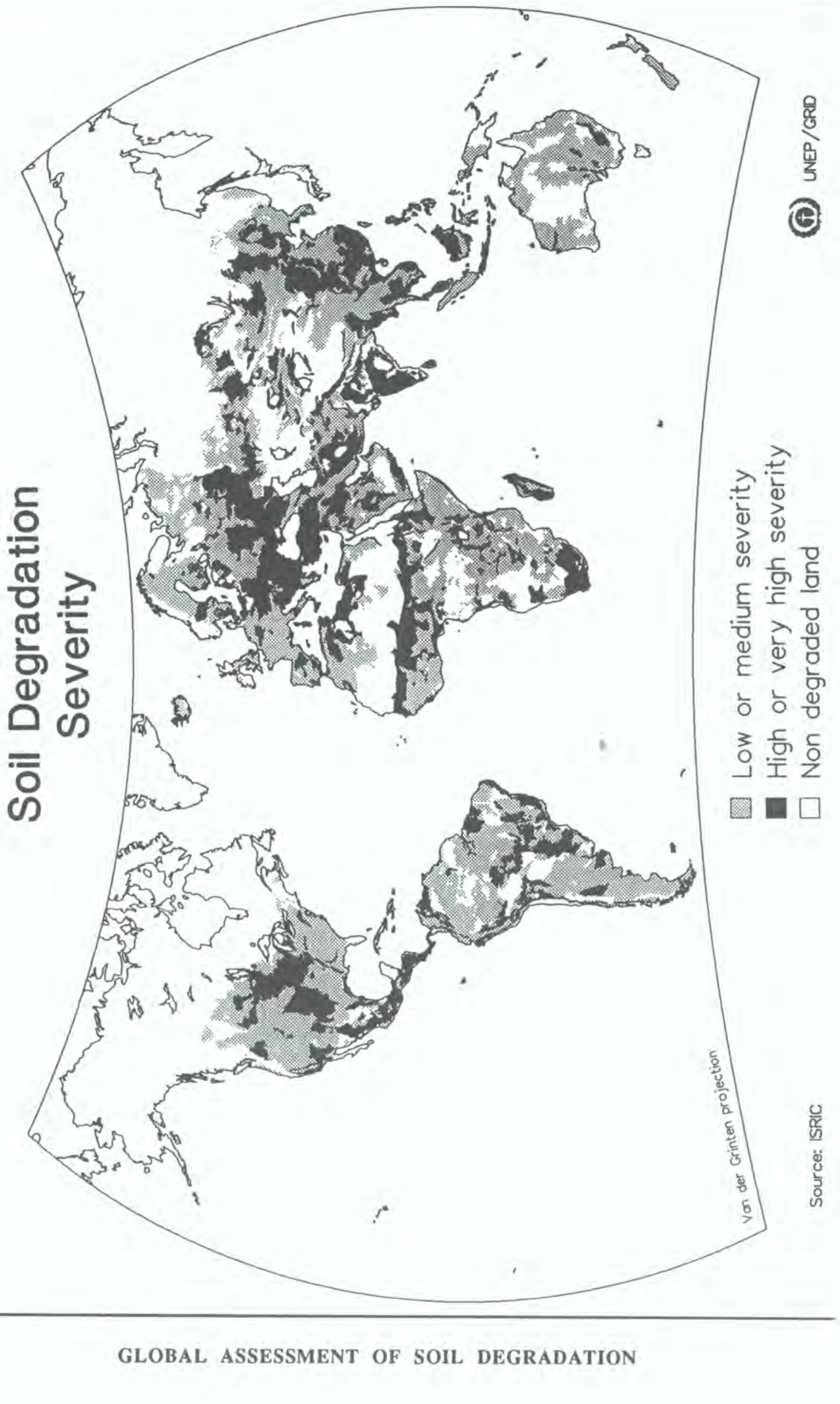

To solve this problem, the soil experts from ISRIC produced another look-up table which links the causative factors to degradation types. A considerable amount of judgement based on expert knowledge and experience was necessary for this, because the sequence of a combined entry (e.g. "ai") does not imply that the first cause is the more important one, or that the first entry refers to the first type. In some cases both causative factors affect both types. In these cases it was assumed that each cause contributed 50% to each soil degradation type.

Besides the various types of soil degradation, the GLASOD database also indicates a number of terrain categories that are not affected by degradation processes: three categories of stable terrain (e.g. stable under natural conditions) and six categories of wastelands (e.g. deserts or arid mountain regions). Wastelands are areas without any vegetative cover or agricultural potential. In the global dataset these types do not have an extent associated with them. It has to be assumed therefore that they occupy the total area of the map unit, except in those cases where type 2 indicates that soil degradation occurs within the map unit as well. In these latter cases, the stable or wasteland type covers the residual area after the area of soil degradation for the map unit has been calculated.

A third case to be considered is when the one or two types of soil degradation do not cover the entire terrain of the map unit. For example, if type 1 has an extent of 1 (2.5%) and type 2 has an extent of 2 (7.5%), 90% of the map unit is unaffected by soil degradation; the area is essentially identical to the stable terrain category.

4. THE GLASOD AFRICAN DATABASE

For the regional section of the atlas of thematic indicators of desertification, ISRIC assembled a more detailed coverage for the African continent at a scale of 1:6 million. The sources of the African dataset are essentially the same questionnaires (matrix tables) that were used to compile the global coverage. Yet, more detail was preserved by representing Africa with some 900 map units compared to the 400 map units in the global dataset. The conventions used to characterize soil degradation processes in the African dataset are essentially the same as for the global one, but with the following important differences.

Both the attribute data and the spatial resolution of the African dataset are more detailed with up to six different degradation processes registered for each polygon. Clearly, this has an implication for the derivation of summary statistics, since for example when calculating the total area affected by water erosion, all six types have to be examined whether they indicate this degradation process.

Each map unit is now completely defined, not only in terms of degradation processes but also with respect to the residual area comprising of stable terrain or wastelands. These latter two categories are included as types and - in contrast to the global dataset - have an extent associated with them. This is a great advantage in the analysis of the dataset. The problem that remains, however, is that in many cases taking the midpoint of the extent ranges leads to total areas greater than 100% of the area. Again, ISRIC was asked to provide guidelines by which for all possible combinations the actual percentages referring to a given extent are adjusted proportionally in such a way that the total always adds up to 100%.

An additional item that was not included in the global dataset is the *combi* variable, which indicates that two degradation types occur in combination *in the same part of the map unit.* The combi types must be considered when calculating areas of individual soil degradation types. The sum of the areas affected by the individual types can be larger than the total degraded area of the map unit, because parts of the map unit can be affected by more than one individual type of degradation. Care has to be taken for area calculations of the four major types (e.g. for wind erosion comprising of all three individual types of wind erosion). If a map unit is affected by both wind/overblowing and wind/loss of topsoil in combination, the area would be considered twice. For the atlas project therefore, only totals for the twelve individual types were calculated because these do not occur more than once for any map unit. If the type of soil degradation is not of interest in the calculation of areas, e.g. when compiling the areas affected by different degrees of degradation, the combi types are not considered since the corresponding area has already been included with one of the previous types.

The treatment of the cause variable in the African dataset facilitates the derivation of area statistics. Instead of only one combined cause as in the global coverage, in the African dataset two cause variables are entered for each type. The correspondence of type and cause is thus clearly defined. Yet, if two causes occur for one type, the problem of splitting up the area remains, and again equal weights have been given to both causes.

Figures 7 - 11 contain sample map output from the African GLASOD database which has been combined with the climate surface which will be described in part 4 of this report. Figure 7 shows the distribution of chemical deterioration processes in the Susceptible Drylands (arid, semi-arid and dry-subhumid areas) and outside these areas. Apart from an overview of the severity of chemical deterioration in Africa, the distribution of three individual types is shown as well. The most important causes of soil degradation in Africa are shown in Figure 8.

Note: A more technical documentation for the global and African GLASOD coverages, considering specific problems of GIS analysis using the Arc/Info system, is in preparation at GRID. This document will be distributed with the digital data sets.

5. REFERENCES

Oldeman, L.R., 1991, Global Assessment of Soil Degradation, Draft report for the UNEP State of the Environment Report, 1992. International Soil Reference and Information Centre, Wageningen, Holland.

Figure 7: Overview of chemical deterioration processes derived from the GLASOD African dataset

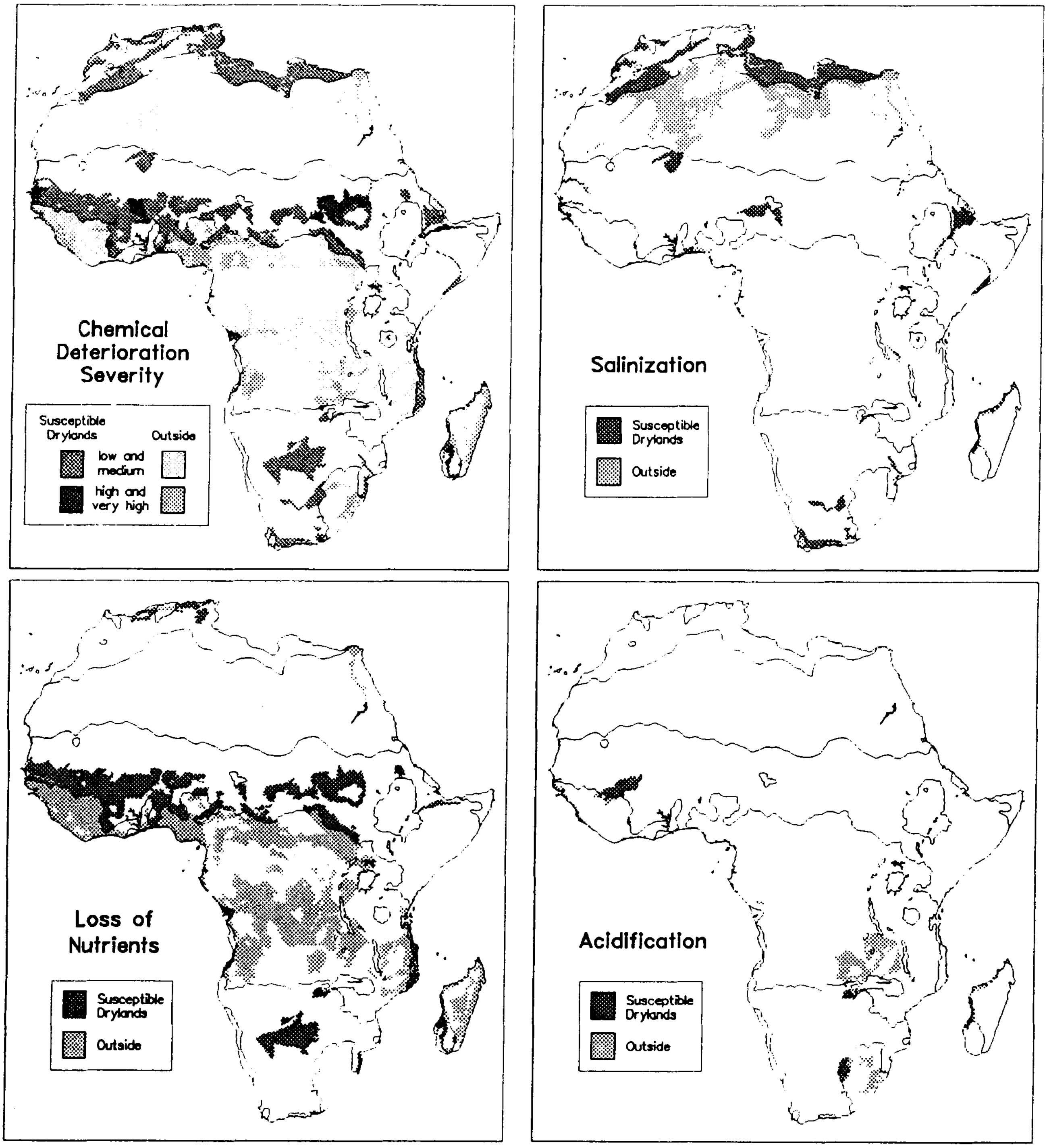

Source: UNEP/ISRIC, CRU/UEA

Approx. Equatorial Scale
1 : 90 million

Van der Grinten Projection

UNEP/GEMS/GRID

Figure 8: Soil degradation causes derived from the GLASOD African dataset

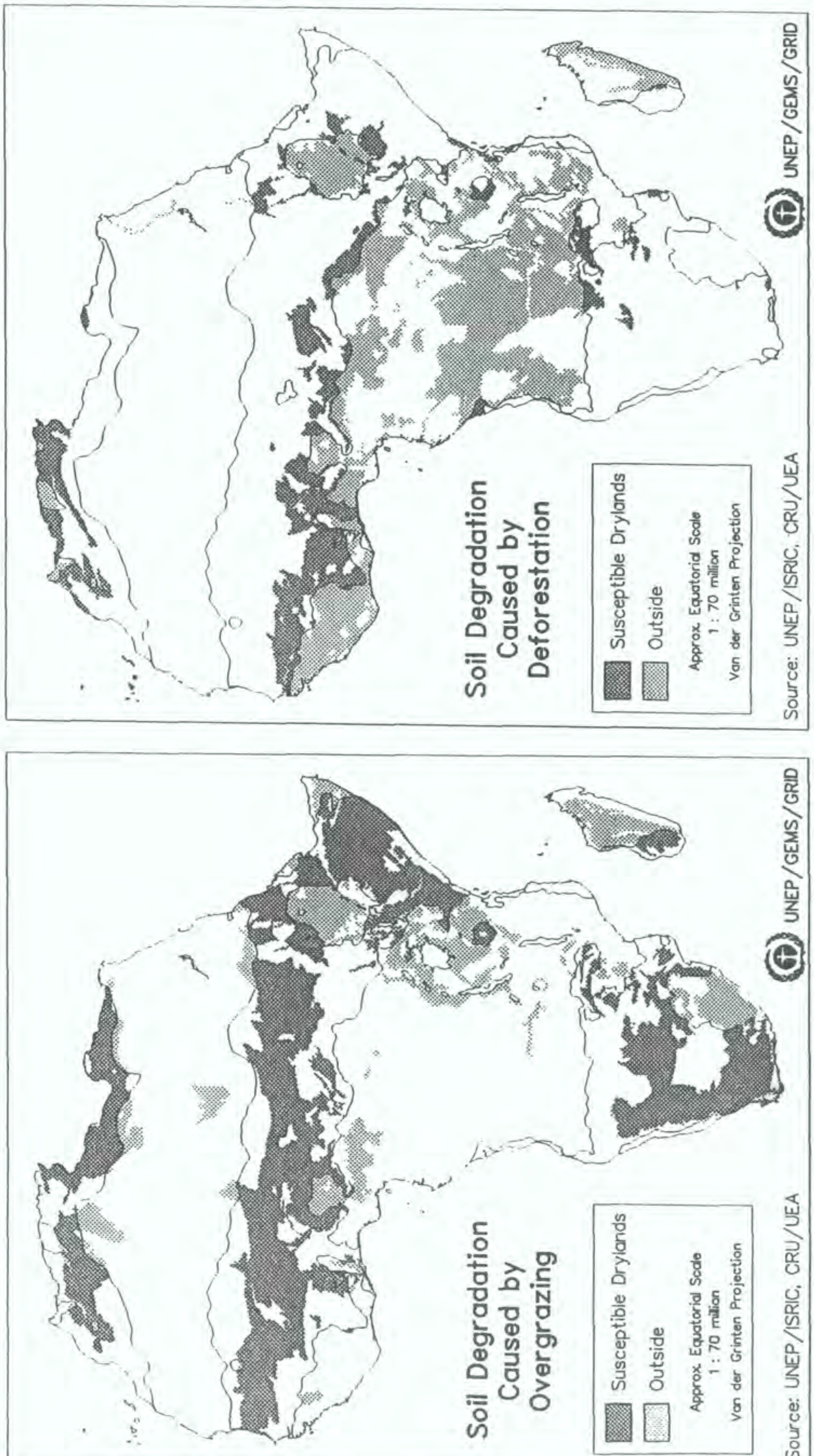

Figure 8 (continued): Soil degradation causes derived from the GLASOD African dataset

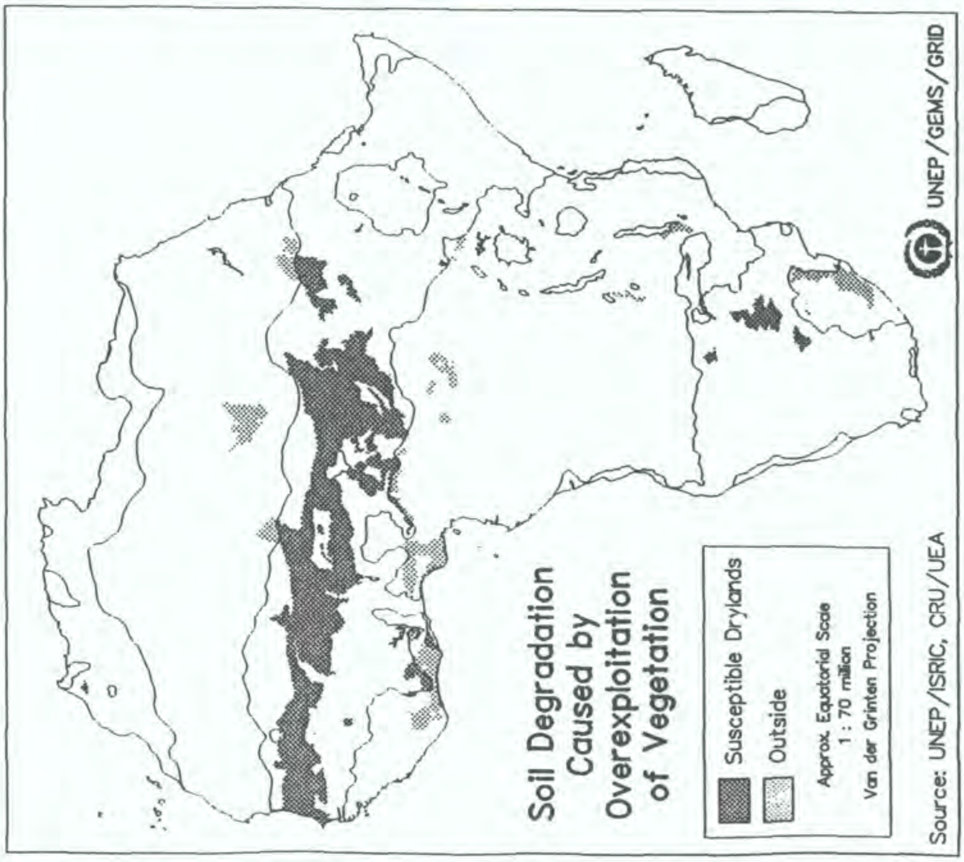

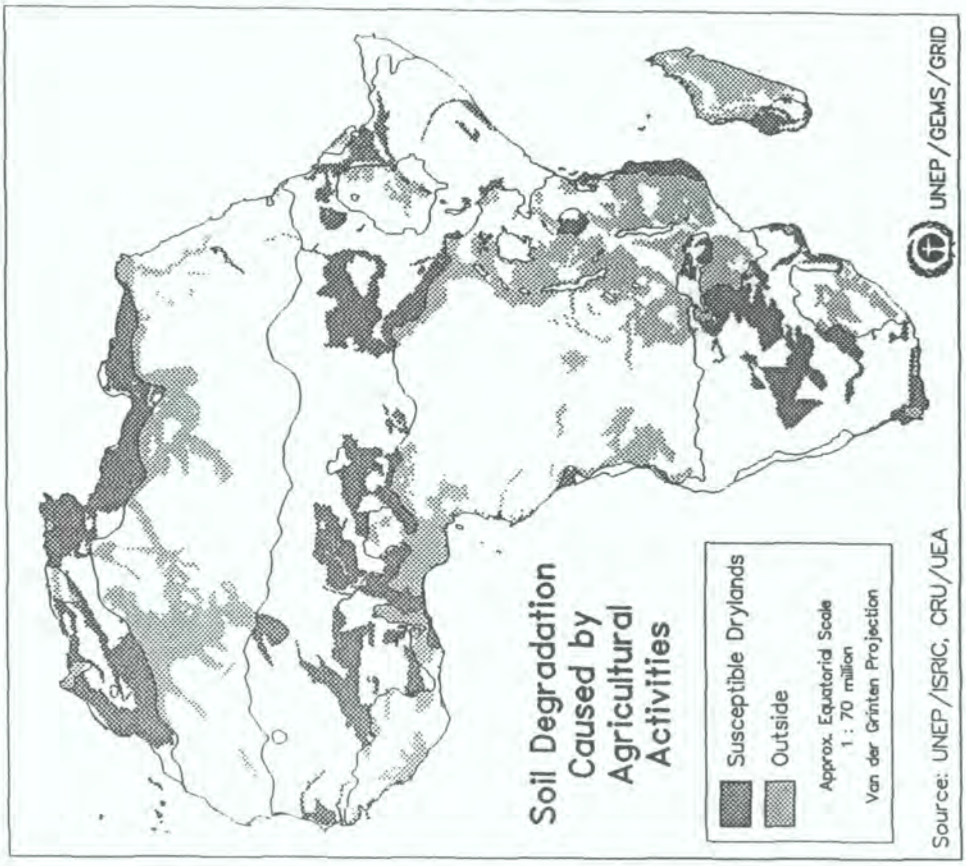

Part 4

THE PREPARATION OF CLIMATIC SURFACES

TABLE OF CONTENTS

1. INTRODUCTION

One of the critical datasets for the Global Assessment of Desertification and the production of a Thematic Atlas is a global climatic index. This index is used to delineate bioclimatic zones representing regimes of moisture availability. The base data for calculating the index was obtained from the Climatic Research Unit (CRU) of the University of East Anglia, UK. A description of the derivation of the raw data as well as a wealth of background information is provided in a number of reports by CRU and in communication (letters, faxes) between CRU and GEMS/GRID (see bibliography). The complete documentation is available at GEMS/GRID. The main focus of this report, therefore, is to describe the work by GRID analysts directed towards the production of global climatic surfaces from the base data.

2. CLIMATIC BASE DATA

The climatic humidity index used in this study is defined as the ratio of precipitation over potential evapotranspiration. The initial proposal by CRU was to provide GRID with climatologies on both precipitation and potential evapotranspiration on a grid with a resolution of 2.5 and 5 degrees respectably (approx. 275 and 550 km at the equator). These datasets are standard products used for CRU's global climate modeling (e.g. to derive climate change scenarios using general circulation models). In these applications, the relatively coarse resolution is used in order to increase the robustness of model results and to keep the computational requirements to a manageable level.

For the purpose of the desertification atlas project, however, different objectives influence the choice of the base data. The global climate surfaces are used for two purposes: for map presentation in the atlas, and for deriving statistics such as area estimates from overlay analysis. For both applications a much finer resolution is required than could be extracted from the coarse grid cell data. As became clear in the course of work, data for a dense network of meteorological stations was the most appropriate basis for the production of global climatic maps. These data can be interpolated on a fine raster by making use of detailed information about the station's location (e.g. latitude, longitude and altitude).

CRU provided station data on precipitation and temperature for two 30-year climatologies: 1930-59 and 1960-89 (CRU July 1990). Thus, a direct analysis of climatic change within the last 60 years could be attempted. In order to compare both derived maps, the interpolation must be based on the same station network. The CRU database contained 950 station values for precipitation and 581 for temperature. First experiments showed that these two networks did not contain enough stations to result in suitable climate surfaces. The resulting surfaces could not be regarded as stable enough to draw meaningful conclusions about climatic changes between the two time periods. Also, due to the interpolation error, area estimates derived from these maps would not be of sufficient accuracy.

After intensive discussions with CRU, the following decisions were made:

- GRID produces a high resolution global climate surface for only one time period for which a maximum of station means are available at CRU. This surface is used by GRID for overlays with other variables (e.g. degradation severity) in the global assessment and to produce map output for the Thematic Atlas of Desertification. With the choice of the time period 1951-80 two issues of prime concern were satisfactorily resolved: (1) The use of a "timeless dataset" is avoided; e.g., one in which all available station means are used regardless of the corresponding time period. An example for timeless datasets are the precipitation and temperature surfaces by Legates and Willmott (1989 and 1990). Although timeless datasets are usually based on a much larger number of stations, and therefore justify the derivation of spatially more detailed maps, their disadvantage is the lack of replicability and comparability in climate change studies (see CRU, July 1990 for a discussion of this issue). (2) More recent data is the basis of this analysis in comparison to most previous studies using the standard 1930-59 climatology. Since the climatic surface is to be combined mainly with the Global Assessment of Soil Degradation (GLASOD), which was compiled in the second half of the eighties, the use of the 1951-80 climatology is much more meaningful: The climatic processes of this period have influenced the results of soil degradation processes that we observe now.

The initial data set for 1951-80 contained 1834 station means for temperature and 2769 for precipitation (CRU, Sept. 1990). Still, a number of problem areas were identified in the precipitation maps in which the station coverage was not sufficient (temperature does not show the same degree of local variation; the interpolation of temperature data is therefore fairly robust). Originally, 568 additional precipitation means were provided by CRU which cover the 1956-75 period (CRU, 21.9.1990). This is only a 20-year period but centered within the complete period. 706 further station means were sent by CRU to take care of some remaining problems in low coverage areas such as the Western Sahara and South America (CRU 11.12.1990). For these means the criterion that a station must include data for 80% of all months in the time period was relaxed to 70%. From these 706 stations, 350 located in problem areas were included in the dataset. Nevertheless, a fourth iteration was necessary because a few key areas displayed a bias which could be traced back to a lack of stations. In these areas (Patagonia, Western Algeria and Southern Madagascar) a small number of additional stations were inserted for which data for 5 to 15 years within the time period was available (CRU 8.1.1991). Although from a strict climatological point of view, these short time periods are not regarded as representative, the stations indicate a trend which greatly improves the interpolation results. The final data set contained 3758 precipitation means. The global distribution of the precipitation and temperature stations is shown in Appendix I and II.

It was further agreed that the analysis of climatic change would be restricted to a much coarser spatial level. CRU provided GRID with 2.5 degree gridded data on precipitation and 5 degree on temperature for the 1930-59 and 1960-89 climatologies (CRU, August 1990). In addition, a global warming scenario for the year 2030 was prepared by CRU. Again, problems of insufficient global coverage of grid cells was encountered for precipitation, because CRU produces grid cell averages only for those cells for which station data is available. An improved coverage was achieved by the derivation of three new 2.5 degree grids by CRU: precipitation averages for a maximum coverage period, 1945-74, and two grids of percentage anomalies for 1930-59 and 1960-89 (CRU, Sept. 1990). The interpolated maximum coverage anomaly surface was used to derive precipitation grids for the two observation periods. A detailed discussion of the climate change analysis will be presented in a later report.

3. INTERPOLATION PROCEDURES

In order to prepare a global humidity index surface, global maps of mean annual precipitation and mean monthly temperature have to be derived. Mean monthly temperature is the basis of the estimation of potential evapotranspiration. A large number of methods for interpolating point (station) data on a continuous surface exist. Because the result of the interpolation will depend on the appropriateness of the method, the choice has to be made carefully. A few of the most common methods are therefore discussed briefly.

Continuous surface in the interpolation context means a fine raster or grid. For each grid cell, a value of the variable is estimated as a function of neighboring station values. The most complex of these methods incorporate some kind of information about the spatial autocorrelation into the estimation. Kriging which is based on the theory of regionalized variables, for example, divides the interpolation process into two steps: first, a semi-variogram is computed in which the average differences between the sample points is plotted against distance (see Huggett 1985, Davis 1973). Information about this optimal sampling distance is then used in the actual interpolation. Apart from the large computational requirements of kriging, the method is not appropriate when the station network is relatively scarce and the sampling of points irregular. For global applications, the method is therefore not necessarily the most suitable. Interpolation methods related to kriging are moving average techniques and trend surfaces. The latter is essentially a multiple regression approach where the locational parameters are used as independent variables.

Triangulated Irregular Networks (TIN) represent a surface as a set of triangles with the endpoints defined as x,y,z values of an irregular network of points (e.g. Arc/Info, see ESRI 1987). From a TIN, contours or interpolated grids can be derived by various methods. Previous experiments by GRID analysts with TINs showed some shortcomings of the method (see also Burroughs 1990). TIN requires a dense network of stations as input into the interpolation procedure. This is rarely available on a global scale. In some instances the resulting maps show unrealistic TIN-shaped patterns. A more appropriate use of TINs might be the interpolation of discontinuous, categorical data.

After evaluating various interpolation methods, it was decided to use the simplest and most robust technique available: distance weighted nearest neighbor interpolation. Hereby, for each grid cell, a value is computed as the average of k nearest station values weighted by a function of distance (usually inverse distance squared). Thus, closer stations have a relatively higher influence (determined by the distance exponent) on the value of the grid cell than stations further away. The number of nearest stations considered, k, usually ranges between 3 and 9. As in all interpolation techniques, the quality of the results depends crucially on the number of input stations and even more on the homogeneity of their distribution. Problems are mostly encountered with variables that show large local variability (like precipitation), or in areas of very rapid change (e.g. for climatic data the coastal deserts on the West Coast of South America and Southern Africa).

The initial global grid onto which the climate data was interpolated had the dimensions 360 rows by 720 columns, representing a 0.5 degree resolution. Despite the fact that a considerably smaller number of station means were available for temperature, the interpolation of this variable is more reliable than that for precipitation. This is due to the fact that temperature does not change as rapidly over space. Secondly, an auxiliary relationship can be utilized for temperature that explains a large part of the local variation: air temperature generally decreases with increasing altitude. The measure for this decrease is the geometric temperature gradient, usually expressed in degrees Celsius per 100m. However, the size of the temperature gradient varies as well temporally as spatially (Weischet 1983). Generally, the daily gradient is highest around noon and annually during Summer. In tropical areas temperature decreases faster with increasing altitude than in proximity of the poles. The upper limit of the gradient is 1 degree/100m (dry-adiabatic gradient). The most common values range from 0.5 to 0.8 degrees. Ideally the local temperature gradient would be calculated using two stations at different altitudes. This is a realistic approach for a small area. For global applications a mean value of 0.6 degrees is usually taken.

Before the temperature values were interpolated, all station means (T_{alt}) were standardized to a value representing sea-level temperatures (T_0):

$$T_0 = T_{alt} + (alt / 100 * 0.6)$$

where *alt* is the altitude in meters. After the estimate for the grid cell is found, the temperature is adjusted to the cell's altitude by subtracting a corresponding value. The altitude for each grid cell was derived from the global digital elevation model of the U.S. Navy (FNOC) which had been resampled from 5 minute to 0.5 degree resolution.

At the time when most of the work on the climate data was conducted, no suitable software package for interpolation was available at GRID. The "Surfer" package (Golden Software 1990), for example, could not be used because the size of the output raster is limited to 65535 cells. Arc/Info's TIN module was not used for reasons outlined above. For this project, an interpolation algorithm was written in the C language on an IBM/PS2. Interpolation is a computationally intensive process, because for each cell the *k* nearest stations have to be found from the full set of stations, in the case of precipitation more than 3600.

To decrease computing time the program uses a modified version of the algorithm outlined in Hodgson (1989). All stations are first sorted into a grid of much coarser resolution (e.g. 36 by 72). A look-up table containing all stations stores the identifier for the large grid-box it is located in as well as the variable value. For a given cell it is known which large grid-boxes surround it and therefore only the stations that fall within these grid-boxes have to be tested for inclusion into the set of *k*-nearest stations. After a number of experiments, a set of 4 nearest stations was used for the final interpolations. However, this rule was not strictly enforced if only 3 or less stations could be found within a specified threshold distance of 20 cell widths. This only occurred in areas of extremely low station density, such as Greenland or various mid-ocean islands. For example, in the precipitation interpolation, about 97% of all valid cells (those which are on land) were calculated with a full set of 4 nearest neighbors.

4. ESTIMATION OF POTENTIAL EVAPOTRANSPIRATION

Long time series data of direct measurements of potential evapotranspiration (PET), e.g. using evaporation pans, are rarely available for climate stations around the world. For the purposes of this study, PET therefore had to be estimated using data that is more readily accessible. The choice of the empirical Thornthwaite PET estimation method is again motivated by the lack of sufficient global data on variables that are necessary to apply estimation methods based on theoretical physical principles (e.g. Penman's formula). For a detailed discussion of this issue see CRU, August 1990.

The Thornthwaite formula requires only two variables for the estimation of mean annual PET: mean temperature for each month of the year and the average number of hours between sunrise and sunset for each month. Average temperature surfaces for each month were produced using the altitude adjusted interpolation outlined above. CRU provided a table of average daylength by month and latitude (in five degree steps). The details of the calculation of Thornthwaite PET estimates are described in the CRU report (ibid., pp.3-5). Using this description, the algorithm for PET calculation was coded into the C language. The results of the global PET estimation, however, did not match prior expectations. Visual inspection of maps of the humidity index, derived using the Thornthwaite PET estimates, showed that in critical areas (e.g. dry-subhumid, semi-arid, or arid regions) PET is generally underestimated. This systematic bias of the Thornthwaite formula for arid regions or seasons is generally known. The magnitude of the impact on the resulting humidity index, however, was not anticipated.

After this problem was identified, CRU estimated an empirical adjustment factor using detailed datasets for Europe and the Sudan. For both datasets Penman estimates of PET were available for the 1951-80 time-period. CRU calibrated a model with Penman PET being a function of Thornthwaite PET. As outlined in the relevant CRU report (October 1990), the error was significantly reduced by using precipitation as an additional explanatory variable. The form of the adjustment is:

$$PET_p = 1.3\ PET_t - 0.428\ PRECIP + 246$$

where PET_p = Penman PET
PET_t = Thornthwaite PET
PRECIP = mean annual precipitation in mm.

The empirical adjustment is greatest in dry regions where the underestimation of Thornthwaite's formula is highest. In humid areas, Thornthwaite and Penman estimates are generally comparable. The introduction of the adjustment factor into the existing program was straightforward using the recommendations given by CRU (ibid. p.5).

To sum up, GRID used the following procedure to derive a raster surface of PET: twelve maps of mean monthly temperature were produced using an altitude adjusted nearest neighbor interpolation of data from 1834 climate stations. These maps were then used as input into a program that calculates a mean annual PET surface using the Thornthwaite method which was adjusted to correspond to Penman PET.

5. CALCULATION OF HUMIDITY INDEX AND DEFINITION OF ARIDITY ZONES

Given global raster maps of mean annual precipitation (P) and PET with identical dimensions, the calculation of the humidity index as the ratio P/PET is straightforward. The classification of the humidity index follows largely the one used in the UNESCO study (1984, p.11, see Appendix III). Adjustments were made for the hyper-arid zone where the boundary was raised to 0.05 to compensate for the perceived underestimation of PET by the Thornthwaite method in this climatic regime. The four aridity zones and the humid zone are defined as follows:

Hyper-Arid Zone:			P/PET	<	0.05
Arid Zone:	0.05	<=	P/PET	<	0.20
Semi-Arid Zone:	0.20	<=	P/PET	<	0.50
Dry-SubHumid Zone:	0.50	<=	P/PET	<	0.65
Humid Zone	0.65	<=	P/PET		

A cold tundra and mountain climate zone, defined using a Koeppen-like climate criterion (Koeppen 1931), was introduced as a sixth zone. It includes those areas in which more than 6 months have an average temperature below 0, and not more than 3 months reach temperatures above 6 degrees (roughly comparable to Koeppen's E, Dc and Df zones). There are two reasons for introducing this additional zone. First, the objectives of the global assessment are focused upon the arid regions in tropical and subtropical areas. Arid mountain regions (e.g. in central Asia) and subarctic regions which can be defined as arid on a purely climatological basis (e.g. Siberia) pose a completely different set of problems not dealt with here. If these tundra and high mountain regions were included in the analysis of global desertification, then the resulting area estimates would be biased. Second, as mentioned in section 4, the adjustment of the Thornthwaite estimates of PET were tailored to a European and a Sudanese dataset covering the warm and hot regions; Thornthwaite himself estimated his formula using data for the USA. Work is currently undertaken at CRU to derive an adjustment factor for cold regions using a suitable dataset from Canada or the Soviet Union, but will not be completed in time for this study.

6. MAP PRODUCTION

Two related maps were derived from the humidity index surface: (1) a continuous raster map showing the large variations of the climate index within each climate zone, and (2) a classified vector coverage that shows the bioclimatic zones as defined above. The raster surface will be used in the regional section of the desertification atlas with the zone vectors overlaid. In addition, the vector boundary is used in combination with other coverages (e.g. GLASOD) to highlight land degradation processes in susceptible dryland areas (arid, semi-arid and dry-subhumid); see Figure 1. Also, statistics are derived from these overlays yielding area estimates of degradation in various aridity zones.

From the classified raster map, a vector coverage was produced using standard Arc/Info commands. In order to improve the appearance of the map, the resulting lines where repeatedly smoothed using the Arc/Info SPLINE command. The use of the resulting maps in the desertification atlas project, required that the latitude/longitude reference system had to be converted into the projections used for all maps: the equal area Mollweide projection for the derivation of statistics, and the Van der Grinten projection for display purposes. While the projection of the vector boundary coverage did not cause any problems using Arc/Info's PROJECT module, the projection change of raster images is not commonly available on standard software packages. The continuous humidity index raster map was therefore converted into the van der Grinten projection by using the Arc/Info compatible NPROJECT command. This module has been written by K. Kundert and utilizes Arc/Info functions.

7. COMPARISON TO UNESCO CLIMATE MAP

To conclude this report some differences of this climatic modeling effort to the one undertaken by UNESCO (1984) for the 1977 assessment of desertification should be mentioned. It will not be possible to avoid comparisons, and thus the major dissimilarities should be pointed out. The UNESCO map used the same ratio of P/PET, and also nearly identical boundary values for the various aridity zones. The climatic boundaries were drawn on the basis of data for 1600 climate stations. A map of the distribution of the stations was not provided. In comparison, GRID/CRU used 1834 for temperature and 3687 for precipitation.

For the calculation of PET, Unesco used Penman's formula employing a significant amount of information on climatic variables such as windspeed, actual vapor pressure, solar radiation etc. for each station. The UNESCO paper does not reveal any information about the time period of the source data. Neither the approximate period, nor the length of the time series for each station that entered the analysis are given. The map is most likely based on a timeless dataset which considers any station available that offers the variables needed regardless of the time frame. This is probably the most significant difference between the two climatic datasets.

A second major point that should be made concerns to the interpolation procedure. For the UNESCO map the climate index for all stations was calculated first; in a second stage, the index was interpolated. In contrast, the GRID/CRU procedure interpolates surfaces for precipitation and temperature first, then PET is estimated for the whole raster, and finally the index is calculated for each cell using the complete surfaces. This strategy is to be preferred because the spatial interpolation of the base variables is more stable than is the interpolation of a ratio. The actual method of interpolation used in the UNESCO study, however, remains unclear from the short explanatory note. It seems that the boundaries were drawn onto a map of the climate stations, and where information was scarce "great attention was given to field observations, using the expertise of specialists on different parts of the world." (UNESCO 1984, p.10). In other words, boundaries were moved where expert knowledge or information on soils, vegetation etc. suggested that the initial interpolation was biased. Both, the use of a timeless dataset to guarantee optimal coverage, and the use of expert knowledge to improve the

Figure 1: Global climate zones defined by the ratio of precipitation over potential evapotranspiration

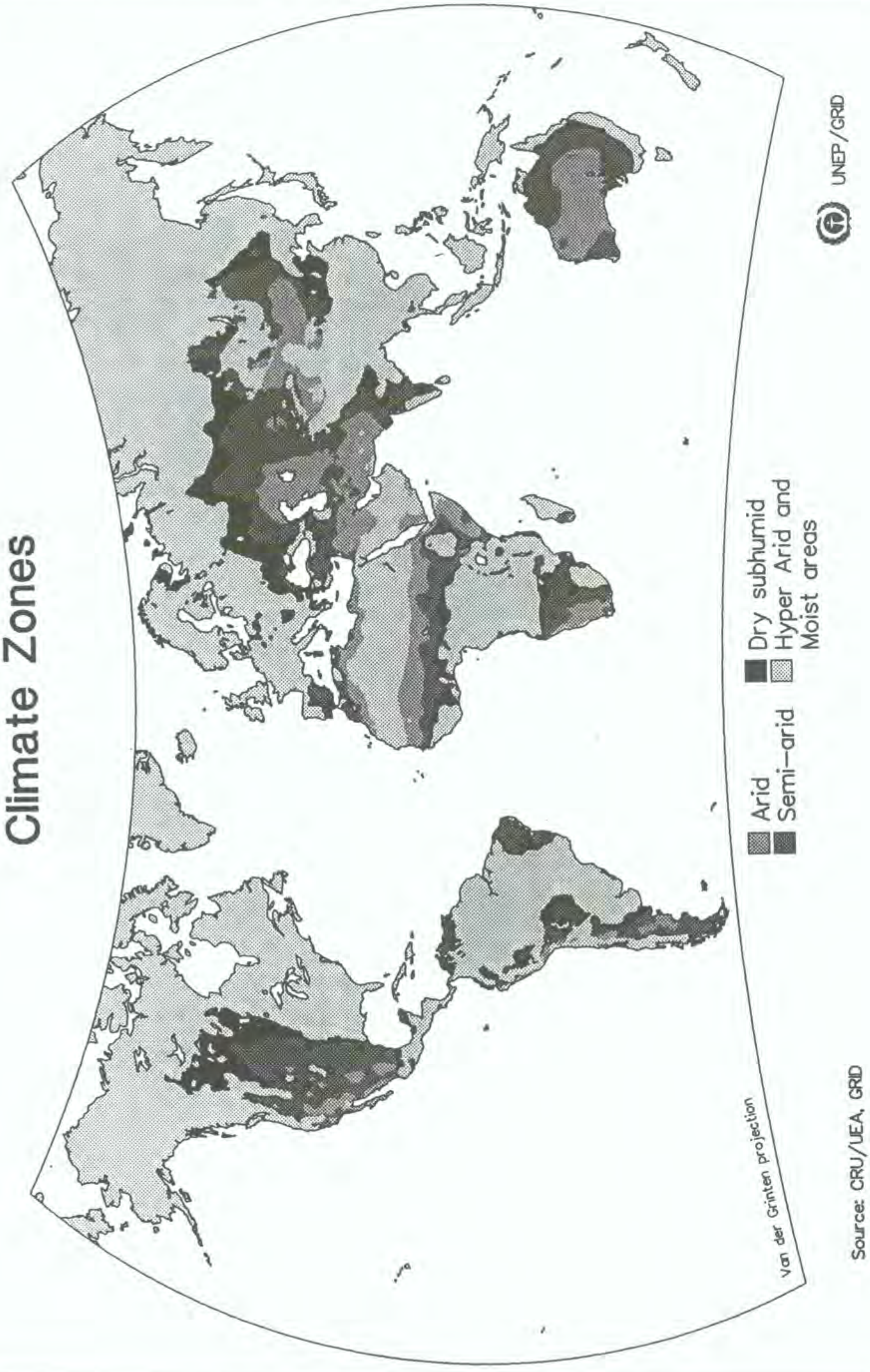

appearance of problem areas, are, of course, perfectly legitimate. However, and this is why GRID and CRU decided to follow a different path, the UNESCO procedure has one important disadvantage: the resulting map is a document that cannot be replicated or compared with any other modeling effort, neither contemporary, nor at any point in the future. While automated interpolation procedures can lead to problems in areas of low coverage (these could be adjusted in an *ad hoc* manner), the resulting maps are completely replicable. Furthermore, the surface produced by GRID/CRU represents the 1951-80 climatology. In a future study, for example highlighting the impacts of climate change, the map could therefore be compared with a newly produced time-dependent map that is based on the same methodology.

Finally, one practical issue should be mentioned. The projections used for the UNESCO map are the *Bipolar Oblique Conformal Projection* for the Americas and the *Miller Oblated Stereographic Projection* (MOS) for the rest of the World. According to UNESCO (1974, p.10) Miller's projection ".. represents surface areas adequately." This is in fact not the case, for MOS was not designed as an equal area projection, but as a reference system that displays the shape of the continents accurately. For purely cartographic purposes the projection is therefore highly suitable. Area statistics derived from the map sheets, however, are biased; for the African continent this bias can be as much as 9% for parts of South Africa and Madagascar. The change of a map coverage from the MOS projection into an equal area system such as *Mollweide*, on the other hand, is not a simple matter, because no standard geographic information system provides this particular option. The reason for this is that while an algorithm to transform latitude/longitude coordinates into MOS units exists (Sprinsky and Snyder 1986), the reverse operation is far more complex. In fact, the only procedure implemented at GRID is based on a rubber sheeting approximation which does not result in exact output coordinates rather than on an exact mathematical solution. It was therefore not feasible to use the UNESCO map in the current UNEP project, since one of the major objectives is to derive area statistics - this was not the case in the UNESCO project. Published area estimates of climate zones derived from the UNESCO mapsheets should thus be interpreted with care, if the exact methodology behind the area calculations is unknown.

The conclusion from this discussion is that the two climatic surfaces derived by UNESCO and GRID/CRU cannot be compared in any objective way. Differences might be due to one of a number of reasons, among others:

- The difference in the observation period. The UNESCO map is most likely based on older data, probably from the standard 1930-60 climatology. Differences in moisture availability between the two maps might therefore be due to actual climate change.
- The PET estimation method. Even though, the Thornthwaite estimates were adjusted to match Penman, the two measures might still diverge in some areas due to common statistical error.
- The station network. The number and distribution of stations has a clear impact on interpolation results.
- "Knowledge based" adjustments in the UNESCO map. These might reflect the expectations of the expert rather than actual data.

8. REFERENCES

Burrough, P.A. (1990), Optimale Methoden zur Interpolation von Umweltvariablen in Geographischen Informationssystemen, *Geographica Helvetica*, vol 45, no. 4, pp. 154-60.

ESRI (1987), Arc/Info Manual, Redlands.

Davis (1973), *Statistics and data analysis in Geology*, Wiley: New York.

Hodgson, M.E. (1989), Searching methods for rapid grid interpolation, *Professional Geographer*, 41(1), pp.51-61.

Huggett R.J. (1985), *Earth Surface Systems*, Springer: Berlin.

Koeppen, W. (1931), Das geographische System der Klimate. *Handbuch der Klimatologie*. Vol 1, Berlin.

Legates, D.R. and C.J. Willmott (forthcoming), Mean seasonal and spatial variability in global surface air temperature, *Theoretical and Applied Climatology*.

Legates, D.R. and C.J. Willmott (1990), Mean seasonal and spatial variability in gauge-corrected, global precipitation, *Int. Journal of Climatology*, 10, pp.111-127.

Golden Software (1990), Surfer Manual, Golden/Colorado.

UNESCO (1984), Map of the world distribution of arid regions. Explanatory note, Paris.

UNIRAS (1989), AGL Kriging. Krigpak User's Manual, UNIRAS A/S, Soborg, DK.

Weischet, W. (1983), *Einfuehrung in die Allgemeine Klimatologie*, Stuttgart: Teubner.

Reports

CRU (July 1990), Phase I: Global Temperature And Precipitation Climatologies for 1930-59 and 1960-89.

CRU (August 1990), Phase II: Global Humidity Index for 1930-59 and 1960-89, Draft Version.

CRU (September 1990), Additional Data for Phases I and II.

CRU (October 1990a), An Empirically Derived Adjustment Factor for Annual Thornthwaite PET Estimates Supplied Under Phase II.

CRU (October 1990b), Average Monthly Global Climate Scenarios (Surface Air Temperature And Precipitation) for The Year 2030.

Communication

CRU (10.9.1990), Fax containing FORTRAN routine for PET calculation.

CRU (21.9.1990), Fax containing information about additional station precipitation means.

CRU (11.12.1990), Letter accompanying diskette containing additional station precipitation means.

CRU (8.1.1991), Fax containing additional station precipitation means for Algeria, Madagascar and South America.

Appendix I: Distribution of stations with temperature means for 1951-80

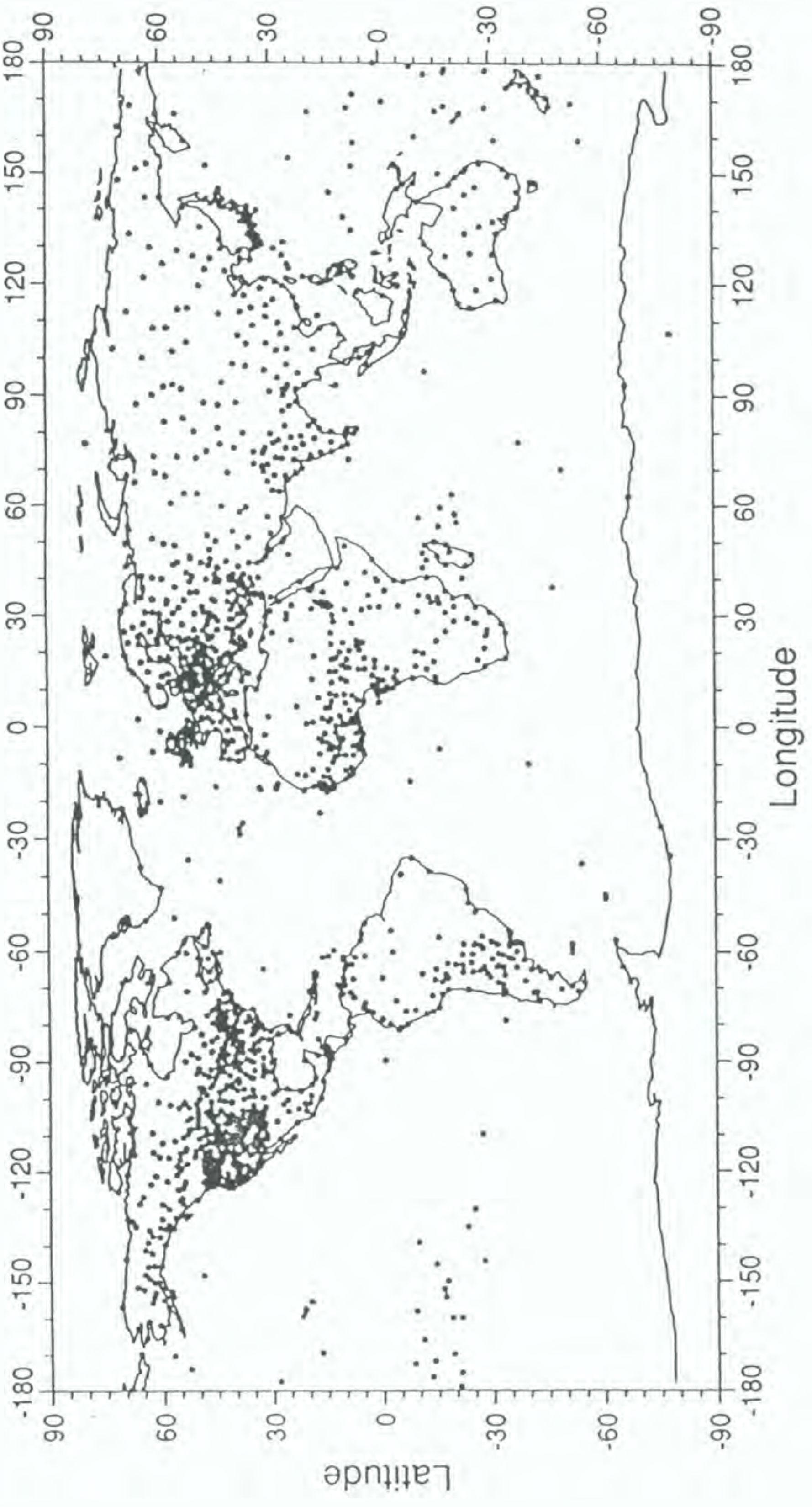

Appendix II: **Distribution of stations with precipitation means for 1951-80 (complete set)**

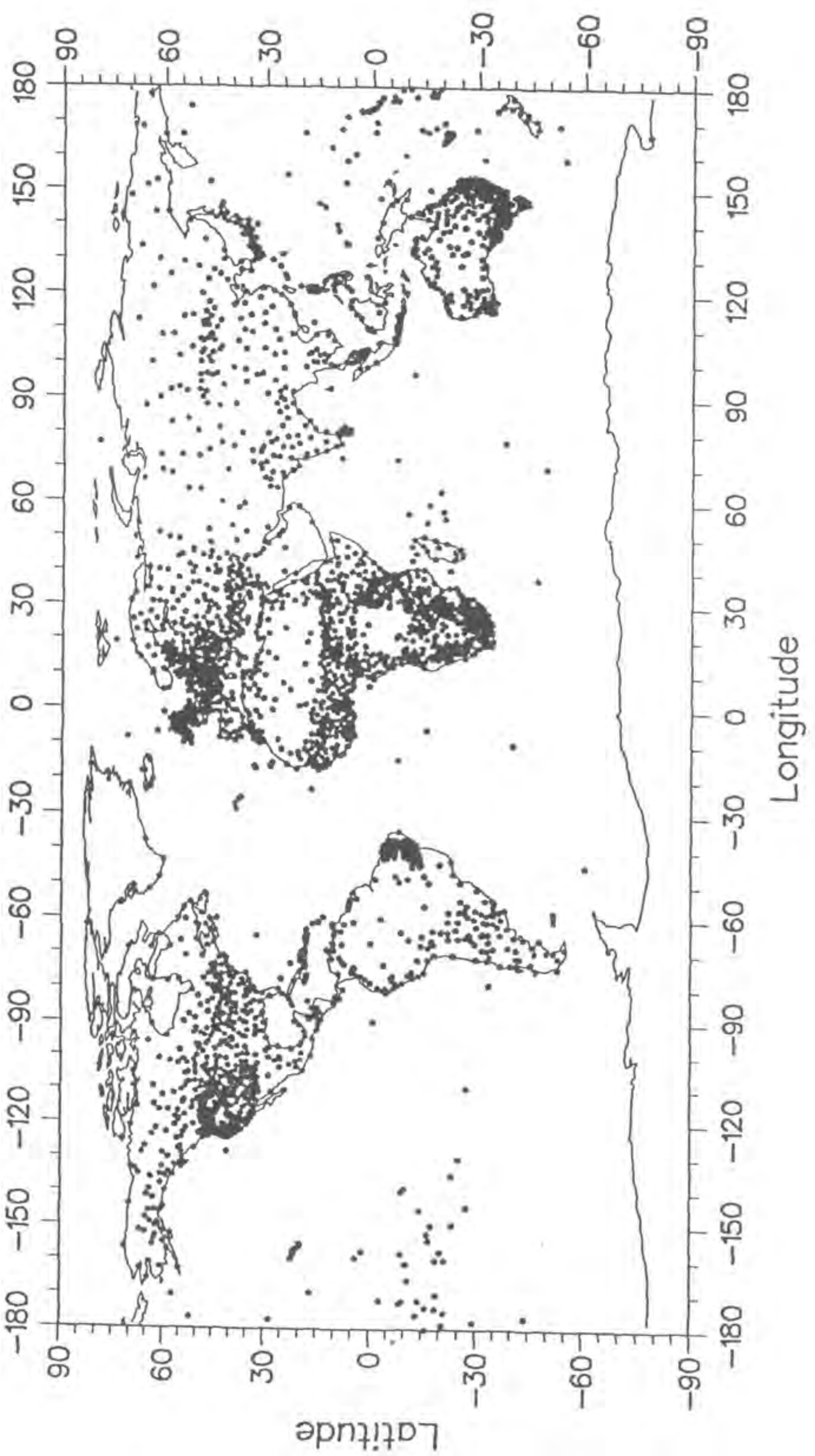

Appendix III: UNESCO description of aridity zones (from UNESCO 1984, p.10)

Four main classes or degrees of aridity have been delimited, corresponding to the major geographic categories generally used by climatologists and biologists.

The *hyper-arid zone* ($P/ETP < 0.03$) is shown on the map by single colours bordered by a continuous flagged black line. It corresponds to real desert climates, with very low and irregular rain which may fall in any season. These regions have almost no perennial vegetation, except some bushes in river beds; annual plants can grow in good years. Agriculture and grazing are generally impossible, except in cases. Interannual variability of rainfall can reach 100 per cent.

The *arid zone* ($0.03 < P/ETP < 0.20$) is shown on the map by single colours bordered by a continuous grey line. The vegetation of this zone is scattered, and includes, according to the region, bushes and small woody, succulent, thorny or leafless shrubs. Very light pastoral use is possible, but no rainfed agriculture. These regions are characterized by annual rainfall of 80-150 mm and 200-350 mm; interannual rainfall variability is 50 to 100 per cent.

The *semi-arid zone* ($0.20 < P/ETP < 0.50$) is shown on the map by colours streaked with white and bordered by a dashed grey line. This is a steppe zone, with some savannahs and tropical scrub. These are sometimes good grazing areas and rainfed agriculture is possible, although the harvest is often irregular due to great rainfall variability. Mean annual rainfall in this zone varies between 300-400 mm and 700 or even 800 mm in summer rainfall regimes, and between 200-250 and 450-500 mm in winter rainfall regimes, at Mediterranean and tropical latitudes. Interannual rainfall variability is between 25 and 50 per cent.

The *sub-humid zone* ($0.50 < P/ETP < 0.75$) is shown on the map by colours overlaid with white diamonds, not bordered towards wetter zones because the transitions are extremely variable. This zone includes mainly certain types of tropical savannah, maquis and chaparral in Mediterranean climates, steppes on chernozem soils, etc. Agriculture is the normal use. Interannual rainfall variability is less than 25 per cent.

Part 5

GLOBAL VEGETATION INDEX

TABLE OF CONTENTS

1. INTRODUCTION

Reliable data on vegetation was seen to be one of the key issues in the land degradation project. Vegetation is usually the most important factor determining the vulnerability of an area to water and wind erosion. Clearing vegetation may in extreme cases lead to irreparable destruction of the soil either as direct loss of the topsoil or through changes in the chemical and physical composition of the soil profiles. A major problem in this context is the lack of suitable vegetation data on a global level. The few existing global vegetation maps available are mostly too general both in terms of spatial coverage and in terms of contents, and are often outdated. Usually their emphasis is on potential vegetation rather than on the actual situation. Furthermore, the vegetation classes traditionally used may not be too well suited to land degradation studies, since the presence of a particular vegetation class may not necessarily tell very much about the soil protective capability of that class on a local level. For land degradation studies, the most important factors are those related to primary production such as canopy and field cover, production of leaf litter, resilience and resistance to grazing and other forms of vegetation utilization. Another factor of great importance is the natural fluctuation of the vegetative cover as a response to seasonal climatic variability and inter-annual changes in weather conditions.

Although satellite data can by no means provide information on all the factors mentioned above, there are still many advantages with a remote sensing approach, and for global or continental studies the use of satellite data may be the only feasible source of information. The scarcity of alternative vegetation data in conjunction with the increasing availability of global time series of satellite data have made the use of such data highly interesting for this study.

2. SATELLITE DATA FOR VEGETATION STUDIES

The early applications of satellite data for vegetation studies were based on data from the first land resources satellites, notably Landsat. The relatively high cost of these high-resolution data in conjunction with the low recurrence frequency of the satellites (one pass every 18 days for Landsat) have however made the data less suitable for dynamic studies of vegetation. The fact that every day roughly half the earths surface is hidden by clouds makes it difficult to obtain more than one cloud-free scene for a whole vegetation cycle for any particular area. During a period when the continuation of the Landsat programme was temporarily threatened the research on using data from other satellites was intensified (Murphy, 1986). The most interesting was data from the Advanced Very High Resolution Radiometer (AVHRR) on board the NOAA (National Oceanographic and Atmospheric Administration) series of polar-orbiting meteorological satellites. Although these data have a coarser resolution and the wavelength bands are less well suited for vegetation studies than those of the land resources satellites, the gains in the temporal domain, the vast area covered and the low cost of the data make the data superior for operational monitoring of vegetation changes on a regional and global scale.

The AVHRR sensor on board the satellite produces data in five wavelength bands, one visible, one near-infrared and three thermal bands. The nominal resolution of the data is 1.1 km, and two operational satellites each cover the same location on the earth every day. Vegetation absorbs light in the red wavelength band and reflects it in the near-infrared band which enables indices between the two bands that are sensitive to light reflected from vegetation to be formed. A widely used index is the Normalized Difference Vegetation Index (NDVI) which is the difference of infrared and red reflection over the sum of the infrared and red reflection. The Global Inventory Monitoring and Modelling Studies (GIMMS) group at NASA/Goddard Space Flight Center Research initiated their research on AVHRR data in 1982 and have produced numerous studies largely emphasizing the use of NDVI for arid and semi-arid areas (Justice, 1986).

The physical and biological functions behind the behaviour of vegetation reflection were examined by Sellers (1985), who found that the influence on the light reflected from vegetation is physically linked to the chlorophyll in the plants. Higher levels of radiation are linked to higher photosynthetic activity. It can thus be argued that the accumulation of vegetation will lead to increased integrated vegetation index values. As discussed by Ripple (1985), the relationship is however asymptotic, meaning that a point will be reached where the addition of more biomass ceases to cause a detectible change in reflectance. This means that NDVI can not be used to detect changes in biomass in areas with very dense vegetation. The relationships between the leaf properties such as chlorophyll, leaf structure, stomatal resistance and moisture availability, and radiation-interception of plant canopies were further discussed by Tucker and Sellers (1986). They emphasized the need for multitemporal measurements of radiation if estimation of primary production is to be attempted. Several publications (e.g. Hielkema et al., 1986; Henricksen & Durkin, 1986 and later Walsh, 1987; Hellden & Eklundh, 1988) discuss the prospects of using the data for monitoring of rainfall and drought. The latter study points out that the relationships between NOAA NDVI and precipitation data are weak outside the arid to semi-arid areas.

Although support for the general principle that long-term integrated images reflect the biomass can be found in several publications, substantial difficulties area encountered when attemting to calibrate the data to ground measurements. This was evaluated in a study by Prince (1986).

3. THE GVI PRODUCT FROM NOAA

The Global Vegetation Index (GVI) is a commercially available product delivered by the NOAA National Environmental Satellite Data and Information Service (NOAA/NESDIS). The NOAA AVHRR 1.1 km data is sampled and averaged on board the satellite to a nominal 4 km resolution and can be obtained in this format under the name of Global Average Cover (GAC) data. These data are further processed at NOAA/NESDIS to form a generalized dataset covering the whole globe on a weekly basis. The daily GAC data are mapped to a grid of 16 km resolution at the equator and a simple vegetation index (NIR-Red) is produced. The seven datafiles for one week are compared on a pixel by pixel basis and for each location only the pixel with the highest index value, the "greenest" pixel, retained, thereby excluding pixels influenced by cloud. For each of these remaining pixels a scaled Normalized Difference Vegetation Index (NDVI) is then calculated. The procedure has several important advantages in that it minimizes the influence of clouds, sun angle, water vapour, aerosols and directional surface reflectance (Holben, 1986), problems that are usually difficult to correct for in land remote sensing. The data are stored and distributed in the projections Polar-Stereographic, Mercator and Plate Carree (lat/long) and can be obtained in digital form or as hardcopies. A more detailed description of the routine data processing at NOAA/NESDIS can be found in Kidwell (1990).

4. DATA PROCESSING

The weekly GVI data are obtained in Plate Carre projection from NOAA and stored on a regular basis at GRID Geneva. There the weekly maximum value images for each month are composited into monthly maximum value images. For each pixel location only one value representing the whole month is retained. This means that the risk of cloud contamination and the negative atmospheric and sun angle effects are further reduced to a minimum. The long time series of monthly maximum value composites (April 1982 to December 1990) stored and constantly updated by GRID opens up great possibilities for time series studies of vegetation, which would previously hardly have been possible.

For the purpose of the land degradation database a different product was also required. The dynamic information in the time series data had to be simplified into a baseline dataset expressing the "normal" vegetation conditions of the globe. It was first assumed that this could be done by extracting the maximum values for all the months to obtain annual composites. Experiments however showed that the method tends to accumulate the noise present in the imagery. This is due to the fact that noise often occurs as very high values in the NDVI data, thereby always being selected and accumulated in the compositing process.

Another method was therefore applied which uses annual mean values instead of the annual maximum values. The 12 monthly composites for each year covering 1983 to 1990 were averaged to create eight annual mean value images which were then averaged in order to create a long term average image representing the whole period. This image was windowed to the area 180 W, 57 S to 180 E, 72 N, to fit the other datasets in the database. A water mask was applied to the data in order to avoid unwanted effects in the water parts of the image. This was done by rasterizing the global template from the Glasod dataset giving oceans and lakes a value of zero. Finally, this image was overlayed with the vegetation index image, and the data were contrast stretched between 1 and 255 for all the land pixels.

The resulting long-term mean value image gives a picture of the average vegetation conditions for the whole globe, integrated for all the growing seasons 1983 to 1990 (Figure 1). This image does not show vegetation classes as such, but rather the "greenness" or vitality of the vegetation averaged over the whole period. This means that quite different biomes can have very similar values, depending on similarities in average primary biomass production, and that one biome can contain areas of very different vegetation greenness, depending on local differences in biomass production. This kind of information is more relevant in a land degradation context than that obtained from a classification of vegetation types.

5. DATA PREPARATION FOR GIS ANALYSIS

The satellite data had first to be stratified or divided into discrete classes in order to combine the vegetation information with data of soil degradation. A histogram of the frequency distribution of digital NDVI levels was computed from the global dataset, and natural clusters were identified and used to form the basis for the stratification into ten discrete classes. A spatial mode value filter was used to decrease the influence of noise and to create more homogeneous classes the image was filtered using . The homogeneous classes could then be converted into vector format. The resulting jagged lines as obtained from the raster data, were smoothed using a mathematical spline function.

Figure 1: NOAA NDVI Composite 1983-1990 produced from weekly maximum value images

The classified GVI data, now in vector format, was then overlayed with the Glasod soil degradation dataset according to the methods outlined in part 2 of this report. The resulting polygon dataset now contains attributes from both two input datasets. This data could now be used to locate occurrences of both variables, such as areas of low NDVI/high soil degradation or high NDVI/low soil degradation, etc. A global map showing this has been produced and is reproduced in the UNEP Global Atlas of Desertification, to be presented in 1992.

Two datasets that emerged as interesting to analyze in conjunction with NOAA NDVI, were the Glasod African dataset (see part 3) and the Population dataset covering Africa (see part 6). These analyses however required a somewhat different approach. First of all a window covering Africa was extracted from the average 1983-1990 GVI image. Since the study was mostly concerned with the arid, semi-arid and dry subhumid areas rather than the moist or hyper-arid areas, these areas were masked out using the moisture availability dataset described in part 4. The resulting raster data were then transformed into a Mollweide projection using software developed at GRID Geneva. This was important in order to insure an equal area representation of the data. A frequency histogram was computed from these data, now only covering the susceptible drylands, and with each pixel representing a constant size on the earths surface. The histogram was stratified into ten equally sized percentiles and the raster image classified accordingly. The classified data was then converted into vector format. The vector data could at this stage be overlayed with the population and soil degradation and any other relevant datasets, and tabular statistics calculated.

6. RESULTS AND DISCUSSION

Although the preparation of the Global Vegetation Index dataset has opened up a lot of interesting possibilities for analysis, only a very preliminary look at the data has so far been attempted. Mostly this was done for data validation purposes. The dynamic information in the time series of the GVI data has at this stage not been studied at all. The few results that are presented here are by no means complete, and should be seen only as the starting point for more detailed GIS studies.

The diagram in Figure 2 shows the relative distribution of each of the four major types of degradation for the GVI zones in the susceptible drylands of Africa. Wind erosion shows a strong increase going from the high to the low GVI areas, with a sharp dip towards the end. This reflects the fact that wind erosion is less active in the well vegetated areas and increases as the vegetation cover diminishes. The dip towards the end of the diagram is caused by the fact that large parts of the dryland areas have been classified as "non reclaimable wastelands" or "stable areas" in the Glasod dataset, the areas thus containing only a very small proportion of the total degradation.

Water erosion is more evenly distributed across the GVI zones, with an increase towards areas with less vegetation. Here the dip at the end of the diagram is also evident, and the same explanation to this applies as for wind erosion. As discussed earlier the relationship between time series of NDVI data and meteorological data has been quite firmly established (e.g. Walsh, 1987), particularly in the arid to semi-arid areas (Hellden and Eklundh, 1988). The vegetated areas thus presumably receives more rainfall, which could cause a lot of erosion. Despite this, the larger proportion of the water erosion occurs in the less vegetated areas. Although it rains less in these areas, the rains are often highly erosive, and the ground not well protected by vegetation. This leads to very strong runoff and erosion caused by rainsplash and vice.

Looking at the total amount of soil degradation in the high vegetation areas, water erosion however still represents the largest part.

Chemical and physical degradation follow each other quite well with a slow decline towards the low vegetation areas. Chemical degradation is often more related to intense utilization of the land that occur in the higher rainfall areas, with the exception of salinization, which can occur on very dry lands, and here probably makes up the largest part of the chemical degradation in the low vegetation areas. Physical degradation occurs under most climatic conditions, although many of the processes are more related to the higher rainfall areas, e.g. waterlogging, aridification and subsidence of organic soils. An investigation of the relationship between specific types of soil degradation and vegetation index could provide more insights into this issue.

The diagram in Figure 3 cannot be explained that easily. It basically tells that the largest part of the light and moderate degrees of degradation occurs in the lowest vegetation areas, whereas the strong and extreme degradation is largely found in medium vegetated areas. Attempts to explain this in more detail will have to be based on a closer analysis of the distribution of degree of degradation by GVI class for each of the specific degradation types.

Figure 4 shows the distribution of population by GVI class in the susceptible drylands of Africa. This data was derived by combining the GVI data with a map of estimated population distribution (see part 6 of this report). As expected, the less vegetated susceptible dryland areas support a lower proportion of the population.

The easy access and availability to GVI/NDVI data means that a number of possibilities for vegetation studies have opened up. The area of investigating time series information was mentioned before as a field which this project has not yet been able to touch. The identification of areas where the annual values deviate from the average situation, and comparing these areas to soil degradation data from the Glasod database is a self-evident field of research.

Although the number of possible applications is substantial, various limitations with the data should be realized. The sampling of data on board the satellite and the subsequent mapping of the digital values onto a geographical grid involve steps where the information is being degraded. Another important source of errors is the lack of calibration of the GVI product. The AVHRR sensor does not produce a signal that is always constant over time, or constant between the different satellites. Dust, water vapour and aerosols also affect the detection of the reflected light. Fortunately, research in this field is quite active, not the least at the NASA/Goddard Space Flight Center, where calibration schemes for the satellite data are being developed. Two recent studies in this field are published by Holben et al. (1990) and Kaufman and Holben (1990). Recently NOAA/NESDIS has started to distribute a Calibrated Vegetation Index (CVI), which is likely to substitute the uncalibrated GVI product.

Figure 2: Degradation type by vegetation index in the susceptible drylands of Africa

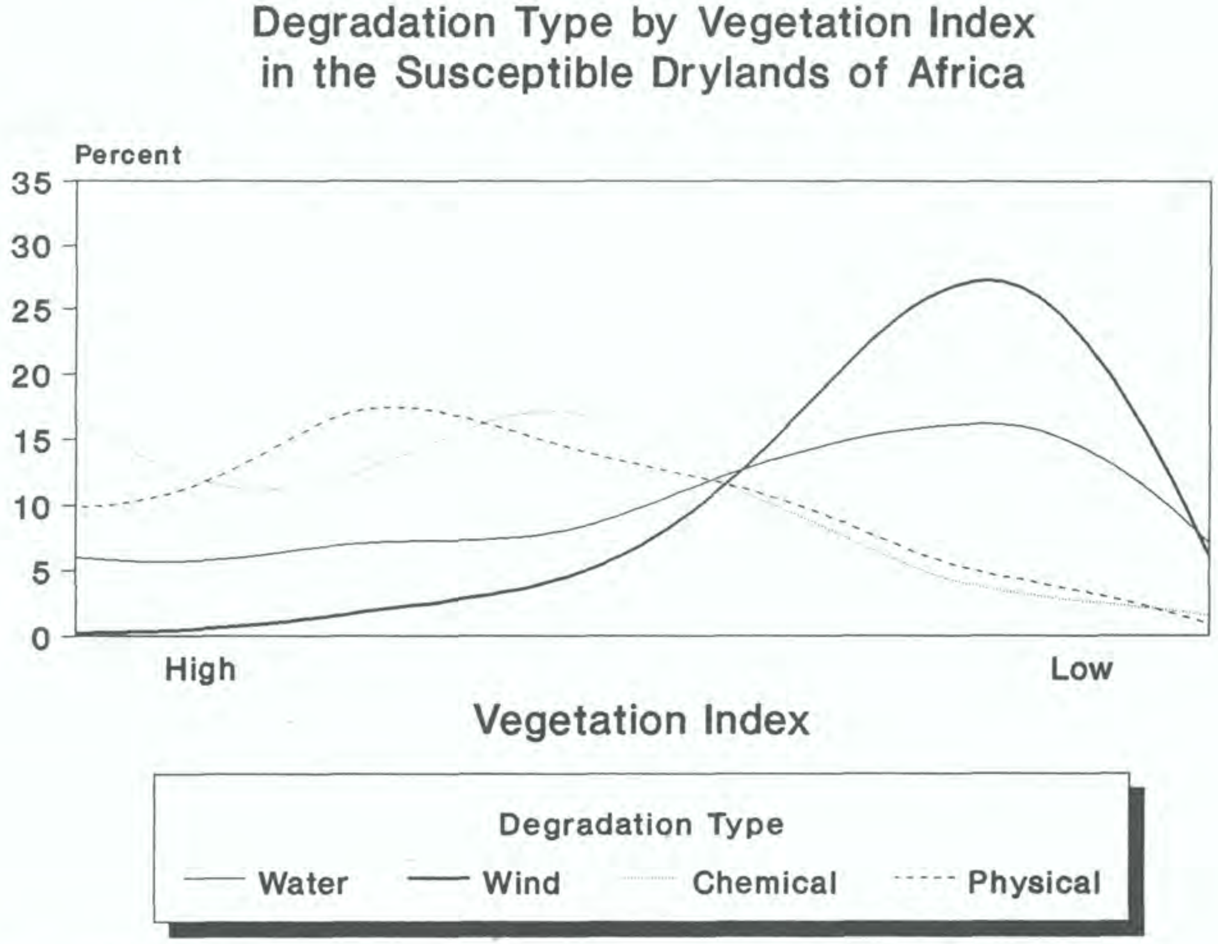

Source: UNEP/ISRIC, NOAA

Figure 3: Degradation degree by vegetation index in the susceptible drylands of Africa

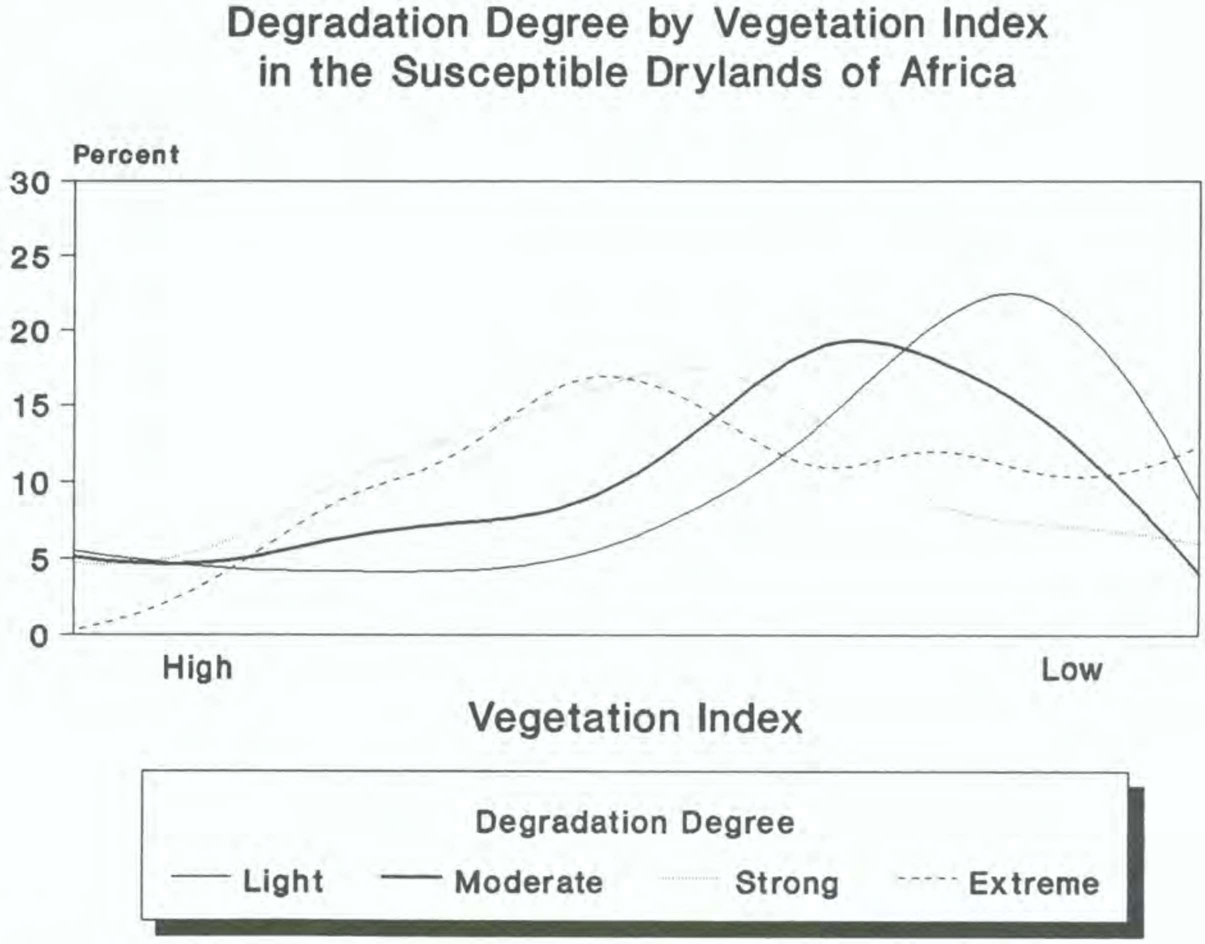

Source: UNEP/ISRIC, NOAA, CRU/UEA

Figure 4: Population by GVI class in the susceptible drylands of Africa

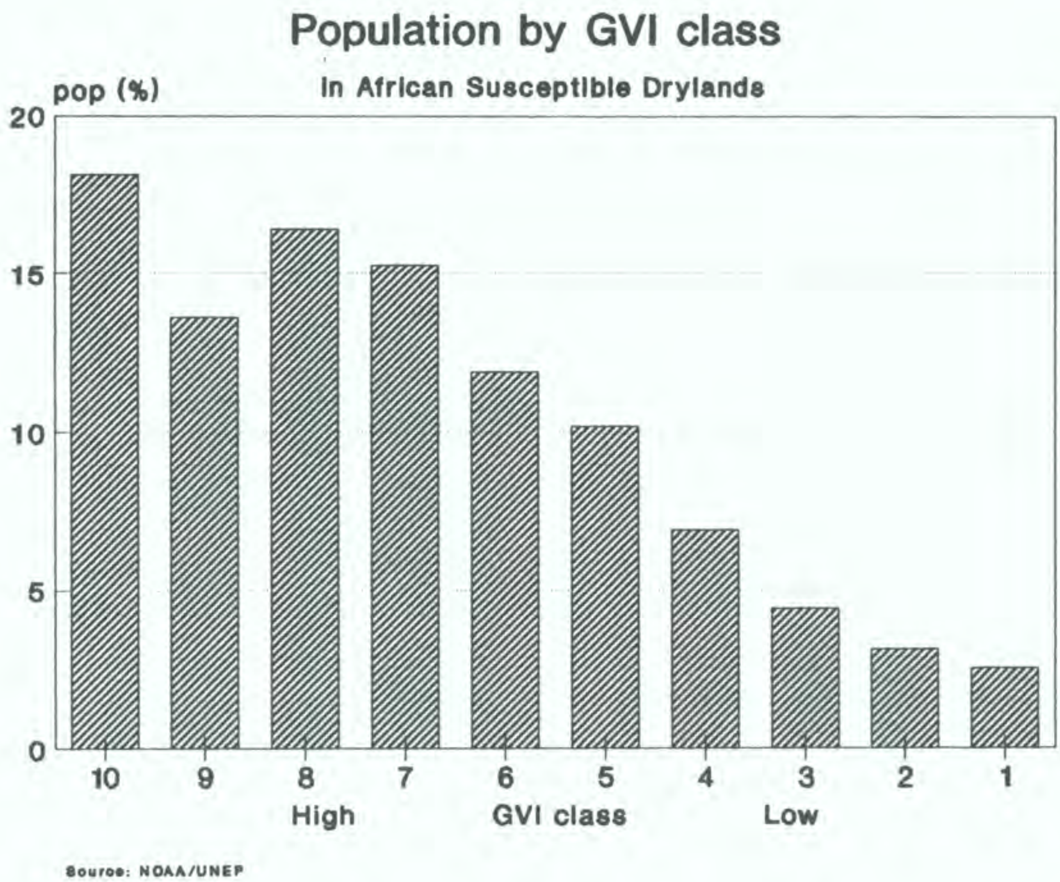

7. REFERENCES

Hellden, U., Eklundh, L.,1988, National Drought Impact Monitoring -A NOAA NDVI and precipitation data study of Ethiopia. *Lund Studies in Geography*, Ser C. No. 15, 55 p.

Henricksen, B.L., Durkin, J.W.,1986, Growing period and drought early warning in Africa using satellite data. *Int. J. Remote Sensing*, Vol 7, No. 11, 1583.

Holben, B.N, 1986, Characteristics of maximum-value composite images from temporal AVHRR data. *Int. J. Remote Sensing*, Vol 7, No. 11, 1417.

Holben, B.N., Kaufman, Y.J., Kendall, J.D., 1990, NOAA-11 AVHRR Visible and Near-IR Inflight Calibration. *Int. J. Remote Sensing*, 1990, Vol 11, No 8, 1511.

Jensen, J.R., 1986: *Introductory Digital Image Processing. A Remote Sensing Perspective.* Prentice-Hall, New Jersey, 379 p.

Justice, C.O., 1986, Monitoring of Grasslands of Semi-arid Africa using NOAA AVHRR Data, *Int. J. Remote Sensing*, Vol 7, No. 11, 1385.

Kaufman, Y.J., Holben, B.N., 1990, Calibration of the AVHRR visible and near-IR bands by atmospheric scattering, ocean glint and desert reflection. *Journal of Applied Meteorology* (Submitted).

Kidwell, K.B., 1990, Global Vegetation Index User's Guide. U.S. Department of Commerce NOAA/NESDIS, Washington D.C.

Lillesand, T.M., Kiefer, R.W, 1979, *Remote Sensing and Image Interpretation*. John Wiley & Sons, 612 p.

Murphy, R.E.,1986, Monitoring of Grasslands of Semi-arid Africa using NOAA AVHRR Data, *Int. J. Remote Sensing*, Vol 7, No. 11, 1391.

Prince, S.W., 1986, Monitoring the Vegetation of Semi-arid Tropical Rangelands with the NOAA-7 Advanced Very High Resolution Radiometer. In *Remote Sensing and Tropical Land Management*, ed. M.J. Eden and J.T. Parry. John Wiley & Sons.

Ripple, W.J.,1985, Asymptotic Reflectance Characteristics of Grass Vegetation. *Photogrammetric Eng. and Remote Sensing*, Vol 51, No. 12, 1915.

Sellers, P.J., 1985, Canopy reflectance, photosynthesis and transpiration. *Int. J. Remote Sensing*, No. 7, 1335.

Tucker, C.J., Sellers, P.J., 1986, Satellite remote sensing of primary production. *Int. J. Remote Sensing*, Vol. 7, No. 11, 1395.

Walsh, S.J., 1987, Comparison of NOAA AVHRR Data to Meteorological Drought Indices. *Photogrammetric Eng. and Remote Sensing*, Vol. 53, No. 8, 1069.

Part 6

ESTIMATED POPULATION DENSITIES FOR AFRICA

TABLE OF CONTENTS

1. INTRODUCTION

Population pressure is a key variable in understanding many human induced environmental degradation processes. Yet, population pressure is an extremely complex concept that touches upon a variety of socio-economic issues such as land use, farming practices, livestock characteristics and land tenure. Data on these factors are difficult to obtain, especially because they show large regional variations even on the subnational level due to characteristics of the land, customs or institutional frameworks. As an approximation to population pressure it was decided to include a map of population densities for the African continent into the regional study of the desertification atlas. This map was constructed on the basis of available data at GRID Nairobi. The methods used to estimate population denities are presented in the following sections.

To clarify the terms used some remarks about the difference between population distribution and population density are necessary (see Bähr 1983). Both terms are closely related, yet not identical. Population distribution indicates the nature of dispersion or concentration of population in a given region; the distance between individuals or groups of people is hereby the major concern. A distribution can be characterized as regular, dispersed, centralized or decentralized. Population distribution is often displayed cartographically using a dot map in which each dot represents an equivalent number of people. Population density on the other hand relates to the ratio of population and a given spatial unit (e.g. inhabitants per km^2). In the approach described in the following sections, the total population of a given country is *distributed* over the total area of the country according to certain criteria. The resulting number of people for each constant spatial unit are then converted into population densities.

Data on rural population densities by country from 1960 to 1985 as well as projections to future years (until 2030) are available from the U.N. Statistical Office in New York. The documentation of the U.N. data did not contain information on the definition of rural population, which generally varies from country to country. For the African countries, this U.N. data are held by GRID as an Arc/Info coverage of country boundaries with the densities stored in the attribute table. For a detailed study that aims at highlighting the links between population density and land degradation, country data is of a much too coarse resolution for it conceals large variations of population densities within a country; the best example being Egypt. GRID analysts improved the data by subtracting wilderness areas in which the population density can be assumed less than one per km^2. This data on the extent of remaining wilderness areas has been estimated by the U.S. Sierra Club (McClosky and Spalding 1989). Yet, the resulting maps were still regarded as unsuitable for the purposes of this study. Therefore it was decided to devise an alternative scheme of estimating population densities on a finer resolution.

2. METHODOLOGY

The methodology chosen is based on relationships between population density and various other variables (see Harrison and Boyce 1972). Information on these variables can be used to derive estimates of population density. The most important regularity of the distribution of population is the fact that it is concentrated rather than dispersed. This can be expressed using the concept of the interaction potential of population which is described in section 2.1. Another regularity is that people tend to live close to man-made or natural features such as roads or rivers. Section 2.2. describes how data on these features can be utilized to improve estimates of population densities. The estimation of population density depends critically on the size of the areas for which control totals of population are available. The collection of these data is discussed in section 2.3. followed by the description of the calculation of the population densities in section 2.4.

2.1. Interaction Potential of Population

Concept

Maybe the most significant among the regularities of population distribution is the fact that people tend to live close together, implying certain concentration effects of population distribution. This means that close to major cities or in proximity to a number of towns or cities, the population density can be assumed higher than in an area distant from urban centres. One way of expressing this in cartographic form would be concentric rings around towns, or the use of Thiessen polygons that delineate the "sphere of influence" of each town (U.S. EPA 1990). Within these a suitable function could show the decrease of densities with increasing distance. The problem with this method is obvious: A large city surrounded by small towns would obtain a smaller Thiessen area than would be justified. A more promising approach is to consider not only the closest urban centre but a number of near cities, or all cities within the region under study (see e.g. Bähr 1983). The basis of this approach is the concept of social gravitation, borrowed from the physical gravity laws. These concepts have been used widely in spatial interaction modeling (Fotheringham and O'Kelly 1989). Urban centres are regarded as physical masses, where the magnitude of attraction or interaction between these towns is proportional to their size (e.g. population) and inversely proportional to some form of spatial friction between them (usually geographic distance, although other measures such as transport costs might often be more meaningful). For a given town (point) *i* the interaction potential of population, V_i, with all other towns in a given region is therefore:

$$V_i = \sum_{j=1}^{n} POP_j / d_{ij}^{\,b}$$

where POP_j is the population of town *j*, and d_{ij} is the distance between towns *i* and *j*. The exponent *b* is a distance weight that determines the structure of the distance decay. Besides estimating the interaction between towns, the approach can also be used to calculate the population potential for any point in the region by using a regular grid draped over the region and calculating the interaction potential with all towns in the region,*V*, for each grid cell. With the choice of the distance parameter *b* knowledge about transport technology and infrastructure, or on assumptions about the homogeneity of population distribution, can be introduced. A larger exponent (e.g. 2 - as in the classical Newtonian gravity formulation) reflects an accelerated decay of population potential with increasing distance from urban centres. A smaller exponent (e.g. 0.5) assumes a more gradual decay.

The interaction potential of population is often simply called *population potential* in the literature. This term, however, has also been used in a number of studies to express the number of people that can be supported by the land. From the previous discussion the difference of these measures to the interaction potential of population should be clear. The latter is simply a measure of the theoretical concentration of people in a given region based on information about urban centers.

Data

The basis for the calculation of the interaction potential of population is data on the size and location of major cities and towns by country. Two datasets were obtained for this purpose:

(a) Birbeck College African Cities. This dataset was commissioned by GRID and assembled at the Department of Geography at Birbeck College (UK) as an ARC/INFO point coverage containing 479 cities for the African continent. The data source given is the Demographic Yearbook published by the U.N. for the years 1973, 1976, 1978, 1979 and 1981 (Table 11: Latest available population estimates of capital cities and towns of 20,000 and more inhabitants since 1970). A similar coverage of global cities with more than 100,000 inhabitants is available in the same format.
The number of cities included for each country varies drastically: while Algeria with 64 cities and towns is very well covered, the inclusion of only 3 for Kenya is clearly unsatisfactory. Similarly the census years of the population figures vary between 1970 for Ghana, and some towns in Madagascar, Senegal and Zaire, and 1985 for a number of towns in South Africa. Minor inconsistencies in the original dataset had to be corrected.

(b) PC Globe digital dataset. PC Globe is an interactive database for Personal Computers containing country based data on a large number of variables (Comwell Systems 1989). For each country, PC Globe provides information on the major cities and towns, their population and exact location (lat/long). For the 51 African countries a total of 363 cities is available. The number of towns included varies between 3 and 12 depending on the size of the country. PC Globe does not provide specific data sources. All numbers refer to the year 1988 but it can be assumed that due to the lack of recent census data, most population figures are projections or estimates.

Both datasets have advantages and disadvantages: The Birbeck dataset provides a wealth of information for a number of countries. Yet, the data is sometimes 20 years old, and for some countries the number of towns included is far from satisfactory. PC Globe on the other hand provides estimates rather than data, and for some countries the number of towns included is far smaller than in the Birbeck data. The datasets were therefore merged in order to maximize the number of cities using the following conventions.

The base data was taken from PC Globe. This was done for two reasons: for 34 countries this dataset contained more cities than Birbeck, and population figures are provided for a much more recent date. The fact that the numbers are mostly estimates is acknowledged. Yet, for the purposes of deriving population densities, estimates are sufficiently exact approximation. The relative magnitudes rather than the precise city sizes are important in computing the population potential.

For 17 countries, the Birbeck data provided a number of additional cities. These are mainly large countries with large total populations (e.g. Algeria, Egypt, Nigeria, South Africa).

In order to bring the whole dataset to match a common base year, the additional Birbeck city populations had to be projected to the year 1988. Two approaches are possible for this purpose: (a) a ratio approach, where the ratio of the country population for 1988 (available from various publications) and the census year country population is employed. Assuming a homogeneous population growth throughout the country this ratio can be used to adjust the individual city populations; (b) an approach based on the country's population growth rate. These growth rates are provided for each country in *World Population Prospects 1988* (U.N. Statistical Office 1989) and in PC Globe. Here a spatially homogeneous population growth is assumed as well. Given the growth rate *r* by country, the target year city population *POP88* can be estimated by

$$\text{POP88} = \text{POP}_{cy} * (1 + r / 100)^{(1988 - cy)}$$

where *cy* is the census year (e.g. 1975) and POP_{cy} is the city population of the census year as provided by Birbeck College.

The second estimation approach was chosen for this study, even though it has a slight disadvantage because growth rates change over time. If the growth rate in a country has increased in recent years, the use of the latest available growth rate will lead to an overestimation of the target year population. Experiments using total country populations for 1975 and 1988, however, showed that this overestimation is generally negligible in the African context and the bias is therefore small. A second reason for using the growth rate approach is ease of computation. While for the ratio approach total country populations for a large number of years have to be used, the computation of target year population given base year data and growth rates is straightforward, even if a number of different census years for cities in a given country occur.

The merged dataset contains 600 cities and towns for the African continent, their exact location in latitude and longitude and their estimated 1988 populations. The table in Appendix I shows the number of cities and towns that were available for each country.

Computation

The interaction potential of population in Africa has been calculated for each cell in a regularly spaced latitude/longitude raster of 960 rows and 1080 columns. The origin (southwest corner) is located at 30 degrees West and 40 degrees South. The raster has a five minute resolution corresponding to about 10km at the equator. A corresponding raster indicating the country into which each cell falls has been derived from the World Database II country boundaries coverage.

The interaction potential of population for all cells in a country has been calculated considering all towns available for that country that fall within a specified threshold distance. A different approach would be to use a specified number of near towns irrespective of the country, since sometimes major cities of different countries are close together (e.g. Kinshasa and Brazzaville). This would, however, assume that the borders between the countries do not represent barriers to interaction; e.g. the flow of people or goods. In the African context this is clearly not the case.

Ideally, the distance exponent *b* should be estimated from a sample of observed data (e.g. for a number of representative countries). Such data, however, were not available, and the distance exponent thus had to be chosen intuitively. Often, inverse distance squared is used in interaction modeling implying a relatively rapid decrease of population potential with increasing distance. This is a reasonable assumption for developed countries where the degree of urbanisation is high (72% for Europe in 1975 according to Bähr, 1983), while rural population (e.g. agricultural labor) is relatively small. For Africa a smaller exponent of 1.5, was seen as more suitable. This acknowledges the fact that large parts of the population are living in rural areas due to labor intensive agricultural practices; the share of urban population in Africa is estimated as 28% in 1975 (ibid.). The large urbanisation tendencies in developing nations due to rural-urban migration are mainly concentrated on the largest cities.

Two more conventions have been used in computing the population potential for each grid cell. The first refers to the impact of megacities (e.g. Cairo, Kinshasa, Lagos). While their attraction is certainly considerable, the use of their actual population (e.g. Cairo's 11 million) would exaggerate the influence of the city and dominate the impact of other towns in the country. It can be reasonably argued that there is a certain threshold where a marginal increase in population does not lead to a comparable increase in attraction. A ceiling of 750,000 inhabitants was therefore introduced as the maximum population for a city.

A second, related aspect is the question of how much a city "influences itself" (more exactly: the grid cell into which it falls, or the immediate neighboring cells); this is reflected in the choice of d_{ii}. For large scale applications a d_{ii} which is larger than one is used which reflects the size of the spatial unit under consideration. Since a larger city can easily cover several cells (e.g. tens of km), a minimum distance of 5 cells was used in this study.

The result of these computations is a raster map for Africa that containes in each cell a theoretical measure of average accessibility or interaction potential. The interaction potential itself does not indicate how many people are living in a particular area. Yet, it can be used as a relative measure of the share of the total regional or national population that is living in a particular cell. Before the estimated number of people living in each cell are calculated, the interaction potentials in the raster were improved by means of auxilliary relationships.

2.2. Adjustment of the Interaction Potential of Population

Concept

Noin (1979, as described in Bähr 1983) has compiled a series of maps for Zambia which show the interdependencies between population distribution and various natural, socio-economic and historical factors (see also Schulz 1976). It is shown that half the Zambian population lives in a narrow corridor along the railway line between Zimbabwe and the copper belt close to the border with Zaire. This phenomenon is closely related to the development of a market oriented agriculture by European settlers along the newly built railroad during the colonization period, and to the location of important mineral resources. This development was the fundament of the current disparities, which have not been reduced since independence. Similar relationships can be found in a number of African countries. The role that the railway line plays in Zambia is assumed by major rivers or lakes in other countries (e.g. the Nile in Egypt, the Zaire river, or Lake Victoria). In addition, since roads are built to connect population centres, it can be assumed that population density is correlated with the proximity to major roads.

In comparison to transport infrastructure - manmade or natural -, the relationship between the distribution of settlements and physical factors is less well defined. The correspondence between average annual rainfall and population distribution is fairly low in Zambia and Tanzania, where regional factors modify and complicate the relationships considerably. The usefulness of employing climatic factors to distinguish regional differences in moderate climatic regimes is therefore limited. The relationship to climatic conditions is much clearer when regions unsuitable for human habitation are considered. Hyperarid areas where potential evapotranspiration far exceeds precipitation are generally not populated (with the exception of oases such as the Nile valley).

A further feature of human population distribution is that on a global scale population density usually increases with proximity to the coast. In 1950, half the world's population lived less than 200 km, 28% less than 50 km from a coast (Bähr 1983). Yet, there exist large variations as well in terms of latitude, as in the distribution on the East and West side of the continents. While the correspondence between human settlements and proximity to the coastline is clearly present in Northern Africa (e.g. Libya), it is much less so in, for example, large parts of Somalia, Namibia or Madagascar.

A number of conclusions can be drawn from the previous discussion. Regularities of the distribution of human population exist on a continental as well as on a regional, national or subnational scale. For physical and topographic factors, a relationship with certain climatic conditions, and the proximity to coastlines, lakes and major rivers can be established. On the socio-economic side, the proximity to manmade infrastructure (rail and road) shows a generally positive correlation with population density.

These relationships, however, are not clearly defined. Variations can be due to a number of reasons ranging from latitude and the resulting climatic conditions to specific historical developments. From this follows that the influence these factors have on regional or national population distribution has to be determined for each region or country individually: while proximity to a river (Nile) explains a large percentage of the population distribution in Egypt, the same parameter has very little value in Somalia or Ethiopia.

The relationships are generally not quantifiable due to the lack of suitable datasets that could be used for model calibration. The variables therefore have to be used in a heuristic process, based on rules of thumb rather than on clearly defined relationships. While this approach could be regarded as somewhat arbitrary, it effectively imitates the process by which a cartographer uses his knowledge and experience in drawing contour lines of population densities on a map. In comparison to a "handdrawn map", the computer based approach has the advantage of perfect replicability.

Data

Two datasets held by GRID show areas that are largely uninhabited: the Sierra Club wilderness areas (McClosky and Spalding 1989) and the Protected Areas in the Afrotropical Realm (MacKinnon and MacKinnon 1986, Burril 1990). The wilderness areas coverage indicates regions of at least 4000 km^2 showing no signs of human habitation or intervention. Most of the wilderness areas in Africa are found in either arid and hyper-arid regions or in the dense tropical forests of West and Equatorial Africa. The protected areas coverage is the result of an inventory of national parks and reserves in Africa.

GRID also holds an extensive African database contains coverages of railroads, major (paved) and secondary (motorable) roads, and major hydrology (lakes and rivers). This database was commissioned jointly by UNEP and FAO (ESRI 1984). Proximity to the coast was derived from a coverage of continental boundaries in this database.

Each of the vector coverages listed above was transformed into a raster compatible with the one used for the interaction potential of population. For the coverages taken from the UNEP/FAO dataset, a buffer was constructed around each feature in these coverages, so that areas up to 3-6 cells (30 to 60 km, depending on the importance of the variable) distant from the coverage feature were considered in the adjustment.

Computation

The first step in the adjustment of the interaction potential of population was to subtract the uninhabited areas, which are indicated by the wilderness and protected areas maps, by reducing the interaction potential drastically. This results in estimated population densities for these areas of less than one per km^2 which allows for the possibility that many of these areas are indeed used by pastoralists and nomads.

In a second step, the interaction potential of population for a given raster cell was increased using a specified weight if it fell within the buffer around the features in the coverages described above. However, as discussed before, the influence of the same variable on population distribution is not the same for all regions or countries. The proximity to a major river in Egypt therefore resulted in a larger upward adjustment of the interaction potential than the same factor in Ethiopia, where river valleys often possess characteristics that constrain habitation (Ethiopian Mapping Authority 1988). Thus, a different set of adjustment weights was used for each African country;

As was mentioned before, the choice of the adjustment weights had to be based on an iterative heuristic approach. Using a number of available cartographic sources (such as the Times Atlas of the World, national atlases and maps etc.), the impact of the weights was estimated and an initial adjustment chosen. After running the model, the resulting population density map was evaluated and the adjustment weights modified in cases where the result did not match auxilliary data sources. This was repeated until a satisfactory result was obtained.

2.3. Control Totals for the Distribution of Population

In the introduction to section 2 it was mentioned that the quality of the population density estimation will depend largely on the size of the areas for which control totals of population are available. These totals are distributed over the cells in each area according to the shares or weights that are derived from the adjusted interaction potential. An effort was therefore made to obtain population statistics on the smallest available spatial level. One of the coverages in the UNEP/FAO African database is a map of administrative districts for all African countries except Madagascar. Population figures and the corresponding census year are included in the attribute information. The level of detail varies from country to country. In some countries only the second level divisions are included while for others third level divisions are displayed as well.

While the topology (e.g. the boundaries) of this coverage is very detailed, the quality of the attribute data is poor. For many countries no information is recorded at all, for example for Burkina Faso, Burundi, Madagascar, Namibia, Somalia, and Western Sahara. For others the data is based on very old census data. The coverage therefore required a considerable amount of work before it was possible to use it for the estimation of population densities in Africa.

Additional and more recent data for administrative districts for a large number of countries was obtained from *Africa South of the Sahara - 1991* (Europa Publ. 1990) and *The Middle East and North Africa - 1990* (Europa Publ. 1989). These publications were also used to correct some errors in the original administrative boundaries cover. In Angola, for example, the Lunda and the Luanda regions were mixed up. Nairobi district had been given the population of Pokot district.

The complete set of data assembled for this study contains 599 administrative districts for Africa. The table included in Appendix I shows the number of administrative districts for each country. The number of administrative units in relation to the size of the country provides an indication of the reliability of the density estimates derived. The best cover was obtained for Algeria, Egypt, Kenya, Mali, Morocco, Niger, and Zambia.

The data on administrative districts had to be adjusted to account for different census years. Rather than projecting the population for each district to the year 1988, it was assumed that the spatial distribution of a country's population had not changed since the last census year; or, in other words, that each administrative district contained the same share of the total country population in the last census year as it did in the year 1988. Thus, the share of the district's population in the last census year was calculated, and this share was then multiplied by the total country population for 1988. In comparison to the use of projected district populations, this approach has the advantage that the total country population could be taken from the same source (PC Globe, which was verified using the estimates published by the U.N. Statistical Office, 1989). As was the case for the projection of city data the assumption of stable proportions is more valid for districts for which more recent census data is available. The table in Appendix I shows that very recent data was available for Angola, Mozambique, Rwanda, South Africa, and Zaire. The result of this data collection is a table of 599 population estimates for administrative districts in Africa. In addition, the vector coverage of administrative districts was rasterized so that for each cell in the raster the corresponding administrative district can be identified.

2.4. Calculation of Population Densities

For the estimation of population densities the values of the interaction potential of population were standardized by dividing the interaction potential of each cell by the sum of the interaction potentials of all cells within the corresponding administrative district. So, the resulting weights or shares for the cells within each administrative district sum up to one. These shares were subsequently multiplied by the number of people living in the corresponding administrative district. While computationally intensive, this step is conceptually straightforward.

The resulting raster of the number of people living within each grid cell was converted into population densities by dividing the number of people by the area of the cell. All computations up to this point were made on a raster that was referenced using geographic coordinates (latitute and longitude). This is not an equal area reference system, which means that the area of grid cells further away from the equator is exaggerated. To adjust for these distortions, the exact area of each grid cell was computed as a function of latitude (see Appendix II).

The result of this exercise is a raster map in geographic coordinates that shows the exact population density for each grid cell. This raster map can be brought directly into another projection, or it can be classified, vectorized and used in combination with other datasets. An example of a classified, vectorized map of estimated population densities for Africa is shown in Figure 1. Combining the raster of the number of people living in each cell with the climatic zones (see Part 4) gives estimates of the number of people living within each climate zone in Africa (Figure 2). The results, however, should be interpreted within the limits of the rather broad scope of analysis, since even within each climatic zone a variety of living conditions due to local factors exist. Figure 3 shows the result of combining population densities with the African GLASOD dataset (see Part 3) for the susceptible drylands of Africa. For each population density class the distribution of the degraded area by degree is displayed.

3. DISCUSSION

The most critical issue in all modeling efforts is the verification of the results. Verification, however, requires some form of truth to which the result can be compared. For the map of African population densities the only available information are a number of national maps of population densities by administrative units. Problems remain however, since these maps are based on the latest available census year. As an example, the National Atlas for Ethiopia (Ethiopian Mapping Authority 1988) contains maps on population distribution as well as on population densities, the latter on the level of third level administrative units. Visual comparison shows that the general features are replicated well in the more detailed map of estimated population densities for Africa. Furthermore, the patterns of distribution of population as displayed in the Ethiopian Atlas are very similar to those in the modeled map. Comparisons with maps from other countries have been made. Visual comparisons were satisfactory but, of course, quantitative measures of fit are not available.

Certainly there are a number of restrictions on the use of this dataset. While a five minute (approx. 10km) resolution is sufficient for most analysis on a continental or regional level, the dataset is not suitable for application to national or subnational studies. For such studies higher resolution data should be employed. It is thus recommended to use the dataset only for large scale analysis, at least involving a number of countries (such as the Sahel region, or sub-saharan Africa).

Climatic and vegetation factors have not been used in the estimation of the population densities, although the explanatory power of these variables could be expected large. Yet, it was anticipated that the population densities will be used in analysis in combination with similar physical factors, e.g. assessing the relationship of population pressure and soil or vegetation degradation in dryland areas. The use of climatic or vegetation (index) data would have imposed a structure on the dataset that would result in an artificial fit in the results of any such analysis.

Potentials for improving the estimates of population densities in Africa exist. As described earlier, data by administrative districts were not available for some countries, for others the data were of poor quality or quite old. The same holds true for the cities dataset. The acquisition of additional subnational data could significantly improve the quality of the population density estimates

Another aspect where improvements are possible is the technique chosen to bring all data to the same temporal basis. The forecasting methods employed in this study are robust but not ideal. The use of cohort survival methods, in which age specific fertility and mortality rates are considered explicitely, is probably not possible for subnational spatial units in Africa due to lack of data on age and sex structure. Nevertheless, the collection of additional data should enable the use of more exact forecasting and estimation techniques, and thus to improve of estimates of up to date city and region populations.

Additional data could also help to estimate rural and urban population densities separately. For many applications the interest is only in rural areas. Yet, the cities and towns dataset is not sufficiently detailed to subtract all urban population from the total population before distributing the remaining population.

Figure 1: Estimated African population densities

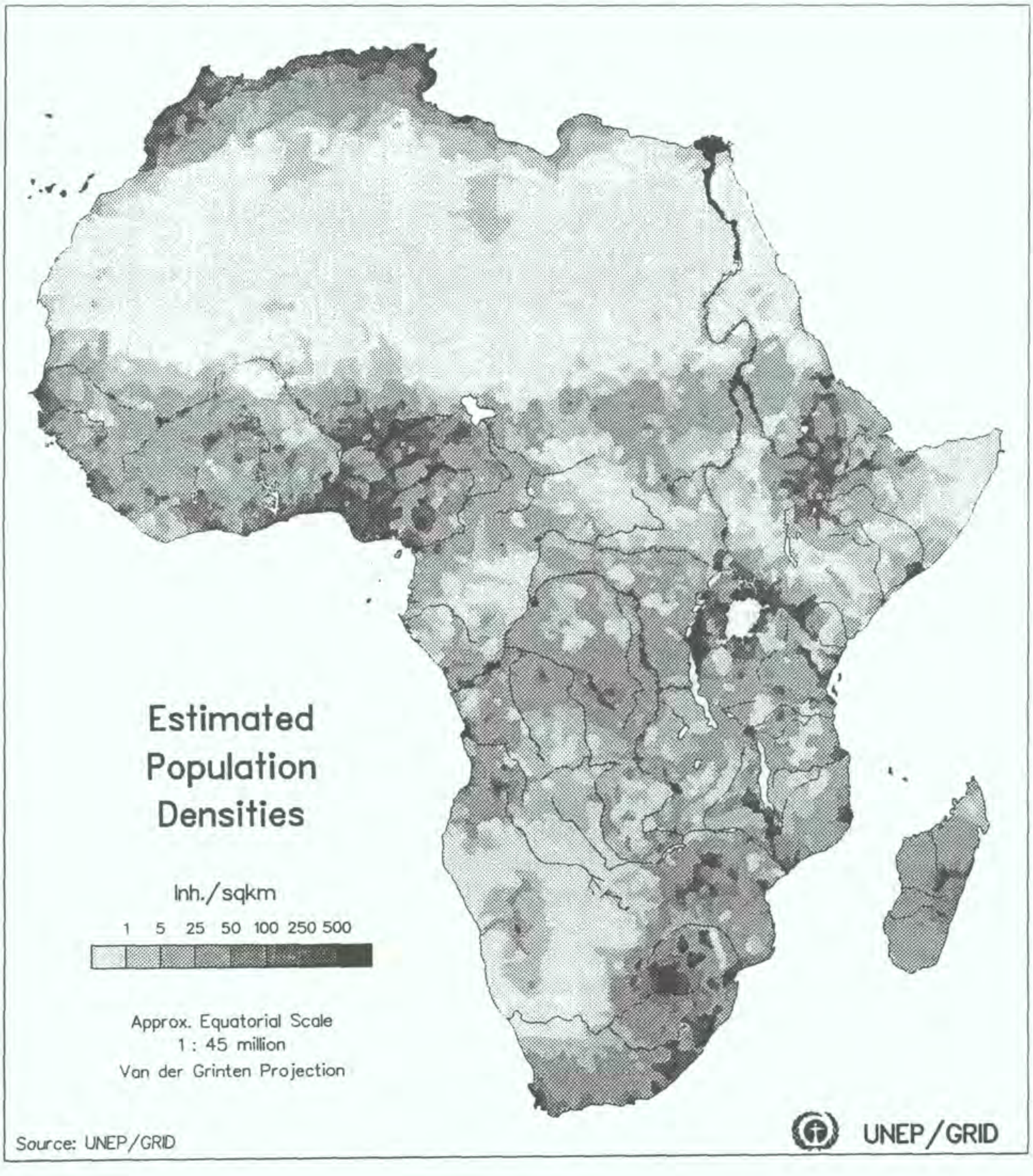

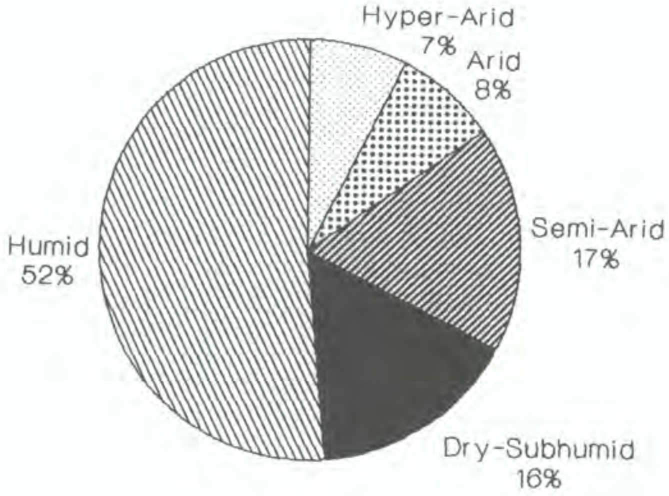

Figure 2: Total African population by climatic zone

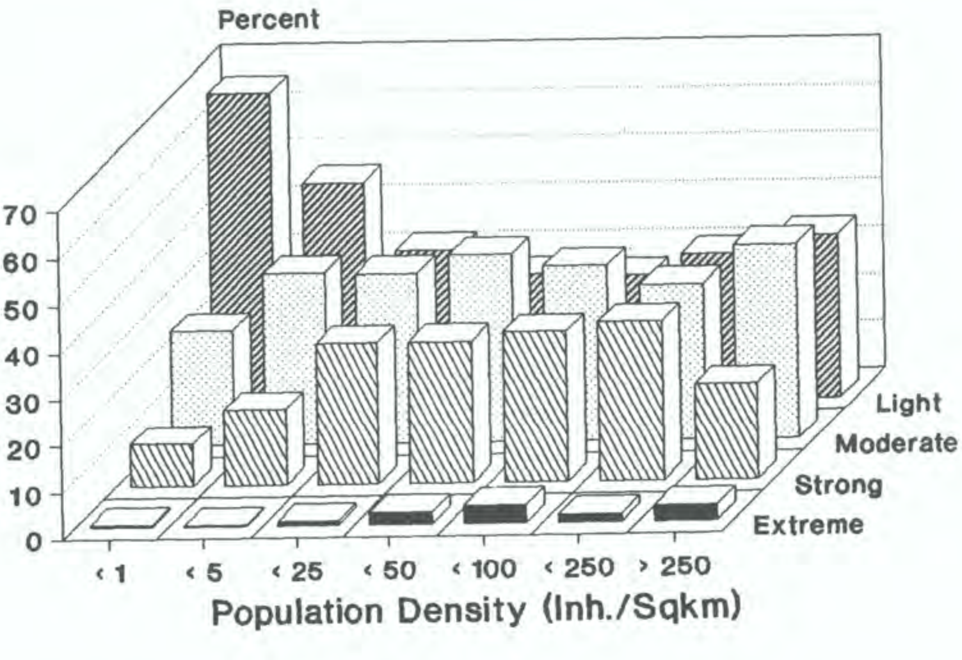

Figure 3: Distribution of soil degradation degree in the susceptible drylands of Africa within each population density class

4. REFERENCES

Bähr, J. (1983), *Bevölkerungsgeographie*, Ulmer, Stuttgart.

Burril, A. (1990), Parks and protected areas: A dataset within UNEP's Global Resource Information Database (GRID), *Mitt. Inst. Allg. Bot.*, 23a.

Comwell Systems Inc. (1989), *PC Globe+ Digital Database*, Tempe.

ESRI (1984), *Final Report: UNEP/FAO World and Africa GIS database*, Redlands, CA.

Ethiopian Mapping Authority (1988), *National Atlas of Ethiopia.*

Europa Publications (1989), *The Middle East and North Africa - 1990.*

Europa Publications (1990), *Africa South of the Sahara - 1991*

Fotheringham, A.S. and M.E. O'Kelly (1989), *Spatial interaction models: formulations and applications*, Kluwer, Dordrecht.

Harrison, G.A. and A.J. Boyce (eds.) (1972), *The structure of human populations*, Clarendon, Oxford.

MacKinnon, J. and K. MacKinnon (1986), *Review of the protected areas system in the Afrotropical realm*, IUCN and UNEP.

McClosky, J.M. and H. Spalding (1989), A reconnaissance level inventory of the amount of wilderness remaining in the world, *Ambio*, 18(4), 221-227.

Noin, D. (1979), *Geographie de la population*, Paris

Schultz, J. (1976), Land use in Zambia, *Afrika Studien*, 95.

Snyder, J.P. (1982), *Map Projections used by the U.S. Geological Survey*, Government Printing Office, Washington.

U.N. Statistical Office (1989), *World Population Prospects 1988*, New York.

U.N. Statistical Office (various), *Demographic Yearbook*, New York.

U.S. Environmental Protection Agency (1990), *Population estimation for risk assessment: A comparison of methods*, Environmental Monitoring and Systems Laboratory, EPA 600/X-90/199, Las Vegas.

Appendix I:

Summary Statistics by Country

Country Id	Country	1988 Population	Number of Admin. Districts	Admin Census Year	Number of Towns and Cities
1	ALGERIA	24195000	31	1980	64
2	ANGOLA	8236000	15	1986	6
3	BENIN	4497000	6	1979	5
4	BOTSWANA	1190000	9	1981	11
5	BURKINA FASO	8486000	1	-	6
6	BURUNDI	5156000	1	-	12
7	CAMEROON	10532000	7	1976	12
8	CAPE VERDE	354000	11	1980	5
9	CENTRAL AFR. REP.	2736000	14	1979	6
10	CHAD	4778000	14	1984	9
11	COMOROS	429000	1	-	4
12	CONGO	2154000	9	1975	7
13	DJIBOUTI	320000	1	-	5
14	EGYPT	53348000	25	1986	20
15	ETHIOPIA	48265000	14	1984	33
16	GABON	1052000	9	1976	6
17	GAMBIA	779000	1	-	7
18	GHANA	14360000	8	1984	19
19	GUINEA	6909000	31	1980	5
20	GUINEA BISSAO	951000	8	1979	7
21	IVORY COAST	11185000	26	1975	16
22	KENYA	23342000	41	1979	11
23	LESOTHO	1666000	9	1979	4
24	LIBERIA	2463000	9	1979	5
25	LIBYA	3956000	10	1978	11
26	MADAGASCAR	11073000	1	-	8
27	MALAWI	7679000	23	1977	6
28	MALI	8666000	41	1976	7
29	MAURITANIA	1919000	12	1977	5
30	MOROCCO	24976000	35	1987	35
31	MOZAMBIQUE	14948000	10	1987	6
32	NAMIBIA	1302000	1	-	6
33	NIGER	7214000	35	1977	7
34	NIGERIA	111904000	19	1986	27
35	RWANDA	7058000	10	1979	6
36	SAO TOME	117000	1	-	2
37	SENEGAL	7281000	7	1976	6
38	SEYCHELLES	69000	1	-	4
39	SIERRA LEONE	3963000	1	-	6
40	SOMALIA	7990000	1	-	7

41	SOUTH AFRICA	35094000	14	1985	22
42	SUDAN	24014000	9	1980	9
43	SWAZILAND	735000	4	1976	3
44	TANZANIA	24295000	22	1978	19
45	TOGO	3336000	19	1980	22
46	TUNISIA	7738000	18	1981	9
47	UGANDA	16447000	18	1969	8
48	WESTERN SAHARA	181000	1	-	3
49	ZAIRE	33294000	9	1985	43
50	ZAMBIA	7546000	45	1980	16
51	ZIMBABWE	9729000	7	1969	11

Appendix II: Adjustment of Areas Calculated on a Latitude-Longitude Grid

The exact equations are taken from Snyder (1982, p.28f). The length in meters of one degree of longitude is:

$$L_{long} = r * \text{cosine}(lat) \ / \ (1 - e^2 * \text{sine}^2(lat))^{1/2} * \pi \ / \ 180$$

and of one degree of latitude:

$$L_{lat} = r * (1 - e^2) \ / \ (1 - e^2 * \text{sine}^2(lat))^{1.5} * \pi \ / \ 180$$

where

r = radius of the ellipsoid of reference, e.g. Hayford: 6,378,388
e^2 = eccentricity (as a function of the ellipsoid's flattening), e.g. 0.00672267
lat = latitude in radians

As an example for the possible distortion for an African coverage: A regular one degree by one degree cell covers the area of 12,309.7 square kilometers at the Equator, but only 9,483.4 square kilometers at 40 degrees North or South latitude.

Part 7

AREA CALCULATIONS DERIVED FROM THE SOIL DEGRADATION DATASETS

GENERAL NOTES

- The template for all maps was derived from the ISRIC/GLASOD coverage. Therefore only areas between 72 degrees North and 57 degrees South were considered in the area calculations.
- For the global region boundaries the conventions used in the *Times Atlas of the World* (1985, p. xiv) were followed.
- All numbers were calculated with a higher precision than is actually displayed. This may be reflected in some of the percentage figures shown. Also, small inconsistencies due to rounding may occur.
- The climatic zones are defined as the ratio of precipitation over potential evapotranspiration (P/PET):

	P/PET
Moist-Subhumid and Humid	> 0.65
Dry-Subhumid	0.51 - 0.65
Semi-Arid	0.21 - 0.50
Arid	0.05 - 0.20
Hyper-Arid	< 0.05

Cold Mountain and Tundra Climates: average temperature in more than 6 months below 0, and in not more than 3 months above 6 degrees Celsius.

TABLE OF CONTENTS

SECTION 1: TABLES DERIVED FROM THE GLASOD 1:10 MILLION DATASET

SECTION 2: TABLES DERIVED FROM THE GLASOD 1:10 MILLION DATASET FOR THE THEMATIC ATLAS

SECTION 3: TABLES DERIVED FROM THE GLASOD 1:6 MILLION DATASET FOR AFRICA

REGIONS AS DEFINED IN THE *TIMES ATLAS OF THE WORLD*

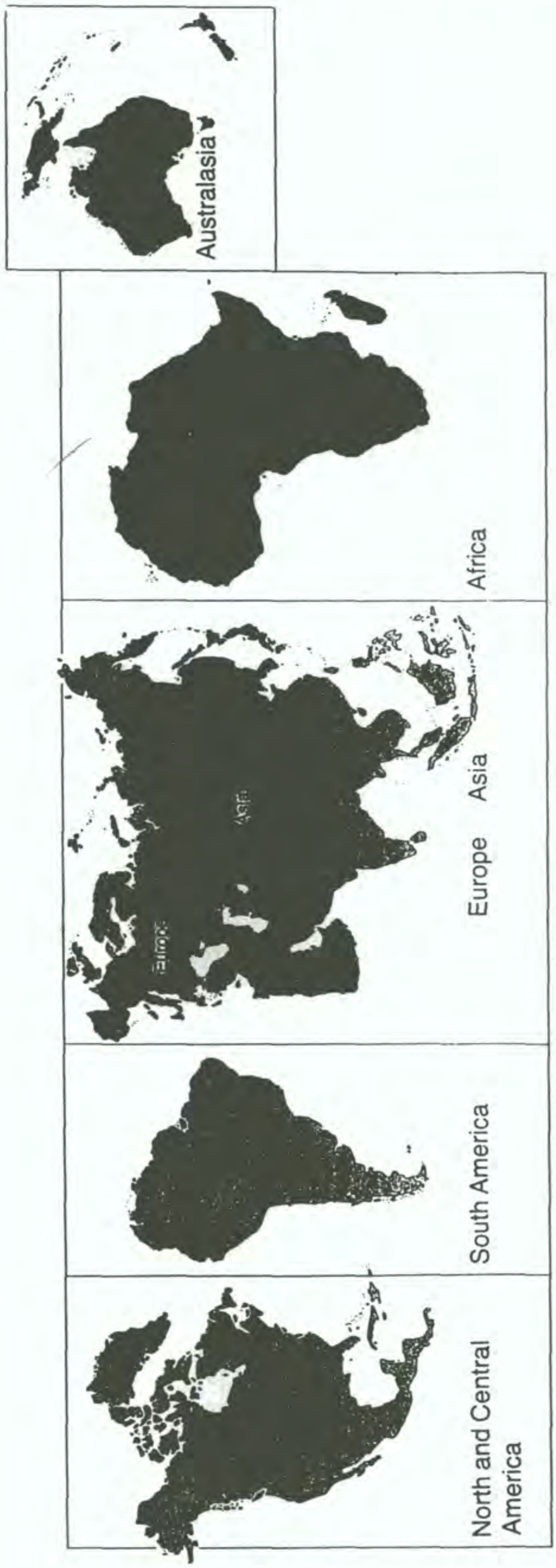

Table 1:
OVERVIEW: DEGRADED AND NON-DEGRADED AREAS

Stable Land, Waste Land and Degraded Areas by Region (millions of hectares)							
	Region						
	AF	AS	AU	EU	NA	SA	Total
Stable Land	1735.6	3023.5	689.0	729.4	1906.4	1496.1	9580.0
Waste Land	735.8	485.5	90.3	2.2	126.4	28.1	1468.3
Degraded	494.2	747.0	102.9	218.9	158.1	243.3	1964.4
Total	2965.6	4256.0	882.2	950.5	2190.9	1767.5	13012.7

Stable Land, Waste Land and Degraded Areas by Region (in percent)							
	Region						
	AF	AS	AU	EU	NA	SA	Total
Stable Land	18.1	31.6	7.2	7.6	19.9	15.6	100.0
Waste Land	50.1	33.1	6.1	0.1	8.6	1.9	100.0
Degraded	25.2	38.0	5.2	11.1	8.0	12.5	100.0
Total	22.8	32.7	6.8	7.3	16.8	13.6	100.0

Regions by Stable Land, Waste Land and Degraded Areas (in percent)							
	Region						
	AF	AS	AU	EU	NA	SA	Total
Stable Land	58.5	71.0	78.1	76.7	87.0	84.6	73.6
Waste Land	24.8	11.4	10.2	0.3	5.8	1.6	11.3
Degraded	16.7	17.6	11.7	23.0	7.2	13.8	15.1
Total	100.0	100.0	100.0	100.0	100.0	100.0	100.0

Regions: AF = Africa, AS = Asia, AU = Australasia, EU = Europe, NA = North America, SA = South America.

Data Source: UNEP/ISRIC, 1990
Data Compilation: UNEP/GRID, 1991

Table 2:
DEGREE OF SOIL DEGRADATION

Degree of Soil Degradation by Region (millions of hectares)							
	Region						
Degree	AF	AS	AU	EU	NA	SA	Total
None	2471.4	3509.0	779.3	731.6	2032.8	1524.2	11048.3
Light	173.6	294.5	96.6	60.6	18.9	104.8	749.0
Moderate	191.8	344.3	3.9	144.4	112.5	113.5	910.5
Strong	123.6	107.7	1.9	10.7	26.7	25.0	295.7
Extreme	5.2	0.5	0.4	3.1	0.0	0.0	9.3
Total	2965.6	4256.0	882.2	950.5	2190.9	1767.5	13012.7

Degree of Soil Degradation by Region (in percent)							
Degree	AF	AS	AU	EU	NA	SA	Total
None	22.4	31.8	7.1	6.6	18.4	13.8	100.0
Light	23.2	39.3	12.9	8.1	2.5	14.0	100.0
Moderate	21.1	37.8	0.4	15.9	12.4	12.5	100.0
Strong	41.8	36.4	0.7	3.6	9.0	8.5	100.0
Extreme	56.2	5.9	4.5	33.4	0.0	0.0	100.0
Total	22.8	32.7	6.8	7.3	16.8	13.6	100.0

Total Area in the Region by Soil Degradation Degree (in percent)							
Degree	AF	AS	AU	EU	NA	SA	Total
None	83.3	82.4	88.3	77.0	92.8	86.2	84.9
Light	5.9	6.9	10.9	6.4	0.9	5.9	5.8
Moderate	6.5	8.1	0.4	15.2	5.1	6.4	7.0
Strong	4.2	2.5	0.2	1.1	1.2	1.4	2.3
Extreme	0.2	0.0	0.0	0.3	0.0	0.0	0.1
Total	100.0	100.0	100.0	100.0	100.0	100.0	100.0

Degraded Area in the Region by Soil Degradation Degree (in percent)							
Degree	AF	AS	AU	EU	NA	SA	Total
Light	35.1	39.4	93.9	27.7	12.0	43.1	38.1
Moderate	38.8	46.1	3.8	66.0	71.2	46.7	46.4
Strong	25.0	14.4	1.9	4.9	16.9	10.3	15.1
Extreme	1.1	0.1	0.4	1.4	0.0	0.0	0.5
Total	100.0	100.0	100.0	100.0	100.0	100.0	100.0

Regions: AF = Africa, AS = Asia, AU = Australasia, EU = Europe, NA = North America, SA = South America.
Data Source: UNEP/ISRIC, 1990
Data Compilation: UNEP/GRID, 1991

Table 3:
TYPE OF SOIL DEGRADATION

Type of Soil Degradation by Region (millions of hectares)							
	Region						
Type	AF	AS	AU	EU	NA	SA	Total
None	2471.4	3509.0	779.3	731.6	2032.8	1524.2	11048.3
Water	227.4	439.6	82.9	114.5	106.1	123.2	1093.7
Wind	186.5	222.1	16.4	42.2	39.2	41.9	548.3
Chemical	61.6	73.2	1.3	25.7	7.0	70.3	239.1
Physical	18.7	12.1	2.3	36.4	5.8	7.9	83.3
Total	2965.6	4256.0	882.2	950.5	2190.9	1767.5	13012.7

Type of Soil Degradation by Region (in percent)							
Type	AF	AS	AU	EU	NA	SA	Total
None	22.4	31.8	7.1	6.6	18.4	13.8	100.0
Water	20.8	40.2	7.6	10.5	9.7	11.3	100.0
Wind	34.0	40.5	3.0	7.7	7.2	7.6	100.0
Chemical	25.8	30.6	0.6	10.8	2.9	29.4	100.0
Physical	22.5	14.6	2.7	43.7	7.0	9.5	100.0
Total	22.8	32.7	6.8	7.3	16.8	13.6	100.0

Total Area in the Region by Soil Degradation Type (in percent)							
Type	AF	AS	AU	EU	NA	SA	Total
None	83.3	82.4	88.3	77.0	92.8	86.2	84.9
Water	7.7	10.3	9.4	12.1	4.8	7.0	8.4
Wind	6.3	5.2	1.9	4.4	1.8	2.4	4.2
Chemical	2.1	1.7	0.2	2.7	0.3	4.0	1.8
Physical	0.6	0.3	0.3	3.8	0.3	0.4	0.6
Total	100.0	100.0	100.0	100.0	100.0	100.0	100.0

Degraded Area in the Region by Soil Degradation Type (in percent)							
Type	AF	AS	AU	EU	NA	SA	Total
Water	46.0	58.8	80.6	52.3	67.1	50.6	55.7
Wind	37.7	29.7	15.9	19.3	24.8	17.2	27.9
Chemical	12.5	9.8	1.3	11.8	4.4	28.9	12.2
Physical	3.8	1.6	2.2	16.6	3.7	3.3	4.2
Total	100.0	100.0	100.0	100.0	100.0	100.0	100.0

Regions: AF = Africa, AS = Asia, AU = Australasia, EU = Europe, NA = North America, SA = South America.

Data Source: UNEP/ISRIC, 1990
Data Compilation: UNEP/GRID, 1991

Table 4:
CLIMATIC ZONES

Climatic Zones by Region (millions of hectares)							
	Region						
Zone	AF	AS	AU	EU	NA	SA	Total
Cold	0.0	1082.5	0.0	27.9	616.9	37.7	1765.0
Humid	1007.7	1224.3	218.9	622.9	838.5	1188.2	5100.5
Dry-Subhumid	268.7	352.7	51.3	183.5	231.5	207.0	1294.7
Semi-Arid	513.8	693.4	309.0	105.2	419.4	264.5	2305.3
Arid	503.5	625.7	303.0	11.0	81.5	44.5	1569.1
Hyper-Arid	672.0	277.3	0.0	0.0	3.1	25.7	978.2
Total	2965.6	4256.0	882.2	950.5	2190.9	1767.5	13012.7

Climatic Zones by Region (in percent)							
Zone	AF	AS	AU	EU	NA	SA	Total
Cold	0.0	61.3	0.0	1.6	34.9	2.1	100.0
Humid	19.8	24.0	4.3	12.2	16.4	23.3	100.0
Dry-Subhumid	20.8	27.2	4.0	14.2	17.9	16.0	100.0
Semi-Arid	22.3	30.1	13.4	4.6	18.2	11.5	100.0
Arid	32.1	39.9	19.3	0.7	5.2	2.8	100.0
Hyper-Arid	68.7	28.4	0.0	0.0	0.3	2.6	100.0
Total	22.8	32.7	6.8	7.3	16.8	13.6	100.0

Region by Climatic Zone (in percent)							
Zone	AF	AS	AU	EU	NA	SA	Total
Cold	0.0	25.4	0.0	2.9	28.2	2.1	13.6
Humid	34.0	28.8	24.8	65.5	38.3	67.2	39.2
Dry-Subhumid	9.1	8.3	5.8	19.3	10.6	11.7	9.9
Semi-Arid	17.3	16.3	35.0	11.1	19.1	15.0	17.7
Arid	17.0	14.7	34.3	1.2	3.7	2.5	12.1
Hyper-Arid	22.7	6.5	0.0	0.0	0.1	1.5	7.5
Total	100.0	100.0	100.0	100.0	100.0	100.0	100.0

Regions: AF = Africa, AS = Asia, AU = Australasia, EU = Europe, NA = North America, SA = South America.

Data Source: CRU/UEA, 1990
Data Compilation: UNEP/GRID, 1991

Table 5:
DEGREE OF SOIL DEGRADATION AND CLIMATIC ZONES

Degree of Soil Degradation by Climatic Zone (millions of hectares)							
	Climatic Zone						
Degree	Cold	Humid	Dry-Subh.	Semi-Arid	Arid	Hyper-Arid	Total
None	1735.4	4302.6	1071.2	1886.0	1176.8	876.4	11048.3
Light	18.7	242.1	66.5	152.5	208.3	60.8	749.0
Moderate	10.2	391.1	129.0	200.2	141.1	39.0	910.5
Strong	0.8	163.0	25.8	63.2	41.1	1.8	295.7
Extreme	0.0	1.7	2.2	3.5	1.7	0.1	9.3
Total	1765.0	5100.5	1294.7	2305.3	1569.1	978.2	13012.7

Degree of Soil Degradation by Climatic Zone (in percent)							
Degree	Cold	Humid	Dry-Subh.	Semi-Arid	Arid	Hyper-Arid	Total
None	15.7	38.9	9.7	17.1	10.7	7.9	100.0
Light	2.5	32.3	8.9	20.4	27.8	8.1	100.0
Moderate	1.1	42.9	14.2	22.0	15.5	4.3	100.0
Strong	0.3	55.1	8.7	21.4	13.9	0.6	100.0
Extreme	0.0	18.8	24.2	38.1	18.4	0.6	100.0
Total	13.6	39.2	9.9	17.7	12.1	7.5	100.0

Total Area in the Climatic Zone by Soil Degradation Degree (in percent)							
Degree	Cold	Humid	Dry-Subh.	Semi-Arid	Arid	Hyper-Arid	Total
None	98.3	84.4	82.7	81.8	75.0	89.6	84.9
Light	1.1	4.7	5.1	6.6	13.3	6.2	5.8
Moderate	0.6	7.7	10.0	8.7	9.0	4.0	7.0
Strong	0.0	3.2	2.0	2.7	2.6	0.2	2.3
Extreme	0.0	0.0	0.2	0.2	0.1	0.0	0.1
Total	100.0	100.0	100.0	100.0	100.0	100.0	100.0

Degraded Area in the Climatic Zone by Soil Degradation Degree (in percent)							
Degree	Cold	Humid	Dry-Subh.	Semi-Arid	Arid	Hyper-Arid	Total
Light	63.1	30.3	29.8	36.4	53.1	59.8	38.1
Moderate	34.3	49.0	57.7	47.7	36.0	38.4	46.4
Strong	2.5	20.4	11.5	15.1	10.5	1.8	15.1
Extreme	0.0	0.2	1.0	0.8	0.4	0.1	0.5
Total	100.0	100.0	100.0	100.0	100.0	100.0	100.0

Data Source: UNEP/ISRIC, 1990 and CRU/UEA, 1990
Data Compilation: UNEP/GRID, 1991

Table 6:
DEGREE AND TYPE OF SOIL DEGRADATION

Degree by Type of Soil Degradation (millions of hectares)					
	Type of Soil Degradation				
Degree	Water	Wind	Chemical	Physical	Total
Light	343.2	268.6	93.0	44.2	749.0
Moderate	526.7	253.6	103.3	26.8	910.5
Strong	217.2	24.3	41.9	12.3	295.7
Extreme	6.6	1.9	0.8	0.0	9.3
Total	1093.7	548.3	239.1	83.3	1964.4

Degree by Type of Soil Degradation (in percent)					
Degree	Water	Wind	Chemical	Physical	Total
Light	45.8	35.9	12.4	5.9	100.0
Moderate	57.8	27.9	11.3	2.9	100.0
Strong	73.5	8.2	14.2	4.1	100.0
Extreme	71.1	20.3	8.6	0.0	100.0
Total	55.7	27.9	12.2	4.2	100.0

Type of Soil Degradation by Degree (in percent)					
Degree	Water	Wind	Chemical	Physical	Total
Light	31.4	49.0	38.9	53.1	38.1
Moderate	48.2	46.3	43.2	32.2	46.4
Strong	19.9	4.4	17.5	14.7	15.1
Extreme	0.6	0.3	0.3	0.0	0.5
Total	100.0	100.0	100.0	100.0	100.0

Data Source: UNEP/ISRIC, 1990
Data Compilation: UNEP/GRID, 1991

Table 7:
TYPE OF SOIL DEGRADATION AND CLIMATIC ZONES

Type of Soil Degradation by Climatic Zone (millions of hectares)							
	Climatic Zone						
Type	Cold	Humid	Dry-Subh.	Semi-Arid	Arid	Hyper-Arid	Total
None	1735.4	4302.6	1071.2	1886.0	1176.8	876.4	11048.3
Water	22.9	592.5	141.0	213.2	113.3	10.9	1093.7
Wind	5.6	30.3	46.8	150.3	235.3	80.0	548.3
Chemical	0.6	127.1	22.5	40.9	37.3	10.8	239.1
Physical	0.5	48.0	13.2	15.1	6.5	0.1	83.3
Total	1765.0	5100.5	1294.7	2305.3	1569.1	978.2	13012.7

Type of Soil Degradation by Climatic Zone (in percent)							
Type	Cold	Humid	Dry-Subh.	Semi-Arid	Arid	Hyper-Arid	Total
None	15.7	38.9	9.7	17.1	10.7	7.9	100.0
Water	2.1	54.2	12.9	19.5	10.4	1.0	100.0
Wind	1.0	5.5	8.5	27.4	42.9	14.6	100.0
Chemical	0.2	53.1	9.4	17.1	15.6	4.5	100.0
Physical	0.6	57.7	15.8	18.1	7.7	0.1	100.0
Total	13.6	39.2	9.9	17.7	12.1	7.5	100.0

Total Area in the Climatic Zone by Soil Degradation Type (in percent)							
Type	Cold	Humid	Dry-Subh.	Semi-Arid	Arid	Hyper-Arid	Total
None	98.3	84.4	82.7	81.8	75.0	89.6	84.9
Water	1.3	11.6	10.9	9.2	7.2	1.1	8.4
Wind	0.3	0.6	3.6	6.5	15.0	8.2	4.2
Chemical	0.0	2.5	1.7	1.8	2.4	1.1	1.8
Physical	0.0	0.9	1.0	0.7	0.4	0.0	0.6
Total	100.0	100.0	100.0	100.0	100.0	100.0	100.0

Degraded Area in the Climatic Zone by Soil Degradation Type (in percent)							
Type	Cold	Humid	Dry-Subh.	Semi-Arid	Arid	Hyper-Arid	Total
Water	77.3	74.3	63.1	50.8	28.9	10.7	55.7
Wind	19.0	3.8	21.0	35.8	60.0	78.7	27.9
Chemical	2.0	15.9	10.1	9.7	9.5	10.6	12.2
Physical	1.7	6.0	5.9	3.6	1.6	0.1	4.2
Total	100.0	100.0	100.0	100.0	100.0	100.0	100.0

Data Source: UNEP/ISRIC, 1990 and CRU/UEA, 1990
Data Compilation: UNEP/GRID, 1991

Table 8:
DEGREE AND TYPE OF SOIL DEGRADATION IN ARID, SEMI-ARID AND DRY-SUBHUMID AREAS

Degree by Type of Soil Degradation (millions of hectares)					
	Type of Soil Degradation				
Degree	Water	Wind	Chemical	Physical	Total
Light	175.1	197.2	44.3	10.8	427.3
Moderate	208.5	215.4	31.4	15.0	470.3
Strong	79.0	18.0	24.2	8.9	130.1
Extreme	4.8	1.8	0.8	0.0	7.5
Total	467.4	432.4	100.7	34.7	1035.2

Degree by Type of Soil Degradation (in percent)					
Degree	Water	Wind	Chemical	Physical	Total
Light	41.0	46.2	10.4	2.5	100.0
Moderate	44.3	45.8	6.7	3.2	100.0
Strong	60.7	13.8	18.6	6.8	100.0
Extreme	64.8	24.5	10.7	0.0	100.0
Total	45.2	41.8	9.7	3.4	100.0

Type by Degree of Soil Degradation (in percent)					
Degree	Water	Wind	Chemical	Physical	Total
Light	37.5	45.6	44.0	31.0	41.3
Moderate	44.6	49.8	31.2	43.4	45.4
Strong	16.9	4.2	24.0	25.6	12.6
Extreme	1.0	0.4	0.8	0.0	0.7
Total	100.0	100.0	100.0	100.0	100.0

Data Source: UNEP/ISRIC, 1990 and CRU/UEA, 1990
Data Compilation: UNEP/GRID, 1991

Table 9:
CAUSATIVE FACTORS

Causative Factors by Region (millions of hectares)							
	Region						
Cause	AF	AS	AU	EU	NA	SA	Total
None	2471.4	3509.0	779.3	731.6	2032.8	1524.2	11048.3
Agriculture	121.4	204.4	7.9	63.9	90.5	63.5	551.6
Overexploit.	62.8	46.1	0.0	0.5	11.4	12.0	132.7
Deforestation	66.8	297.8	12.3	83.8	17.9	100.1	578.6
Overgrazing	243.0	197.3	82.5	50.0	37.9	67.9	678.7
Bioindustr. Act.	0.2	1.4	0.1	20.6	0.4	0.0	22.8
Total	2965.6	4256.0	882.2	950.5	2190.9	1767.5	13012.7

Causative Factors by Region (in percent)							
Cause	AF	AS	AU	EU	NA	SA	Total
None	22.4	31.8	7.1	6.6	18.4	13.8	100.0
Agriculture	22.0	37.1	1.4	11.6	16.4	11.5	100.0
Overexploit.	47.3	34.7	0.0	0.4	8.6	9.0	100.0
Deforestation	11.5	51.5	2.1	14.5	3.1	17.3	100.0
Overgrazing	35.8	29.1	12.2	7.4	5.6	10.0	100.0
Bioindustr. Act.	0.9	6.3	0.4	90.6	1.8	0.0	100.0
Total	22.8	32.7	6.8	7.3	16.8	13.6	100.0

Total Area in the Region by Causative Factors (in percent)							
Cause	AF	AS	AU	EU	NA	SA	Total
None	83.3	82.4	88.3	77.0	92.8	86.2	84.9
Agriculture	4.1	4.8	0.9	6.7	4.1	3.6	4.2
Overexploit.	2.1	1.1	0.0	0.1	0.5	0.7	1.0
Deforestation	2.3	7.0	1.4	8.8	0.8	5.7	4.4
Overgrazing	8.2	4.6	9.4	5.3	1.7	3.8	5.2
Bioindustr. Act.	0.0	0.0	0.0	2.2	0.0	0.0	0.2
Total	100.0	100.0	100.0	100.0	100.0	100.0	100.0

Degraded Area in the Region by Causative Factors (in percent)							
Cause	AF	AS	AU	EU	NA	SA	Total
Agriculture	24.6	27.4	7.7	29.2	57.2	26.1	28.1
Overexploit.	12.7	6.2	0.0	0.2	7.2	4.9	6.8
Deforestation	13.5	39.9	12.0	38.3	11.3	41.1	29.5
Overgrazing	49.2	26.4	80.2	22.9	24.0	27.9	34.5
Bioindustr. Act.	0.0	0.2	0.1	9.4	0.3	0.0	1.2
Total	100.0	100.0	100.0	100.0	100.0	100.0	100.0

Regions: AF = Africa, AS = Asia, AU = Australasia, EU = Europe, NA = North America, SA = South America.
Data Source: UNEP/ISRIC, 1990; *Data Compilation:* UNEP/GRID, 1991

Table 10:
DEGREE AND CAUSE OF SOIL DEGRADATION

Degree by Cause of Soil Degradation (millions of hectares)						
	Cause of Soil Degradation					
Degree	Agriculture	Overexploit.	Deforestation	Overgrazing	Bioind. Act.	Total
Light	180.8	57.2	176.2	328.8	6.1	749.0
Moderate	285.0	51.8	288.7	268.3	16.6	910.5
Strong	83.3	23.7	113.5	75.0	0.1	295.7
Extreme	2.5	0.0	0.2	6.5	0.0	9.3
Total	551.6	132.7	578.6	678.7	22.8	1964.4

Degree by Cause of Soil Degradation (in percent)						
Degree	Agriculture	Overexploit.	Deforestation	Overgrazing	Bioind. Act.	Total
Light	24.1	7.6	23.5	43.9	0.8	100.0
Moderate	31.3	5.7	31.7	29.5	1.8	100.0
Strong	28.2	8.0	38.4	25.4	0.0	100.0
Extreme	27.1	0.0	2.4	70.5	0.0	100.0
Total	28.1	6.8	29.5	34.5	1.2	100.0

Cause by Type of Soil Degradation (in percent)						
Degree	Agriculture	Overexploit.	Deforestation	Overgrazing	Bioind. Act.	Total
Light	32.8	43.1	30.4	48.4	26.8	38.1
Moderate	51.7	39.0	49.9	39.5	72.9	46.4
Strong	15.1	17.9	19.6	11.1	0.3	15.1
Extreme	0.5	0.0	0.0	1.0	0.0	0.5
Total	100.0	100.0	100.0	100.0	100.0	100.0

Data Source: UNEP/ISRIC, 1990
Data Compilation: UNEP/GRID, 1991

Table 11:
TYPE AND CAUSE OF SOIL DEGRADATION

Type by Cause of Soil Degradation (millions of hectares)						
	Cause of Soil Degradation					
Type	Agriculture	Overexploit.	Deforestation	Overgrazing	Bioind. Act.	Total
Water	265.5	36.2	471.3	319.6	1.1	1093.7
Wind	87.0	85.6	44.2	331.6	0.0	548.3
Chemical	133.2	10.4	61.8	13.9	19.8	239.1
Physical	66.0	0.5	1.3	13.6	1.9	83.3
Total	551.6	132.7	578.6	678.7	22.8	1964.4

Type by Cause of Soil Degradation (in percent)						
Type	Agriculture	Overexploit.	Deforestation	Overgrazing	Bioind. Act.	Total
Water	24.3	3.3	43.1	29.2	0.1	100.0
Wind	15.9	15.6	8.1	60.5	0.0	100.0
Chemical	55.7	4.4	25.8	5.8	8.3	100.0
Physical	79.2	0.6	1.6	16.3	2.3	100.0
Total	28.1	6.8	29.5	34.5	1.2	100.0

Cause by Type of Soil Degradation (in percent)						
Type	Agriculture	Overexploit.	Deforestation	Overgrazing	Bioind. Act.	Total
Water	48.1	27.3	81.5	47.1	4.8	55.7
Wind	15.8	64.5	7.6	48.9	0.0	27.9
Chemical	24.1	7.9	10.7	2.0	86.8	12.2
Physical	12.0	0.4	0.2	2.0	8.3	4.2
Total	100.0	100.0	100.0	100.0	100.0	100.0

Data Source: UNEP/ISRIC, 1990
Data Compilation: UNEP/GRID, 1991

Table 12:
DEGREE OF SOIL DEGRADATION AND CLIMATIC ZONES
AFRICA

Degree of Soil Degradation by Climatic Zone (millions of hectares)							
	Climatic Zone						
Degree	Cold	Humid	Dry-Subh.	Semi-Arid	Arid	Hyper-Arid	Total
None	0.0	868.9	231.4	404.3	331.0	635.9	2471.5
Light	0.0	42.9	13.8	23.7	80.5	12.8	173.6
Moderate	0.0	43.0	11.4	46.2	69.6	21.6	191.8
Strong	0.0	51.2	11.3	38.1	21.3	1.7	123.6
Extreme	0.0	1.7	0.7	1.5	1.2	0.1	5.2
Total	0.0	1007.7	268.7	513.8	503.5	672.0	2965.7

Degree of Soil Degradation by Climatic Zone (in percent)							
Degree	Cold	Humid	Dry-Subh.	Semi-Arid	Arid	Hyper-Arid	Total
None	0.0	35.2	9.4	16.4	13.4	25.7	100.0
Light	0.0	24.7	7.9	13.7	46.3	7.4	100.0
Moderate	0.0	22.4	6.0	24.1	36.3	11.2	100.0
Strong	0.0	41.4	9.2	30.9	17.2	1.4	100.0
Extreme	0.0	32.6	14.4	28.8	23.2	1.0	100.0
Total	0.0	34.0	9.1	17.3	17.0	22.7	100.0

Total Area in the Climatic Zone by Soil Degradation Degree (in percent)							
Degree	Cold	Humid	Dry-Subh.	Semi-Arid	Arid	Hyper-Arid	Total
None	0.0	86.2	86.1	78.7	65.7	94.6	83.3
Light	0.0	4.3	5.1	4.6	16.0	1.9	5.9
Moderate	0.0	4.3	4.3	9.0	13.8	3.2	6.5
Strong	0.0	5.1	4.2	7.4	4.2	0.2	4.2
Extreme	0.0	0.2	0.3	0.3	0.2	0.0	0.2
Total	100.0	100.0	100.0	100.0	100.0	100.0	100.0

Degraded Area in the Climatic Zone by Soil Degradation Degree (in percent)							
Degree	Cold	Humid	Dry-Subh.	Semi-Arid	Arid	Hyper-Arid	Total
Light	0.0	30.9	36.9	21.7	46.6	35.4	35.1
Moderate	0.0	31.0	30.7	42.1	40.3	59.8	38.8
Strong	0.0	36.9	30.4	34.8	12.3	4.6	25.0
Extreme	0.0	1.2	2.0	1.4	0.7	0.1	1.1
Total	100.0	100.0	100.0	100.0	100.0	100.0	100.0

Data Source: UNEP/ISRIC, 1990 and CRU/UEA, 1990
Data Compilation: UNEP/GRID, 1991

Table 13:
DEGREE OF SOIL DEGRADATION AND CLIMATIC ZONES
ASIA

Degree of Soil Degradation by Climatic Zone (millions of hectares)							
	Climatic Zone						
Degree	Cold	Humid	Dry-Subh.	Semi-Arid	Arid	Hyper-Arid	Total
None	1060.6	933.6	274.4	552.0	475.0	213.3	3508.9
Light	15.7	74.0	24.0	57.7	75.0	48.1	294.5
Moderate	5.4	152.8	46.6	66.6	56.9	15.9	344.3
Strong	0.8	63.9	7.7	17.1	18.2	0.0	107.7
Extreme	0.0	0.0	0.0	0.1	0.5	0.0	0.5
Total	1082.5	1224.3	352.7	693.4	625.7	277.3	4255.9

Degree of Soil Degradation by Climatic Zone (in percent)							
Degree	Cold	Humid	Dry-Subh.	Semi-Arid	Arid	Hyper-Arid	Total
None	30.2	26.6	7.8	15.7	13.5	6.1	100.0
Light	5.3	25.1	8.1	19.6	25.5	16.3	100.0
Moderate	1.6	44.4	13.5	19.3	16.5	4.6	100.0
Strong	0.7	59.3	7.1	15.9	16.9	0.0	100.0
Extreme	0.0	0.0	0.0	9.8	90.2	0.0	100.0
Total	25.4	28.8	8.3	16.3	14.7	6.5	100.0

Total Area in the Climatic Zone by Soil Degradation Degree (in percent)							
Degree	Cold	Humid	Dry-Subh.	Semi-Arid	Arid	Hyper-Arid	Total
None	98.0	76.3	77.8	79.6	75.9	76.9	82.4
Light	1.5	6.0	6.8	8.3	12.0	17.3	6.9
Moderate	0.5	12.5	13.2	9.6	9.1	5.7	8.1
Strong	0.1	5.2	2.2	2.5	2.9	0.0	2.5
Extreme	0.0	0.0	0.0	0.0	0.1	0.0	0.0
Total	100.0	100.0	100.0	100.0	100.0	100.0	100.0

Degraded Area in the Climatic Zone by Soil Degradation Degree (in percent)							
Degree	Cold	Humid	Dry-Subh.	Semi-Arid	Arid	Hyper-Arid	Total
Light	71.8	25.5	30.7	40.8	49.8	75.1	39.4
Moderate	24.8	52.6	59.5	47.1	37.8	24.9	46.1
Strong	3.4	22.0	9.8	12.1	12.1	0.0	14.4
Extreme	0.0	0.0	0.0	0.0	0.3	0.0	0.1
Total	100.0	100.0	100.0	100.0	100.0	100.0	100.0

Data Source: UNEP/ISRIC, 1990 and CRU/UEA, 1990
Data Compilation: UNEP/GRID, 1991

Table 14:
DEGREE OF SOIL DEGRADATION AND CLIMATIC ZONES
AUSTRALASIA

Degree of Soil Degradation by Climatic Zone (millions of hectares)							
	Climatic Zone						
Degree	Cold	Humid	Dry-Subh.	Semi-Arid	Arid	Hyper-Arid	Total
None	0.0	203.5	46.5	275.1	254.1	0.0	779.3
Light	0.0	13.0	3.8	32.4	47.4	0.0	96.6
Moderate	0.0	1.6	0.4	0.5	1.5	0.0	3.9
Strong	0.0	0.8	0.6	0.6	0.0	0.0	1.9
Extreme	0.0	0.0	0.0	0.4	0.0	0.0	0.4
Total	0.0	218.9	51.3	309.0	303.0	0.0	882.2

Degree of Soil Degradation by Climatic Zone (in percent)							
Degree	Cold	Humid	Dry-Subh.	Semi-Arid	Arid	Hyper-Arid	Total
None	0.0	26.1	6.0	35.3	32.6	0.0	100.0
Light	0.0	13.4	4.0	33.6	49.1	0.0	100.0
Moderate	0.0	40.5	9.6	12.3	37.6	0.0	100.0
Strong	0.0	41.8	29.0	29.1	0.0	0.0	100.0
Extreme	0.0	0.0	0.1	99.9	0.0	0.0	100.0
Total	0.0	24.8	5.8	35.0	34.3	0.0	100.0

Total Area in the Climatic Zone by Soil Degradation Degree (in percent)							
Degree	Cold	Humid	Dry-Subh.	Semi-Arid	Arid	Hyper-Arid	Total
None	0.0	93.0	90.7	89.0	83.9	0.0	88.3
Light	0.0	5.9	7.4	10.5	15.6	0.0	10.9
Moderate	0.0	0.7	0.7	0.2	0.5	0.0	0.4
Strong	0.0	0.4	1.1	0.2	0.0	0.0	0.2
Extreme	0.0	0.0	0.0	0.1	0.0	0.0	0.0
Total	100.0	100.0	100.0	100.0	100.0	100.0	100.0

Degraded Area in the Climatic Zone by Soil Degradation Degree (in percent)							
Degree	Cold	Humid	Dry-Subh.	Semi-Arid	Arid	Hyper-Arid	Total
Light	0.0	84.3	80.2	95.7	97.0	0.0	93.9
Moderate	0.0	10.4	7.9	1.4	3.0	0.0	3.8
Strong	0.0	5.3	11.9	1.7	0.0	0.0	1.9
Extreme	0.0	0.0	0.0	1.2	0.0	0.0	0.4
Total	100.0	100.0	100.0	100.0	100.0	100.0	100.0

Data Source: UNEP/ISRIC, 1990 and CRU/UEA, 1990
Data Compilation: UNEP/GRID, 1991

Table 15:
DEGREE OF SOIL DEGRADATION AND CLIMATIC ZONES
EUROPE

Degree of Soil Degradation by Climatic Zone (millions of hectares)							
	Climatic Zone						
Degree	Cold	Humid	Dry-Subh.	Semi-Arid	Arid	Hyper-Arid	Total
None	26.6	504.8	122.2	71.8	6.2	0.0	731.6
Light	0.8	45.9	9.5	4.2	0.2	0.0	60.6
Moderate	0.5	63.3	49.6	26.6	4.6	0.0	144.4
Strong	0.0	8.9	0.8	1.0	0.0	0.0	10.7
Extreme	0.0	0.0	1.5	1.6	0.0	0.0	3.1
Total	27.9	622.9	183.5	105.2	11.0	0.0	950.5

Degree of Soil Degradation by Climatic Zone (in percent)							
Degree	Cold	Humid	Dry-Subh.	Semi-Arid	Arid	Hyper-Arid	Total
None	3.6	69.0	16.7	9.8	0.9	0.0	100.0
Light	1.4	75.7	15.6	7.0	0.3	0.0	100.0
Moderate	0.3	43.8	34.3	18.4	3.2	0.0	100.0
Strong	0.0	83.3	7.1	9.6	0.0	0.0	100.0
Extreme	0.0	1.4	48.2	50.4	0.0	0.0	100.0
Total	2.9	65.5	19.3	11.1	1.2	0.0	100.0

Total Area in the Climatic Zone by Soil Degradation Degree (in percent)							
Degree	Cold	Humid	Dry-Subh.	Semi-Arid	Arid	Hyper-Arid	Total
None	95.4	81.0	66.6	68.2	56.8	0.0	77.0
Light	3.0	7.4	5.2	4.0	1.6	0.0	6.4
Moderate	1.6	10.2	27.0	25.3	41.6	0.0	15.2
Strong	0.0	1.4	0.4	1.0	0.0	0.0	1.1
Extreme	0.0	0.0	0.8	1.5	0.0	0.0	0.3
Total	100.0	100.0	100.0	100.0	100.0	100.0	100.0

Degraded Area in the Climatic Zone by Soil Degradation Degree (in percent)							
Degree	Cold	Humid	Dry-Subh.	Semi-Arid	Arid	Hyper-Arid	Total
Light	65.1	38.8	15.5	12.7	3.7	0.0	27.7
Moderate	34.9	53.6	80.9	79.6	96.2	0.0	66.0
Strong	0.0	7.6	1.2	3.1	0.1	0.0	4.9
Extreme	0.0	0.0	2.4	4.7	0.0	0.0	1.4
Total	100.0	100.0	100.0	100.0	100.0	100.0	100.0

Data Source: UNEP/ISRIC, 1990 and CRU/UEA, 1990
Data Compilation: UNEP/GRID, 1991

Table 16:
DEGREE OF SOIL DEGRADATION AND CLIMATIC ZONES
NORTH AMERICA

Degree of Soil Degradation by Climatic Zone (millions of hectares)							
	Climatic Zone						
Degree	Cold	Humid	Dry-Subh.	Semi-Arid	Arid	Hyper-Arid	Total
None	616.7	760.1	213.2	366.1	73.6	3.0	2032.8
Light	0.2	5.3	4.5	7.8	1.1	0.0	18.9
Moderate	0.0	53.7	10.5	43.1	5.2	0.0	112.5
Strong	0.0	19.4	3.2	2.3	1.6	0.1	26.7
Extreme	0.0	0.0	0.0	0.0	0.0	0.0	0.0
Total	616.9	838.5	231.5	419.4	81.5	3.1	2190.9

Degree of Soil Degradation by Climatic Zone (in percent)							
Degree	Cold	Humid	Dry-Subh.	Semi-Arid	Arid	Hyper-Arid	Total
None	30.3	37.4	10.5	18.0	3.6	0.1	100.0
Light	0.8	28.2	23.7	41.5	5.8	0.0	100.0
Moderate	0.0	47.7	9.4	38.3	4.6	0.0	100.0
Strong	0.0	72.5	12.1	8.7	6.1	0.5	100.0
Extreme	0.0	0.0	0.0	0.0	0.0	0.0	100.0
Total	28.2	38.3	10.6	19.1	3.7	0.1	100.0

Total Area in the Climatic Zone by Soil Degradation Degree (in percent)							
Degree	Cold	Humid	Dry-Subh.	Semi-Arid	Arid	Hyper-Arid	Total
None	100.0	90.6	92.1	87.3	90.3	95.5	92.8
Light	0.0	0.6	1.9	1.9	1.3	0.0	0.9
Moderate	0.0	6.4	4.5	10.3	6.4	0.0	5.1
Strong	0.0	2.3	1.4	0.6	2.0	4.5	1.2
Extreme	0.0	0.0	0.0	0.0	0.0	0.0	0.0
Total	100.0	100.0	100.0	100.0	100.0	100.0	100.0

Degraded Area in the Climatic Zone by Soil Degradation Degree (in percent)							
Degree	Cold	Humid	Dry-Subh.	Semi-Arid	Arid	Hyper-Arid	Total
Light	90.2	6.8	24.6	14.7	13.7	0.0	12.0
Moderate	9.8	68.5	57.7	80.9	65.8	0.0	71.2
Strong	0.0	24.7	17.7	4.4	20.4	100.0	16.9
Extreme	0.0	0.0	0.0	0.0	0.0	0.0	0.0
Total	100.0	100.0	100.0	100.0	100.0	100.0	100.0

Data Source: UNEP/ISRIC, 1990 and CRU/UEA, 1990
Data Compilation: UNEP/GRID, 1991

Table 17:
DEGREE OF SOIL DEGRADATION AND CLIMATIC ZONES
SOUTH AMERICA

Degree of Soil Degradation by Climatic Zone (millions of hectares)							
	Climatic Zone						
Degree	Cold	Humid	Dry-Subh.	Semi-Arid	Arid	Hyper-Arid	Total
None	31.5	1031.7	183.4	216.6	36.9	24.1	1524.2
Light	2.0	61.0	10.9	26.6	4.2	0.0	104.8
Moderate	4.3	76.6	10.5	17.3	3.3	1.6	113.5
Strong	0.0	18.8	2.2	4.0	0.0	0.0	25.0
Extreme	0.0	0.0	0.0	0.0	0.0	0.0	0.0
Total	37.7	1188.2	207.0	264.5	44.5	25.7	1767.6

Degree of Soil Degradation by Climatic Zone (in percent)							
Degree	Cold	Humid	Dry-Subh.	Semi-Arid	Arid	Hyper-Arid	Total
None	2.1	67.7	12.0	14.2	2.4	1.6	100.0
Light	1.9	58.3	10.4	25.4	4.0	0.0	100.0
Moderate	3.7	67.5	9.2	15.2	2.9	1.4	100.0
Strong	0.0	75.1	8.8	16.0	0.1	0.0	100.0
Extreme	0.0	0.0	0.0	0.0	0.0	0.0	100.0
Total	2.1	67.2	11.7	15.0	2.5	1.5	100.0

Total Area in the Climatic Zone by Soil Degradation Degree (in percent)							
Degree	Cold	Humid	Dry-Subh.	Semi-Arid	Arid	Hyper-Arid	Total
None	83.5	86.8	88.6	81.9	83.0	94.0	86.2
Light	5.2	5.1	5.3	10.1	9.4	0.0	5.9
Moderate	11.3	6.5	5.1	6.5	7.5	6.0	6.4
Strong	0.0	1.6	1.1	1.5	0.0	0.0	1.4
Extreme	0.0	0.0	0.0	0.0	0.0	0.0	0.0
Total	100.0	100.0	100.0	100.0	100.0	100.0	100.0

Degraded Area in the Climatic Zone by Soil Degradation Degree (in percent)							
Degree	Cold	Humid	Dry-Subh.	Semi-Arid	Arid	Hyper-Arid	Total
Light	31.7	39.0	46.3	55.6	55.6	0.0	43.1
Moderate	68.3	49.0	44.3	36.1	44.2	100.0	46.7
Strong	0.0	12.0	9.4	8.4	0.3	0.0	10.3
Extreme	0.0	0.0	0.0	0.0	0.0	0.0	0.0
Total	100.0	100.0	100.0	100.0	100.0	100.0	100.0

Data Source: UNEP/ISRIC, 1990 and CRU/UEA, 1990
Data Compilation: UNEP/GRID, 1991

Table 18:
DEGREE AND TYPE OF SOIL DEGRADATION
AFRICA

Degree by Type of Soil Degradation (millions of hectares)					
	Type of Soil Degradation				
Degree	Water	Wind	Chemical	Physical	Total
Light	57.5	88.3	26.0	1.8	173.6
Moderate	67.4	89.3	27.0	8.1	191.8
Strong	98.3	7.9	8.6	8.8	123.6
Extreme	4.2	1.0	0.0	0.0	5.2
Total	227.4	186.5	61.6	18.7	494.2

Degree by Type of Soil Degradation (in percent)					
Degree	Water	Wind	Chemical	Physical	Total
Light	33.1	50.8	15.0	1.1	100.0
Moderate	35.2	46.6	14.1	4.2	100.0
Strong	79.5	6.4	6.9	7.1	100.0
Extreme	80.6	19.4	0.0	0.0	100.0
Total	46.0	37.7	12.5	3.8	100.0

Type of Soil Degradation by Degree (in percent)					
Degree	Water	Wind	Chemical	Physical	Total
Light	25.3	47.3	42.2	9.8	35.1
Moderate	29.6	47.9	43.8	43.1	38.8
Strong	43.2	4.2	13.9	47.1	25.0
Extreme	1.8	0.5	0.0	0.0	1.1
Total	100.0	100.0	100.0	100.0	100.0

Data Source: UNEP/ISRIC, 1990
Data Compilation: UNEP/GRID, 1991

Table 19:
DEGREE AND TYPE OF SOIL DEGRADATION
ASIA

Degree by Type of Soil Degradation (millions of hectares)					
	Type of Soil Degradation				
Degree	Water	Wind	Chemical	Physical	Total
Light	124.5	132.4	31.8	5.7	294.5
Moderate	241.7	75.1	21.5	6.0	344.3
Strong	73.4	14.5	19.5	0.4	107.7
Extreme	0.0	0.2	0.4	0.0	0.5
Total	439.6	222.1	73.2	12.1	747.0

Degree by Type of Soil Degradation (in percent)					
Degree	Water	Wind	Chemical	Physical	Total
Light	42.3	45.0	10.8	2.0	100.0
Moderate	70.2	21.8	6.2	1.7	100.0
Strong	68.1	13.5	18.1	0.3	100.0
Extreme	0.0	30.3	69.7	0.0	100.0
Total	58.8	29.7	9.8	1.6	100.0

Type of Soil Degradation by Degree (in percent)					
Degree	Water	Wind	Chemical	Physical	Total
Light	28.3	59.6	43.5	47.4	39.4
Moderate	55.0	33.8	29.4	49.7	46.1
Strong	16.7	6.5	26.6	2.9	14.4
Extreme	0.0	0.1	0.5	0.0	0.1
Total	100.0	100.0	100.0	100.0	100.0

Data Source: UNEP/ISRIC 1990
Data Compilation: UNEP/GRID, 1991

Table 20:
DEGREE AND TYPE OF SOIL DEGRADATION
AUSTRALASIA

Degree by Type of Soil Degradation (millions of hectares)					
	Type of Soil Degradation				
Degree	Water	Wind	Chemical	Physical	Total
Light	79.4	16.3	0.2	0.7	96.6
Moderate	3.2	0.0	0.7	0.0	3.9
Strong	0.2	0.1	0.0	1.6	1.9
Extreme	0.0	0.0	0.4	0.0	0.4
Total	82.9	16.4	1.3	2.3	102.9

Degree by Type of Soil Degradation (in percent)					
Degree	Water	Wind	Chemical	Physical	Total
Light	82.2	16.9	0.2	0.7	100.0
Moderate	82.5	0.0	17.5	0.0	100.0
Strong	11.8	5.2	0.0	83.0	100.0
Extreme	0.0	0.0	100.0	0.0	100.0
Total	80.6	15.9	1.3	2.2	100.0

Type of Soil Degradation by Degree (in percent)					
Degree	Water	Wind	Chemical	Physical	Total
Light	95.8	99.4	17.1	29.3	93.9
Moderate	3.9	0.0	51.6	0.0	3.8
Strong	0.3	0.6	0.0	70.7	1.9
Extreme	0.0	0.0	31.3	0.0	0.4
Total	100.0	100.0	100.0	100.0	100.0

Data Source: UNEP/ISRIC, 1990
Data Compilation: UNEP/GRID, 1991

Table 21:
DEGREE AND TYPE OF SOIL DEGRADATION
EUROPE

Degree by Type of Soil Degradation (millions of hectares)					
	Type of Soil Degradation				
Degree	Water	Wind	Chemical	Physical	Total
Light	21.4	3.2	8.1	27.9	60.6
Moderate	81.0	38.2	17.1	8.1	144.4
Strong	9.8	0.0	0.6	0.4	10.7
Extreme	2.4	0.7	0.0	0.0	3.1
Total	114.5	42.2	25.7	36.4	218.9

Degree by Type of Soil Degradation (in percent)					
Degree	Water	Wind	Chemical	Physical	Total
Light	35.2	5.3	13.4	46.1	100.0
Moderate	56.1	26.5	11.8	5.6	100.0
Strong	91.1	0.3	5.2	3.4	100.0
Extreme	77.1	22.9	0.0	0.0	100.0
Total	52.3	19.3	11.8	16.6	100.0

Type of Soil Degradation by Degree (in percent)					
Degree	Water	Wind	Chemical	Physical	Total
Light	18.6	7.6	31.5	76.7	27.7
Moderate	70.7	90.6	66.3	22.3	66.0
Strong	8.5	0.1	2.2	1.0	4.9
Extreme	2.1	1.7	0.0	0.0	1.4
Total	100.0	100.0	100.0	100.0	100.0

Data Source: UNEP/ISRIC, 1990
Data Compilation: UNEP/GRID, 1991

Table 22:
DEGREE AND TYPE OF SOIL DEGRADATION
NORTH AMERICA

Degree by Type of Soil Degradation (millions of hectares)					
	Type of Soil Degradation				
Degree	Water	Wind	Chemical	Physical	Total
Light	14.5	2.6	0.5	1.3	18.9
Moderate	68.2	34.9	5.7	3.8	112.5
Strong	23.4	1.7	0.7	0.8	26.7
Extreme	0.0	0.0	0.0	0.0	0.0
Total	106.1	39.2	7.0	5.8	158.1

Degree by Type of Soil Degradation (in percent)					
Degree	Water	Wind	Chemical	Physical	Total
Light	76.5	13.9	2.9	6.7	100.0
Moderate	60.6	31.0	5.0	3.4	100.0
Strong	87.8	6.5	2.8	2.9	100.0
Extreme	0.0	0.0	0.0	0.0	100.0
Total	67.1	24.8	4.4	3.7	100.0

Type of Soil Degradation by Degree (in percent)					
Degree	Water	Wind	Chemical	Physical	Total
Light	13.6	6.7	7.8	21.8	12.0
Moderate	64.3	88.9	81.5	65.0	71.2
Strong	22.1	4.5	10.7	13.2	16.9
Extreme	0.0	0.0	0.0	0.0	0.0
Total	100.0	100.0	100.0	100.0	100.0

Data Source: UNEP/ISRIC, 1990
Data Compilation: UNEP/GRID, 1991

Table 23:
DEGREE AND TYPE OF SOIL DEGRADATION
SOUTH AMERICA

Degree by Type of Soil Degradation (millions of hectares)					
	Type of Soil Degradation				
Degree	Water	Wind	Chemical	Physical	Total
Light	45.9	25.8	26.3	6.8	104.8
Moderate	65.1	16.1	31.4	0.8	113.5
Strong	12.1	0.0	12.6	0.3	25.0
Extreme	0.0	0.0	0.0	0.0	0.0
Total	123.2	41.9	70.3	7.9	243.4

Degree by Type of Soil Degradation (in percent)					
Degree	Water	Wind	Chemical	Physical	Total
Light	43.8	24.6	25.1	6.5	100.0
Moderate	57.4	14.2	27.7	0.7	100.0
Strong	48.5	0.0	50.3	1.3	100.0
Extreme	0.0	0.0	0.0	0.0	100.0
Total	50.6	17.2	28.9	3.3	100.0

Type of Soil Degradation by Degree (in percent)					
Degree	Water	Wind	Chemical	Physical	Total
Light	37.3	61.5	37.4	85.8	43.1
Moderate	52.9	38.5	44.7	10.3	46.7
Strong	9.9	0.0	17.9	4.0	10.3
Extreme	0.0	0.0	0.0	0.0	0.0
Total	100.0	100.0	100.0	100.0	100.0

Data Source: UNEP/ISRIC, 1990
Data Compilation: UNEP/GRID, 1991

Table 24:
TYPE OF SOIL DEGRADATION AND CLIMATIC ZONES
AFRICA

Type of Soil Degradation by Climatic Zone (millions of hectares)							
	Climatic Zone						
Type	Cold	Humid	Dry-Subh.	Semi-Arid	Arid	Hyper-Arid	Total
None	0.0	868.9	231.4	404.3	331.0	635.9	2471.5
Water	0.0	104.7	25.1	59.2	34.8	3.6	227.4
Wind	0.0	0.8	1.6	30.7	127.5	25.8	186.5
Chemical	0.0	28.5	7.7	11.3	7.6	6.5	61.6
Physical	0.0	4.8	2.9	8.4	2.6	0.1	18.7
Total	0.0	1007.7	268.7	513.8	503.5	672.0	2965.7

Type of Soil Degradation by Climatic Zone (in percent)							
Type	Cold	Humid	Dry-Subh.	Semi-Arid	Arid	Hyper-Arid	Total
None	0.0	35.2	9.4	16.4	13.4	25.7	100.0
Water	0.0	46.0	11.0	26.0	15.3	1.6	100.0
Wind	0.0	0.4	0.9	16.4	68.4	13.9	100.0
Chemical	0.0	46.3	12.5	18.3	12.3	10.6	100.0
Physical	0.0	25.4	15.7	44.6	14.0	0.4	100.0
Total	0.0	34.0	9.1	17.3	17.0	22.7	100.0

Total Area in the Climatic Zone by Soil Degradation Type (in percent)							
Type	Cold	Humid	Dry-Subh.	Semi-Arid	Arid	Hyper-Arid	Total
None	0.0	86.2	86.1	78.7	65.7	94.6	83.3
Water	0.0	10.4	9.3	11.5	6.9	0.5	7.7
Wind	0.0	0.1	0.6	6.0	25.3	3.8	6.3
Chemical	0.0	2.8	2.9	2.2	1.5	1.0	2.1
Physical	0.0	0.5	1.1	1.6	0.5	0.0	0.6
Total	100.0	100.0	100.0	100.0	100.0	100.0	100.0

Degraded Area in the Climatic Zone by Soil Degradation Type (in percent)							
Type	Cold	Humid	Dry-Subh.	Semi-Arid	Arid	Hyper-Arid	Total
Water	0.0	75.4	67.2	54.1	20.2	10.0	46.0
Wind	0.0	0.6	4.3	28.0	73.9	71.6	37.7
Chemical	0.0	20.5	20.6	10.3	4.4	18.1	12.5
Physical	0.0	3.4	7.9	7.6	1.5	0.2	3.8
Total	100.0	100.0	100.0	100.0	100.0	100.0	100.0

Data Source: UNEP/ISRIC,1990 and CRU/UEA, 1990
Data Compilation: UNEP/GRID, 1991

Table 25:
TYPE OF SOIL DEGRADATION AND CLIMATIC ZONES
ASIA

Type of Soil Degradation by Climatic Zone (millions of hectares)							
	Climatic Zone						
Type	Cold	Humid	Dry-Subh.	Semi-Arid	Arid	Hyper-Arid	Total
None	1060.6	933.6	274.4	552.0	475.0	213.3	3508.9
Water	19.4	255.6	54.9	69.9	32.7	7.1	439.6
Wind	2.4	13.8	15.1	52.1	85.9	52.8	222.1
Chemical	0.0	18.9	6.0	15.6	28.6	4.1	73.2
Physical	0.1	2.4	2.3	3.8	3.5	0.0	12.1
Total	1082.5	1224.3	352.7	693.4	625.7	277.3	4255.9

Type of Soil Degradation by Climatic Zone (in percent)							
Type	Cold	Humid	Dry-Subh.	Semi-Arid	Arid	Hyper-Arid	Total
None	30.2	26.6	7.8	15.7	13.5	6.1	100.0
Water	4.4	58.1	12.5	15.9	7.4	1.6	100.0
Wind	1.1	6.2	6.8	23.5	38.7	23.8	100.0
Chemical	0.0	25.9	8.2	21.3	39.0	5.6	100.0
Physical	1.2	19.8	19.3	31.1	28.6	0.0	100.0
Total	25.4	28.8	8.3	16.3	14.7	6.5	100.0

Total Area in the Climatic Zone by Soil Degradation Type (in percent)							
Type	Cold	Humid	Dry-Subh.	Semi-Arid	Arid	Hyper-Arid	Total
None	98.0	76.3	77.8	79.6	75.9	76.9	82.4
Water	1.8	20.9	15.6	10.1	5.2	2.6	10.3
Wind	0.2	1.1	4.3	7.5	13.7	19.0	5.2
Chemical	0.0	1.5	1.7	2.3	4.6	1.5	1.7
Physical	0.0	0.2	0.7	0.5	0.6	0.0	0.3
Total	100.0	100.0	100.0	100.0	100.0	100.0	100.0

Degraded Area in the Climatic Zone by Soil Degradation Type (in percent)							
Type	Cold	Humid	Dry-Subh.	Semi-Arid	Arid	Hyper-Arid	Total
Water	88.4	87.9	70.1	49.4	21.7	11.1	58.8
Wind	10.9	4.7	19.2	36.9	57.0	82.5	29.7
Chemical	0.0	6.5	7.7	11.0	19.0	6.4	9.8
Physical	0.6	0.8	3.0	2.7	2.3	0.0	1.6
Total	100.0	100.0	100.0	100.0	100.0	100.0	100.0

Data Source: UNEP/ISRIC, 1990 and CRU/UEA, 1990
Data Compilation: UNEP/GRID, 1991

Table 26:
TYPE OF SOIL DEGRADATION AND CLIMATIC ZONES
AUSTRALASIA

Type of Soil Degradation by Climatic Zone (millions of hectares)							
	Climatic Zone						
Type	Cold	Humid	Dry-Subh.	Semi-Arid	Arid	Hyper-Arid	Total
None	0.0	203.5	46.5	275.1	254.1	0.0	779.3
Water	0.0	13.2	4.1	26.3	39.3	0.0	82.9
Wind	0.0	0.4	0.0	6.4	9.5	0.0	16.4
Chemical	0.0	0.7	0.1	0.6	0.0	0.0	1.3
Physical	0.0	1.1	0.6	0.6	0.0	0.0	2.3
Total	0.0	218.9	51.3	309.0	303.0	0.0	882.2

Type of Soil Degradation by Climatic Zone (in percent)							
Type	Cold	Humid	Dry-Subh.	Semi-Arid	Arid	Hyper-Arid	Total
None	0.0	26.1	6.0	35.3	32.6	0.0	100.0
Water	0.0	16.0	5.0	31.7	47.4	0.0	100.0
Wind	0.0	2.3	0.2	39.3	58.2	0.0	100.0
Chemical	0.0	50.9	4.5	44.6	0.0	0.0	100.0
Physical	0.0	47.5	25.0	25.5	1.9	0.0	100.0
Total	0.0	24.8	5.8	35.0	34.3	0.0	100.0

Total Area in the Climatic Zone by Soil Degradation Type (in percent)							
Type	Cold	Humid	Dry-Subh.	Semi-Arid	Arid	Hyper-Arid	Total
None	0.0	93.0	90.7	89.0	83.9	0.0	88.3
Water	0.0	6.0	8.0	8.5	13.0	0.0	9.4
Wind	0.0	0.2	0.1	2.1	3.1	0.0	1.9
Chemical	0.0	0.3	0.1	0.2	0.0	0.0	0.2
Physical	0.0	0.5	1.1	0.2	0.0	0.0	0.3
Total	100.0	100.0	100.0	100.0	100.0	100.0	100.0

Degraded Area in the Climatic Zone by Soil Degradation Type (in percent)							
Type	Cold	Humid	Dry-Subh.	Semi-Arid	Arid	Hyper-Arid	Total
Water	0.0	86.0	86.2	77.5	80.4	0.0	80.6
Wind	0.0	2.5	0.6	19.0	19.5	0.0	15.9
Chemical	0.0	4.4	1.3	1.8	0.0	0.0	1.3
Physical	0.0	7.1	12.0	1.7	0.1	0.0	2.2
Total	100.0	100.0	100.0	100.0	100.0	100.0	100.0

Data Source: UNEP/ISRIC, 1990 and CRU/UEA, 1990
Data Compilation: UNEP/GRID, 1991

Table 27:
TYPE OF SOIL DEGRADATION AND CLIMATIC ZONES
EUROPE

Type of Soil Degradation by Climatic Zone (millions of hectares)							
	Climatic Zone						
Type	Cold	Humid	Dry-Subh.	Semi-Arid	Arid	Hyper-Arid	Total
None	26.6	504.8	122.2	71.8	6.2	0.0	731.6
Water	0.4	66.0	34.7	12.8	0.6	0.0	114.5
Wind	0.1	3.4	17.4	17.3	4.0	0.0	42.2
Chemical	0.6	21.1	2.4	1.7	0.0	0.0	25.7
Physical	0.3	27.6	6.8	1.7	0.1	0.0	36.4
Total	27.9	622.9	183.5	105.2	11.0	0.0	950.5

Type of Soil Degradation by Climatic Zone (in percent)							
Type	Cold	Humid	Dry-Subh.	Semi-Arid	Arid	Hyper-Arid	Total
None	3.6	69.0	16.7	9.8	0.9	0.0	100.0
Water	0.3	57.7	30.3	11.2	0.6	0.0	100.0
Wind	0.3	8.1	41.3	41.0	9.4	0.0	100.0
Chemical	2.2	82.0	9.1	6.5	0.1	0.0	100.0
Physical	0.7	75.7	18.7	4.6	0.3	0.0	100.0
Total	2.9	65.5	19.3	11.1	1.2	0.0	100.0

Total Area in the Climatic Zone by Soil Degradation Type (in percent)							
Type	Cold	Humid	Dry-Subh.	Semi-Arid	Arid	Hyper-Arid	Total
None	95.4	81.0	66.6	68.2	56.8	0.0	77.0
Water	1.3	10.6	18.9	12.2	5.7	0.0	12.1
Wind	0.4	0.5	9.5	16.4	36.0	0.0	4.4
Chemical	2.0	3.4	1.3	1.6	0.3	0.0	2.7
Physical	0.9	4.4	3.7	1.6	1.2	0.0	3.8
Total	100.0	100.0	100.0	100.0	100.0	100.0	100.0

Degraded Area in the Climatic Zone by Soil Degradation Type (in percent)							
Type	Cold	Humid	Dry-Subh.	Semi-Arid	Arid	Hyper-Arid	Total
Water	27.2	55.9	56.7	38.3	13.3	0.0	52.3
Wind	9.2	2.9	28.4	51.8	83.3	0.0	19.3
Chemical	44.1	17.9	3.8	5.0	0.8	0.0	11.8
Physical	19.5	23.3	11.1	5.0	2.7	0.0	16.6
Total	100.0	100.0	100.0	100.0	100.0	100.0	100.0

Data Source: UNEP/ISRIC, 1990 and CRU/UEA, 1990
Data Compilation: UNEP/GRID, 1991

Table 28:
TYPE OF SOIL DEGRADATION AND CLIMATIC ZONES NORTH AMERICA

Type of Soil Degradation by Climatic Zone (millions of hectares)

	Climatic Zone						
Type	Cold	Humid	Dry-Subh.	Semi-Arid	Arid	Hyper-Arid	Total
None	616.7	760.1	213.2	366.1	73.6	3.0	2032.8
Water	0.1	67.7	10.7	24.4	3.3	0.0	106.1
Wind	0.0	1.2	6.8	27.3	3.7	0.1	39.2
Chemical	0.0	4.7	0.3	1.2	0.7	0.0	7.0
Physical	0.1	4.8	0.4	0.4	0.2	0.0	5.8
Total	616.9	838.5	231.5	419.4	81.5	3.1	2190.9

Type of Soil Degradation by Climatic Zone (in percent)

Type	Cold	Humid	Dry-Subh.	Semi-Arid	Arid	Hyper-Arid	Total
None	30.3	37.4	10.5	18.0	3.6	0.1	100.0
Water	0.1	63.8	10.1	23.0	3.1	0.0	100.0
Wind	0.0	3.2	17.4	69.6	9.5	0.3	100.0
Chemical	0.0	68.0	4.4	17.3	9.6	0.6	100.0
Physical	1.8	81.4	7.1	6.3	3.4	0.0	100.0
Total	28.2	38.3	10.6	19.1	3.7	0.1	100.0

Total Area in the Climatic Zone by Soil Degradation Type (in percent)

Type	Cold	Humid	Dry-Subh.	Semi-Arid	Arid	Hyper-Arid	Total
None	100.0	90.6	92.1	87.3	90.3	95.5	92.8
Water	0.0	8.1	4.6	5.8	4.1	0.0	4.8
Wind	0.0	0.1	3.0	6.5	4.6	3.2	1.8
Chemical	0.0	0.6	0.1	0.3	0.8	1.3	0.3
Physical	0.0	0.6	0.2	0.1	0.2	0.0	0.3
Total	100.0	100.0	100.0	100.0	100.0	100.0	100.0

Degraded Area in the Climatic Zone by Soil Degradation Type (in percent)

Type	Cold	Humid	Dry-Subh.	Semi-Arid	Arid	Hyper-Arid	Total
Water	38.1	86.3	58.5	45.8	41.9	0.0	67.1
Wind	0.0	1.6	37.5	51.3	47.1	70.6	24.8
Chemical	0.0	6.0	1.7	2.3	8.5	29.4	4.4
Physical	61.9	6.1	2.3	0.7	2.5	0.0	3.7
Total	100.0	100.0	100.0	100.0	100.0	100.0	100.0

Data Source: UNEP/ISRIC, 1990 and CRU/UEA, 1990
Data Compilation: UNEP/GRID, 1991

Table 29:
TYPE OF SOIL DEGRADATION AND CLIMATIC ZONES
SOUTH AMERICA

Type of Soil Degradation by Climatic Zone (millions of hectares)							
	Climatic Zone						
Type	Cold	Humid	Dry-Subh.	Semi-Arid	Arid	Hyper-Arid	Total
None	31.5	1031.7	183.4	216.6	36.9	24.1	1524.2
Water	3.1	85.3	11.5	20.6	2.5	0.1	123.2
Wind	3.1	10.6	5.9	16.4	4.6	1.3	41.9
Chemical	0.0	53.1	6.1	10.5	0.4	0.1	70.3
Physical	0.0	7.5	0.1	0.3	0.0	0.0	7.9
Total	37.7	1188.2	207.0	264.5	44.5	25.7	1767.6

Type of Soil Degradation by Climatic Zone (in percent)							
Type	Cold	Humid	Dry-Subh.	Semi-Arid	Arid	Hyper-Arid	Total
None	2.1	67.7	12.0	14.2	2.4	1.6	100.0
Water	2.5	69.2	9.4	16.7	2.0	0.1	100.0
Wind	7.4	25.3	14.0	39.1	11.0	3.1	100.0
Chemical	0.0	75.5	8.7	15.0	0.6	0.2	100.0
Physical	0.0	94.4	1.4	4.2	0.0	0.0	100.0
Total	2.1	67.2	11.7	15.0	2.5	1.5	100.0

Total Area in the Climatic Zone by Soil Degradation Type (in percent)							
Type	Cold	Humid	Dry-Subh.	Semi-Arid	Arid	Hyper-Arid	Total
None	83.5	86.8	88.6	81.9	83.0	94.0	86.2
Water	8.2	7.2	5.6	7.8	5.7	0.4	7.0
Wind	8.3	0.9	2.8	6.2	10.4	5.1	2.4
Chemical	0.0	4.5	2.9	4.0	1.0	0.5	4.0
Physical	0.0	0.6	0.1	0.1	0.0	0.0	0.4
Total	100.0	100.0	100.0	100.0	100.0	100.0	100.0

Degraded Area in the Climatic Zone by Soil Degradation Type (in percent)							
Type	Cold	Humid	Dry-Subh.	Semi-Arid	Arid	Hyper-Arid	Total
Water	49.8	54.5	48.8	43.0	33.3	7.4	50.6
Wind	50.0	6.8	24.9	34.3	61.0	84.6	17.2
Chemical	0.2	33.9	25.8	22.0	5.7	8.1	28.9
Physical	0.0	4.8	0.5	0.7	0.0	0.0	3.3
Total	100.0	100.0	100.0	100.0	100.0	100.0	100.0

Data Source: UNEP/ISRIC, 1990 and CRU/UEA, 1990
Data Compilation: UNEP/GRID, 1991

SECTION 2:
TABLES DERIVED FROM THE 1:10 MILLION GLASOD DATASET FOR THE THEMATIC ATLAS

Table 1:
SOIL DEGRADATION DEGREE BY REGION INSIDE AND OUTSIDE SUSCEPTIBLE DRYLAND AREAS

Soil Degradation Degree by Region Inside and Outside Susceptible Dryland Areas (millions of hectares)								
Region		Light	Moderate	Strong	Extreme	Total Degraded	Non-Degraded	Total
Africa	Drylands	118.0	127.2	70.7	3.5	319.4	966.6	1286.0
	Others	55.7	64.6	52.8	1.7	174.8	1504.9	1679.7
Asia	Drylands	156.7	170.1	43.0	0.5	370.3	1301.5	1671.8
	Others	137.8	174.2	64.6	0.0	376.6	2207.5	2584.1
Australasia	Drylands	83.6	2.4	1.1	0.4	87.5	575.8	663.3
	Others	13.0	1.6	0.8	0.0	15.4	203.5	218.9
Europe	Drylands	13.8	80.7	1.8	3.1	99.4	200.2	299.6
	Others	46.7	63.8	8.9	0.0	119.4	531.4	650.8
N-America	Drylands	13.4	58.8	7.3	0.0	79.5	652.9	732.4
	Others	5.5	53.7	19.5	0.0	78.7	1379.8	1458.5
S-America	Drylands	41.8	31.1	6.2	0.0	79.1	436.9	516.0
	Others	63.0	82.4	18.9	0.0	164.3	1087.3	1251.6
World	Drylands	427.2	470.3	130.2	7.5	1035.2	4133.9	5169.1
	Others	321.7	440.3	165.5	1.7	929.2	6914.4	7843.6
Total		748.9	910.6	295.7	9.2	1964.4	11048.3	13012.7

Data Source: UNEP/ISRIC, 1990 and CRU/UEA, 1990
Data Compilation: UNEP/GRID, 1991

Table 2:
SOIL DEGRADATION DEGREE BY REGION AND CLIMATE ZONE IN SUSCEPTIBLE DRYLAND AREAS

Soil Degradation Degree by Region and Climatic Zone Susceptible Dryland Areas (millions of hectares)				
Region	Bioclimatic Zone	Light and Moderate	High and Very High	Total
Africa	Dry-Subhumid	25.2	12.1	37.3
	Semi-Arid	69.9	39.6	109.5
	Arid	150.1	22.4	172.5
Asia	Dry-Subhumid	70.6	7.7	78.3
	Semi-Arid	124.2	17.2	141.4
	Arid	131.9	18.8	150.7
Australasia	Dry-Subhumid	4.2	0.6	4.8
	Semi-Arid	32.9	1.0	33.9
	Arid	48.9	0.0	48.9
Europe	Dry-Subhumid	59.0	2.3	61.3
	Semi-Arid	30.8	2.6	33.4
	Arid	4.8	0.0	4.8
N-America	Dry-Subhumid	15.0	3.2	18.3
	Semi-Arid	50.9	2.3	53.3
	Arid	6.3	1.6	7.9
S-America	Dry-Subhumid	21.4	2.3	23.7
	Semi-Arid	43.9	4.0	47.9
	Arid	7.5	0.0	7.5
Total		897.6	137.6	1035.2

Data Source: UNEP/ISRIC, 1990 and CRU/UEA, 1990
Data Compilation: UNEP/GRID, 1991

Table 3:
SOIL DEGRADATION DEGREE OF DEGRADATION TYPES BY REGION IN SUSCEPTIBLE DRYLAND AREAS

Degree of Wind Erosion by Region in Susceptible Dryland Areas (millions of hectares)							
	Africa	Asia	Australasia	Europe	N-America	S-America	Total
Light	78.1	80.5	15.9	1.3	2.6	18.8	197.2
Moderate	74.2	62.9	0.0	36.6	33.6	8.1	215.4
Strong	6.6	9.7	0.1	0.0	1.6	0.0	18.0
Extreme	1.0	0.1	0.0	0.7	0.0	0.0	1.8
Total	159.9	153.2	16.0	38.6	37.8	26.9	432.4

Degree of Water Erosion by Region in Susceptible Dryland Areas (millions of hectares)							
	Africa	Asia	Australasia	Europe	N-America	S-America	Total
Light	28.5	49.6	67.5	6.4	10.3	12.8	175.1
Moderate	36.6	91.2	2.1	38.0	23.9	16.7	208.5
Strong	51.5	16.7	0.0	1.4	4.2	5.2	79.0
Extreme	2.5	0.0	0.0	2.3	0.0	0.0	4.8
Total	119.1	157.5	69.6	48.1	38.4	34.7	467.4

Degree of Chemical Deterioration by Region in Susceptible Dryland Areas (millions of hectares)							
	Africa	Asia	Australasia	Europe	N-America	S-America	Total
Light	10.2	22.2	0.0	1.5	0.3	10.1	44.3
Moderate	10.4	11.1	0.2	2.2	1.3	6.2	31.4
Strong	5.9	16.5	0.0	0.4	0.6	0.7	24.1
Extreme	0.0	0.4	0.4	0.0	0.0	0.0	0.8
Total	26.5	50.2	0.6	4.1	2.2	17.0	100.6

Degree of Physical Deterioration by Region in Susceptible Dryland Areas (millions of hectares)							
	Africa	Asia	Australasia	Europe	N-America	S-America	Total
Light	1.2	4.4	0.2	4.8	0.2	0.0	10.8
Moderate	6.0	5.0	0.0	3.8	0.0	0.2	15.0
Strong	6.7	0.2	1.0	0.0	0.8	0.2	8.9
Extreme	0.0	0.0	0.0	0.0	0.0	0.0	0.0
Total	13.9	9.6	1.2	8.6	1.0	0.4	34.7

Data Source: UNEP/ISRIC, 1990 and CRU/UEA, 1990
Data Compilation: UNEP/GRID, 1991

Table 4:
CAUSE OF SOIL DEGRADATION BY REGION IN SUSCEPTIBLE DRYLANDS AND OTHER AREAS

Cause of Soil Degradation by Region in Susceptible Drylands and Other Areas (millions of hectares)									
Region	Climate Zone	Deforest -ation	Over-grazing	Agric. Activity	Overex-ploit.	Bioind. Activity	Total Degraded	Non-Degraded	Total
Africa	Drylands	18.6	184.6	62.2	54.0	0.0	319.4	966.6	1286.0
	Others	48.2	58.5	59.2	8.7	0.2	174.8	1504.9	1679.7
Asia	Drylands	111.5	118.8	96.7	42.3	1.0	370.3	1301.5	1671.8
	Others	186.3	78.5	107.6	3.8	0.4	376.6	2207.5	2584.1
Australasia	Drylands	4.2	78.5	4.8	0.0	0.0	87.5	575.8	663.3
	Others	8.1	4.0	3.2	0.0	0.1	15.4	203.5	218.9
Europe	Drylands	38.9	41.3	18.3	0.0	0.9	99.4	200.2	299.6
	Others	44.9	8.7	45.6	0.5	19.7	119.4	531.4	650.8
N-America	Drylands	4.3	27.7	41.4	6.1	0.0	79.5	652.9	732.4
	Others	13.6	10.2	49.1	5.4	0.4	78.7	1379.8	1458.5
S-America	Drylands	32.2	26.2	11.6	9.1	0.0	79.1	436.9	516.0
	Others	67.8	41.7	51.9	2.9	0.0	164.3	1087.3	1251.6
Total		578.6	678.7	551.6	132.7	22.8	1964.4	11048.3	13012.7

SECTION 3: TABLES DERIVED FROM THE 1:6 MILLION GLASOD DATASET FOR AFRICA

Table 1: DEGREE OF SOIL DEGRADATION IN AFRICA BY CLIMATE ZONE IN SUSCEPTIBLE DRYLANDS

Degree of Soil Degradation by Climatic Zone (millions of hectares)				
	Climatic Zone			
Degree	Arid	Semi-Arid	Dry-Subhumid	Total
Light	98.5	28.8	16.8	144.1
Moderate	56.3	43.8	12.1	112.2
Strong	20.7	41.2	10.8	72.7
Extreme	1.3	1.1	0.7	3.1
Unaffected	324.4	398.8	230.6	953.8
Total	501.2	513.7	271.0	1285.9

Data Source: UNEP/ISRIC, 1990 and CRU/UEA, 1990
Data Compilation: UNEP/GRID, 1991

Table 2:
SPECIFIC TYPES OF SOIL DEGRADATION IN AFRICA BY CLIMATIC ZONE IN SUSCEPTIBLE DRYLANDS

Water Erosion - Loss of Topsoil (millions of hectares)				
	Climatic Zone			
Degree	Arid	Semi-Arid	Dry-Subhumid	Total
Light	21.6	13.5	9.7	44.8
Moderate	7.9	19.9	9.3	37.1
Strong	16.3	27.4	6.0	49.7
Extreme	0.1	0.4	0.5	1.0
Total	45.9	61.2	25.5	132.6

Water Erosion - Terrain Deformation (millions of hectares)				
	Climatic Zone			
Degree	Arid	Semi-Arid	Dry-Subhumid	Total
Light	1.0	1.5	0.3	2.8
Moderate	0.3	3.2	1.5	5.0
Strong	0.5	1.8	1.5	3.8
Extreme	0.6	0.5	0.1	1.2
Total	2.4	7.0	3.4	12.8

Wind Erosion - Loss of Topsoil (millions of hectares)				
	Climatic Zone			
Degree	Arid	Semi-Arid	Dry-Subhumid	Total
Light	86.4	18.8	3.8	109.0
Moderate	53.0	17.9	1.3	72.2
Strong	3.6	4.9	0.0	8.5
Extreme	0.0	0.0	0.0	0.0
Total	143.0	41.6	5.1	189.7

Wind Erosion - Terrain Deformation (millions of hectares)				
	Climatic Zone			
Degree	Arid	Semi-Arid	Dry-Subhumid	Total
Light	37.6	5.1	0.0	42.7
Moderate	3.2	2.8	0.0	6.0
Strong	0.0	0.0	0.0	0.0
Extreme	0.0	0.0	0.0	0.0
Total	40.8	7.9	0.0	48.7

AREA CALCULATIONS

Table 2 (cont.):

Wind Erosion - Overblowing (millions of hectares)				
	Climatic Zone			
Degree	Arid	Semi-Arid	Dry-Subhumid	Total
Light	2.8	2.2	0.3	5.3
Moderate	1.9	1.3	0.0	3.2
Strong	0.3	0.2	0.0	0.5
Extreme	0.6	0.2	0.0	0.8
Total	5.6	3.9	0.3	9.8

Chemical Degradation - Loss of Nutrients (millions of hectares)				
	Climatic Zone			
Degree	Arid	Semi-Arid	Dry-Subhumid	Total
Light	0.7	16.6	9.8	27.1
Moderate	2.3	4.3	2.1	8.7
Strong	0.6	4.2	1.2	6.0
Extreme	0.0	0.0	0.0	0.0
Total	3.6	25.1	13.1	41.8

Chemical Degradation - Salinization (millions of hectares)				
	Climatic Zone			
Degree	Arid	Semi-Arid	Dry-Subhumid	Total
Light	2.2	1.2	0.2	3.6
Moderate	1.2	0.8	0.1	2.1
Strong	0.0	0.0	0.0	0.0
Extreme	0.0	0.0	0.0	0.0
Total	3.4	2.0	0.3	5.7

Chemical Degradation - Acidification (millions of hectares)				
	Climatic Zone			
Degree	Arid	Semi-Arid	Dry-Subhumid	Total
Light	0.0	1.2	1.4	2.6
Moderate	0.0	0.0	0.0	0.0
Strong	0.0	0.0	0.0	0.0
Extreme	0.0	0.0	0.0	0.0
Total	0.0	1.2	1.4	2.6

Table 2 (cont.):

Physical Degradation - Compaction/Crusting (millions of hectares)				
	Climatic Zone			
Degree	Arid	Semi-Arid	Dry-Subhumid	Total
Light	1.9	12.0	5.3	19.2
Moderate	2.6	8.6	1.4	12.6
Strong	1.0	4.1	2.1	7.2
Extreme	0.0	0.0	0.0	0.0
Total	5.5	24.7	8.8	39.0

Physical Degradation - Waterlogging (millions of hectares)				
	Climatic Zone			
Degree	Arid	Semi-Arid	Dry-Subhumid	Total
Light	0.0	0.1	0.2	0.3
Moderate	0.0	0.1	0.0	0.1
Strong	0.0	0.0	0.0	0.0
Extreme	0.0	0.0	0.0	0.0
Total	0.0	0.2	0.2	0.4

Data Source: UNEP/ISRIC, 1990 and CRU/UEA, 1990
Data Compilation: UNEP/GRID, 1991

Table 3:
CAUSE OF SOIL DEGRADATION IN AFRICA
BY CLIMATE ZONE IN SUSCEPTIBLE DRYLANDS

Cause of Soil Degradation by Climatic Zone (millions of hectares)				
	Climatic Zone			
Cause	Arid	Semi-Arid	Dry-Subhumid	Total
Deforestation	3.9	7.6	10.5	22.0
Overgrazing	119.9	61.9	12.6	194.4
Agricult. Activ.	11.1	33.8	15.5	60.4
Overexploitation	42.0	11.7	1.8	55.5
Total	176.9	115.0	40.4	332.3

Data Source: UNEP/ISRIC, 1990 and CRU/UEA, 1990
Data Compilation: UNEP/GRID, 1991